Advances in Raw Material Industries for Sustainable Development Goals

Editor
Vladimir Litvinenko

CRC Press
Taylor & Francis Group

ADVANCES IN RAW MATERIAL INDUSTRIES FOR SUSTAINABLE DEVELOPMENT GOALS

Advances in Raw Material Industries for Sustainable Development Goals

Editor

Vladimir Litvinenko

Rector of Saint-Petersburg Mining University, Saint-Petersburg, Russia
Co-chairman of Russian-German Raw Materials Forum

CRC Press
Taylor & Francis Group
Boca Raton London New York

CRC Press is an imprint of the
Taylor & Francis Group, an **informa** business

A BALKEMA BOOK

CRC Press/Balkema is an imprint of the Taylor & Francis Group, an informa business

Typeset by Integra Software Services Pvt. Ltd., Pondicherry, India

Library of Congress Cataloging-in-Publication Data

Applied for

Published by: CRC Press/Balkema
Schipholweg 107C, 2316XC Leiden, The Netherlands
e-mail: Pub.NL@taylorandfrancis.com
www.routledge.com – www.taylorandfrancis.com

ISBN: 978-0-367-75881-3 (Hbk)
ISBN: 978-1-003-16439-5 (eBook)
DOI: 10.1201/9781003164395
https://doi.org/10.1201/9781003164395

Advances in Raw Material Industries for Sustainable Development Goals – Litvinenko (Ed)
© 2021 Taylor & Francis Group, London, ISBN 978-0-367-75881-3

Table of contents

Advances in Raw Material Industries for Sustainable Development Goals – Litvinenko (Ed)
© 2021 Taylor & Francis Group, London, ISBN 978-0-367-75881-3

Preface

Here are the results of joint scientific research conducted in the context of the Russian-German Raw Materials Forum. These results reflect the main promising areas of cooperation between Russian Federation and Germany.

Today Russia and Germany are exploring various forms of cooperation in the field of mining, geology, mineralogy, mechanical engineering and energy. The Forum accumulates information on current trends – the development of raw materials markets and the world economy or environmental issues and new technologies in the industry – to respond to modern challenges efficiently. In 2018, we decided to annually publish the collection of research articles to promote relevant information discussed at the Forum, and to highlight socially significant problems of the raw materials sector, and this has now become a strong tradition.

For more than 12 years of its existence, the Russian-German Raw Materials Forum has proven its effectiveness and social and political significance, becoming an important platform for discussing the most pressing relations issues between Russia and Germany, not only in the mineral and raw materials sector, but also in international economic and geopolitical aspects.

Economic and technological cooperation have always played an important and sometimes decisive role in Russian-German relations. At the same time, Russian oil and gas exports remain the most important economic link between Russia and Germany. But in addition, the access to German technologies traditionally stimulating the economy development continues to be essential for the Russian side.

We focus on the main fields of cooperation, development areas and business opportunities for technological cooperation in the mineral sector.

At the same time, we have significantly expanded the scope of the Russian-German cooperation: not only traditional oil and gas issues are raised now, but also the topics of energy of the future, digitalization of the raw materials industry, raw materials processing, circular economy and joint scientific projects on Earth exploration.

Taking into account the traditionally high interest of young people in the Forum, as well as thanks to the support of the International Competence Centre for Mining Engineering Education under the auspices of UNESCO, the programme for young scientists has also been significantly expanded recently.

We are very glad that, at present, despite the world political challenges, the interest in the Russian-German Raw Materials Forum is constantly growing, and the joint projects with various Russian regions and cooperation of scientists make the Raw Materials Forum the main dialogue platform for both countries here and now.

We are confident that exactly such deep and dynamic Russian-German scientific and academic dialogue will continue contributing to strong, wide-ranging, mutually beneficial and equal relations between the countries. And we will do everything in our power to maintain and develop such relationships.

Vladimir Litvinenko
Doctor of Engineering, Professor; Rector of Saint Petersburg Mining University

Organizers

International Competence Centre for Mining Engineering Education under the auspices of UNESCO

United Nations Educational, Scientific and Cultural Organization

International Competence Centre for Mining-Engineering Education under the auspices of UNESCO

Russian-German Raw Materials Forum

Rohstoff-Forum
Российско-Германский сырьевой форум

Saint Petersburg Mining University

SAINT-PETERSBURG MINING UNIVERSITY

SIBUR

SIBUR

PhosAgro

PHOSAGRO®

Freiberg University of Mining and Technology

TU BERGAKADEMIE FREIBERG

VNG

VNG

Advances in Raw Material Industries for Sustainable Development Goals – Litvinenko (Ed)
© 2021 Taylor & Francis Group, London, ISBN 978-0-367-75881-3

Processing of oil products by hydrocarbon-oxidizing microorganisms

O.M. Prishchepa
Doctor of geological and mineralogical Sciences, Head of department, Saint-Petersburg Mining University, Saint-Petersburg, Russia

Y.V. Nefedov
PhD in Geology and Mineralogy, Associate Professor, Deputy Head of Oil and Gas Geology Department, Saint-Petersburg Mining University, Saint-Petersburg, Russia

P.A. Morgunov
PhD in Chemisty, All-Russia Petroleum Research Exploration Institute» JSC ("VNIGRI" JSC)

ABSTRACT: This paper presents the results of laboratory studies concerning biodegradation of oil and diesel fuel put into actions by strains of hydrocarbon-oxidizing microorganisms. The degree of biodegradation of oil and oil products in the laboratory is estimated by balance calculations, according to which the destruction could reach up to 56.6-71.6%, while the destruction of individual fractions of the oil pollutant could exceeds 80-90%. A theoretical explanation of the activity of hydrocarbon-oxidizing microorganism strains is presented.

Keywords: Hydrocarbon-oxidizing bacteria, strains of microorganisms, biodegradation of oil and oil products

1 INTRODUCTION

The purpose of experimental and scientific activity is to determine in the laboratory the capacity and efficiency of transformation of oil and oil products by selected strains of hydrocarbon-oxidizing microorganisms. Long-term researches of VNIGRI allowed to create a collection of microorganisms possessing high oil-oxidizing and bio emulsifying properties.

Studies of biodegradation properties of individual strains related to oil degradation are aimed for compiling a data base of microorganisms "destructors" clearing of oil (including the conditions of high concentration of oil products, in a wide temperature and pH range) suitable for soil and water ecosystems.

2 PROBLEM STATEMENT

Samples of diesel fuel and oil were selected as research objects on the hydrocarbon ecology problem. Samples of polluting oil were analyzed according to the scheme of detailed complex genuine chemical and bituminological analysis, developed and used in the laboratory practice of VNIGRI, in order to be able to compare the results in pre- and post-experimental stages.

Identification of the most active strains of hydrocarbon-oxidizing microorganisms based on the capacity to dispose of polluting oils is aimed to creating the basis of the new biological products.

The results obtained and subsequent balance calculations based on them will allow to determine not only the activity of strains for the utilization of oil pollution in general, but also its specific fractions.

3 OIL AND OIL PRODUCTS BIODEGRADATION BY HYDROCARBON-OXIDIZING STRAINS OF MICROORGANISMS

In the special literature the studies about the utilization of various classes of oil hydrocarbons by pure cultures of hydrocarbon-oxidizing microorganisms devoted a significant amount of work.

Since oil and oil products are among the most common pollutants of the biosphere, the problem of cleaning the environment from oil pollution is becoming increasingly acute due to both limited possibilities (and sometimes environmental harm) of using mechanical and physic and chemical cleaning methods for these purposes. Oil is a toxin, which, covering the surface of the soil, destroys vegetation, creates conditions of oxygen starvation in the soil, has a toxic effect on humans and all living organisms, etc. Accordingly, oil, getting into the soil, changes its physical characteristics. It has brightly expressed hydrophobic properties, which are transmitted to soil particles. There are significant violations of water and air regimes of soils, leading to the development of anaerobic processes, which adversely affects soil fertility. Oil pollution causes an increase in the carbon content in the soil, leading to a high ratio of carbon to nitrogen; in addition, there is a decrease in the concentration of mobile phosphorus (Rueter et al., 1994).

Oil components, interacting with soil particles in different ways, are distributed along the vertical profile of the soil. For the vertical movement of oil down the soil section in the humus level is going high-molecular oil components, the beneath layers penetrate mostly low molecular compounds: the simplest structure of the paraffinic, naphthenic and aromatic oil hydrocarbons. On the surface of the soil oil undergoes chemical oxidation, partially photo-oxidation. However, it should be noted that abiotic oxidation is rather slow, therefore, to a greater extent the destruction of oil hydrocarbons is associated with the process of their biological oxidation, which occurs only with the participation of oil-oxidizing microorganisms.

In this regard, in recent years, more and more attention of environmentalists attracts biological method of purification from oil pollution. The method is based on the use of microorganisms capable of using oil hydrocarbons as the only source of carbon. This makes it possible to reduce the oil content to background values (the values of background concentrations vary widely depending on the area) at low operating costs and facility of decision.

4 MECHANISMS OF HYDROCARBON OXIDATION BY MICROORGANISMS

The processes of biogenic oxidation of hydrocarbons are so complex that currently there is not clear enough to define this mechanism. This question is complicated because the direction of the biogenic oxidation process is influenced by many factors: hydrogen potential (Ph), oxidative-reductive potential (Rh2), temperature, lighting, osmotic pressure, etc. In addition to these factors, the physiological characteristics of the microorganisms themselves, which are obvious related to the oxidation of individual hydrocarbons and their mixtures, are also very important.

Microorganisms have the property of selective attitude to different hydrocarbons, and this capacity is determined not only by the difference in the structure of the substance, but even by the number of carbon atoms contained in the structure. For example, selected and described by V. Petrov and I. Tauch Bacterium aliphaticum and Bacterium aliphaticum liquefaciens oxidized n-hexane, n-octane, decan, hexadecan, triacontane and tetra trioctane. Bacterium paraffinicum described by the same authors, oxidized only the higher homologues of this series, starting with hexadecane.

Oxidation of hydrocarbons by the majority of well-known microorganisms is carried out by adaptive enzymes (ferments). This fact is established by numerous experiments about the oxidation of hydrocarbons by the cells of microorganisms grown on non-hydrocarbon substrates. It has been shown, for example, that cells of heptane-oxidant bacteria grown on glucose are unable to oxidize hydrocarbons in the presence of chloramphenicol. This compound inhibits protein synthesis and thus prevents the emergence of adaptive enzymes.

Ways of microbiological oxidation of hydrocarbons are established by various methods:

– The simultaneous adaptation method proposed by R.Y. Stanier (1947) is based on the high specificity of adaptive enzymes induced by hydrocarbons to intermediate oxidation products. The basic principles of this method are: cells adapted to the oxidation of hydrocarbon are simultaneously adapted to the oxidation of subsequent intermediate products. Hence, if cells grown on hydrocarbon are simultaneously adapted to oxidation of any compound, this compound can be a member of a series of hydrocarbon metabolites.
– A method of checking the growth of microorganisms on the expected intermediate product.

The methods give the indirect evidence of metabolic pathways. Direct evidence of metabolism is obtained by the following two methods:

– Separation and determination of intermediate products of oxidation of hydrocarbons. In recent years, more advanced methods of separation and identification of products of microorganisms – gas and liquid chromatography, infrared spectrophotometry, ultraviolet rays and mass spectrometry have been used. The most accurate and reliable evidence is provided by the method of application marked by isotope substrates and mark detection in oxidation products.
– Making of enzymatic preparations out of microbial cells that catalyze specific reactions in the metabolic chain.

5 DISPERSION OF HYDROCARBON-OXIDIZING MICROORGANISMS IN NATURE

Microorganisms degrading hydrocarbons are widely spread in the nature. There are 22 species of bacteria, 31 species of microscopic fungi, including 19 species of yeast selected from soil ecosystems capable of biodegradation of various oil hydrocarbons. There are 25 species of hydrocarbon-degrading bacteria and 27 species of hydrocarbon-using microscopic fungi that were isolated from the marine environment.

Among them:

– bacteria (Achromobacter, Acinetobacter, Alcaligenes, Arthrobacter, Bacillus, Brevibacterium, Citrobacter, Clostridium, Corynebacterium, Desulfovibrio, Eneribacer, Escherichia, Flavobacterium, Methanobacterium, Micrococcus, Micromonospora, Mycobacterium, Nocardia, Rhodococcus, Pseudomonas, Sarcina, Serratia, Spirillum, Streptomyces, Thiobacillus, Vibrio),
– mycelial fungi (Aspergillus, Cephalosporium, Penicillium, Mucor, Fusarium, Trichoderma),
– yeast (Candida, Debaryomyces, Endomyces, Endomycopsis, Hansenula, Rhodotorula, Saccharomyces, Torulopsis, Trichosporon),
– cyanobacteriums (Agmenellum, Aphanocapsa, Lyngbya, Microcoleus, Oscillatoria, Phormidium, Plectonema).

Most hydrocarbon-oxidizing microorganisms are found both in soil and water habitats (Petrikov et. al., 2008).

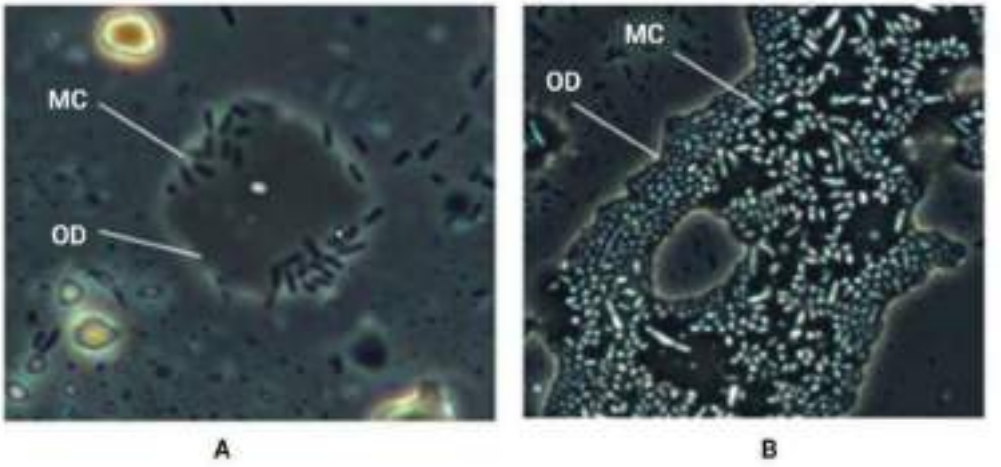

Figure 1. Pure cultures of microorganisms in the process of oil destruction (optical microscopy).
A - Pseudomonas putida BS3701 (pBS1141, pBS1142), B - Rhodococcus sp. S67: MC – microbe cells, OD – oil drop.

6 OIL EFFECT ON SOIL MICROORGANISMS

The effect of long-term impact of oil on the soil can be emerged in the change of its microbiological properties. All soils contain a large number of microorganisms capable of oxidizing various hydrocarbons. The breeding effect of oil on the soil microbiota is primarily expressed in the fact that in contaminated soils there are microorganisms using n-alkanes and aromatic hydrocarbons much more than in soils without oil. There is an increase in the number of highly specialized forms of microorganisms oxidizing gaseous hydrocarbons, solid paraffin's, aromatic hydrocarbons. The effect of oil on living organisms of the soil is largely determined by its composition and concentration. It is well known that at low concentrations oil has a stimulating effect on soil biota, as it is an energy substrate for a large group of microorganisms and contains substances that stimulate the growth of plants. On the other hand, the massive oil pollution caused by accidental spills is accompanied by an acute toxic effect of oil on living organisms (Petrikov et al., 2008).

With the help of optical microscope, the behavior of strains belonging to different species and having a different structure of the cell wall with growth in a medium with crude oil was studied. As it can be seen from Figure 1, the nature of interaction with oil gram-negative cells Pseudomonas putida BS3701 and gram-positive cells Rhodococcus sp. S67 differ significantly.

Optical studies of these cultures after three days of cultivation in medium with crude oil showed that Pseudomonas are localized on the oil drops surface, and the cells *Rhodococcus* are inside of oil drops (Nikulin et al., 2017).

7 HYDROCARBONS ENTRYWAYS INTO BACTERIAL CELLS

Today there are no reliable experimental data on the oxidation of hydrocarbons by extracellular enzymes of microorganisms. Special studies have shown that in the growth of yeast in the medium with hexadecane p. Candida enzymes responsible for the oxidation of hydrocarbons, as well as products of primary oxidation of the substrate – cetyl alcohol and palmitic aldehyde – they were contained only in cells and were not found in the culture medium. The available various data on the hydrocarbons diffusing into the cells of microorganisms, localization of hydrocarbon-oxidizing enzymes and the resulting products leave no doubt that

hydrocarbons are oxidized intracellularly. Hence the need arises to explain the entry of water-insoluble substrate into the cell (Gottslak, 2008).

There are the following known types of transport of hydrocarbons into the cells of microorganisms:

Passive transfer:

a) simple diffusion - a non-specific flow of substances into the cell, where various compounds penetrate the cell without interacting with any carrier;
b) facilitated diffusion - a specific process in which the transferred substance reversibly binds to the carrier located in the membrane and enters the cell in the form of a substrate-protein complex;

In this case, the rate of entry of substances is equal to the rate of its release from the cell.

Both of these processes and their speed depends on the concentration of the substrate in the medium.

Active transfer: the substance enters the cell against the concentration gradient in the medium; the process requires energy and occurs with the help of specific protein-carriers (permeases).

Further restrictions are related to the solubility of the substrate in water. The substrate can enter the microbial cell either from the state of the true solution or by its direct contact with the cell.

The absorption process is defined as active transport according to the following parameters:

– specificity with respect to the substrate; on the outer surface of the membrane formed a complex carrier-substrate;
– the need for metabolic energy; the carrier has a high affinity for the substrate, if it is facing the outer surface of the membrane, and low affinity to it, if it is facing its inner surface. These changes in the carrier consume metabolic energy;
– transport of the corresponding substrate against the concentration gradient; this is due to a change in the affinity of the carrier to the substrate during the transition from outside to inside;
– release of unmodified substrate into cytoplasm (as opposite to group transfer) (Skryabin, G. K., 2008).

Only low molecular weight liquid hydrocarbons from C5 to C11, as well as some aromatic hydrocarbons, can slightly dissolve in water, higher molecular weight homologues are practically insoluble (Gottslak, 2008).

8 MICROBIOLOGICAL OXIDATION OF OIL HYDROCARBONS AND OIL PRODUCTS

Microbiological transformations of hydrocarbons are a special area because of some features of these processes. Their specificity is due to the peculiarity of hydrocarbons as chemical compounds with the maximum recovery associated with these hydrophobic properties. It turned out that the hydrophobicity of the hydrocarbon molecule is of great importance for the chemistry of microbiological oxidation of these compounds, their transport to the microbial cell, the dynamics of culture growth, their physiology, and many aspects of the processes technology associated with the use of hydrocarbon substrates.

All reactions of microbiological transformation of hydrocarbons are oxidation reaction. The limiting recovery of these substances makes it necessary for their oxidation the presence of oxygen. The hydrophobic nature of the molecule is the reason that the oxidation processes are carried out by oxygenases, in contrast to the oxidation of more hydrophilic substances that occur under the action of dehydrogenases. The hydrophobicity of hydrocarbon substrates and their poor solubility in water determine the methods of transport of substances into the cell, that was discussed above (Petrikov et. al., 2008).

A characteristic feature of the process of assimilation of hydrocarbons as a carbon source is the frequent accumulation of intermediate products in the culture medium of microorganisms growing due to such substrates (Nikulin, A., Epifancev, K. 2017).

Let us consider these processes by the example of normal paraffins oxidation. The ways of oxidation of normal paraffins by microorganisms using these compounds as sources of carbon and energy were studied in sufficient detail.

In the vast majority of cases, as a result of the primary enzymatic attack of the n-paraffin molecule, the oxidation of the terminal carbon atom occurs.

The first stable products of oxidation of hydrocarbons are primary alcohols. The next stage is the usual biological transformation of alcohol into aldehyde and aldehyde into acid. The general scheme of reaction is as follows.

R-CH2-CH3+ [O] R-CH2-CH2OH- 2H R-CH2-CHO - 2H + HOH R-CH2-COOH

The further mechanism of fatty acids assimilation, arising during hydrocarbons oxidation, proceeds by β-oxidation, which consists in successive spliting of two-carbon fragments in the form of active acetate entering the tricarboxylic acid cycle.

Further reduction of fatty acid formed as a result of microbiological oxidation of n-alkanes along with classical β-oxidation may include a number of minor products:

1) ω-hydroxylation, leading to the formation of ω - oxycarboxylic acids, and then dicarboxylic acids with further partitioning. This oxidation way has been experimentally proven in many microorganisms;
2) α-oxidation, decarboxylation, which is proven in cases where the carbon subterminal atom carries a ketogroup or hydroxyl; 3) dehydrogenation of fatty acid followed by oxidative cleavage of the double bond. The existence of this mechanism is suggested by a group of researchers (W.R. Finnerty, R.E. Kallio, 1964).

The terminal oxidation mechanism described above is not the only way to degrade n-alkanes. In some microorganisms, the oxidation of subterminal or internal carbon atoms is described, which leads to the formation of secondary alcohols and ketones. This way sometimes goes as a minor along with terminal oxidation.

H.B. Lukins and J.W. Foster (1963) found that some mycobacteria metabolize n-alkanes through methylketone with the intermediate formation of peroxide and secondary alcohol. Further oxidation of ketones has not been sufficiently studied. In the experiments of J.R. Vestal and J.J. Perry (1969) Brevibacterium sp. was oxidized propane through acetone with subsequent attack on the terminal methyl and decarboxylation:

CH3CH2CH3 → CH3CHOHCH3 → CH3COCH3 → CH3COCH2OH → CH3COOH

Based on the works of F.W. Forney and A.J. Markovetz (1970) the degradation of tridecane by culture of Pseudomonas aeruginosa appears to be as follows:

CH3(CH2)11CH3→ CH3(CH2)10CHOHCH3→ CH3(CH2)10COCH3→
CH3(CH2)9CH2OCOCH3→
CH3(CH2)9CH2OH + CH3COOH
↓
CH3(CH2)9COOH

9 BIOGENIC OXIDATION OF OILS OF DIFFERENT CHEMICAL COMPOSITION

In the process of oil oxidation, the mutual influence of hydrocarbon and non-hydrocarbon components included in its composition plays an important role (Khotimskii et. al., 1970).

With anaerobic and aerobic microbial destruction, regardless of the type of oil, their density increases, the content of resinous-asphaltene compounds, sulfur increases and the concentration of paraffin hydrocarbons in the system decreases. The residual accumulation of naphthenic hydrocarbons was noticed (Bruheim et al., 1998).

Reduction of paraffin potential of oils in biochemical oxidation is due to the removal of model systems of n-alkanes as substances mainly consumed by microorganisms. Among n-alkanes, bacteria are better able to absorb low molecular weight compounds, which has

Table 1. The classification of the components of the oils according to their capacity to biodegradation.

Group	Attitude to the microorganism effects	Degree of biodegradation, % to the original content	Oil components
I	Highly sensitive	80-100	n-alkanes; isoalkane
II	Sensitive	60-80	cycloalkanes with 6, 1, 5 and 2 rings; s-aromatics; monoaromatic
III	Moderately sensitive	45-60	cycloalkanes with 3 and 4 rings; three aromatic hydrocarbons
IV	Resistant	30-45	tetra-aromatic hydrocarbons; sterane; triterpene; naphtene aromatic hydrocarbons
V	Highly resistant	0-30	pentha-aromatic hydrocarbons; asphaltenes; resins

been proven on the range of C14 to C20 hydrocarbons. In addition, no selectivity has been found in the biooxidation of hydrocarbons with an even or uneven number of C atoms in the molecule (Bruheim et al., 1998).

From the physiological characteristics of each kind of microorganisms depends on the direction of the process of destruction of individual hydrocarbons and their mixtures with different degrees of resistance to oxidation (Table 1).

The above-mentioned, undoubtedly complicates obtaining unambiguous results of research of predictability of transformation of various classes of oils. However, oil microbiology has research works, in the results of which can be traced geochemical changes in the composition of oils during biodegradation.

In 1960-1970-ies in "VNIGRI" JSC under the guidance of doctor of biological sciences T. L. Simakova were conducted long-term comprehensive studies of the change pecularities of different chemical composition of oils, some of their fractions and individual hydrocarbons in

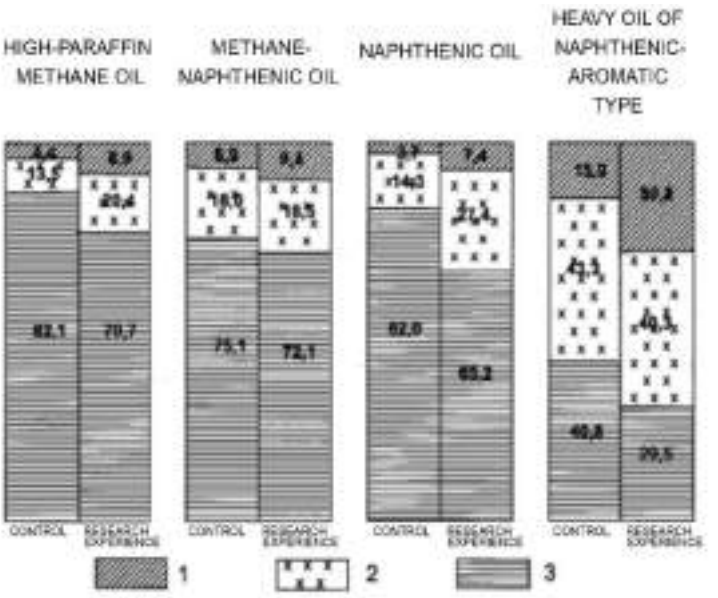

Figure 2. Changes of the chemical group composition of oils under the influence of biogenic factor.
1 — asphalt-resinous components; 2 — aromatic hydrocarbons; 3 — methane and naphthenic hydrocarbons.

biodegradation. Biocenoses of microorganisms were isolated from formation waters of the same wells, from which oil was selected for experiments.

As a result of these studies on a large factual material, it was shown that as a result of biogenic oxidation in aerobic conditions, there are significant changes in the group hydrocarbon composition of oils, leading to the transition of one geochemical type of oil to another (Skryabin, G. K., 2008)., (Figure 2).

The authors came to the following main conclusions (Khotimskii et. al., 1970):

- High-paraffin methane oil under the influence of microorganisms becomes heavier, its viscosity and the content of asphalt-resinous substances increase, the content of solid paraffins decreases. In the group hydrocarbon composition, it is redistributed in the content of separate groups of hydrocarbons with a decrease in the amount of methane (normal and isostructure), as well as aromatic hydrocarbons that are part of the kerosene fractions. The total content of naphthenic and aromatic hydrocarbons in oil as a whole increase. Thus, methane oils under the influence of the biogenic factor change with the approach to the methane-naphthenic type.
- Methane-naphthenic oil type under the influence of the biogenic factor changes in the same direction, as a result of which it is weighted, it also increases the content of asphalt-resinous substances, the number of saponification due to the ethereal number and the number of solid paraffins decreases. Its hydrocarbon composition changes, as in methane oil, with a decrease in the amount of methane hydrocarbons and aromatic hydrocarbons, but the last one is only in kerosene fractions. In general, methane-naphthenic oils change with increasing content of naphthenic and aromatic hydrocarbons in their composition.
- Naphthenic oil type with a high content of naphthenic hydrocarbons under conditions of biogenic oxidation changes with increasing specific gravity, viscosity, content of asphalt-resinous components and acid number in oils. Its hydrocarbon composition reduces the content of methane and naphthenic hydrocarbons. In contrast to the above types of oils, the amount of aromatic hydrocarbons included in the composition of kerosene fractions increases. Thus, as a result of the vital activity of microorganisms, the oxidation of naphthenic oil is accompanied by an increase in its aromatic fraction and a decrease in methane and naphthenic hydrocarbons.
- Oxidation of heavy oil of naphthenic-aromatic type is accompanied by its tarring with a significant increase in specific gravity and viscosity. Unlike other types of oils studied by the authors, as a result of biogenic oxidation in oils of naphthenic-aromatic oil, both acid and ethereal number increases. The hydrocarbon composition of this oil reduces the content of all groups of hydrocarbons: methane, naphthenic and aromatic — by increasing the asphalt-resinous components.

According to the above, during biodegradation of the studied types of oils in their group composition, there are serious changes: the relative content of the asphalt—resinous components increase in 1.4-2 times, aromatic hydrocarbons increases in 1.02-1.9 times (the exception is naphthene-aromatic oil). The relative content of methane and methane-naphthenic hydrocarbons, compared with the control, is reduced in 0.12—1.4 times.

Changes in the group composition of oils should be taken into account in the development of technology for cleaning soils from oil pollution.

The practical help of oil microbiology in solving this problem is the allocation of pure cultures of hydrocarbon-oxidizing microorganisms, the establishing of their origin and the degree of activity in the oxidation of oils and oil products.

The most active strains of hydrocarbon-oxidizing microorganisms, oxidizing to a large extent resistant to biodegradation components of oil, are the most promising for the creation on their basis of biological products for soil purification from oil pollutant.

The study of the ability of microorganisms to oxidize specific classes of hydrocarbons in the composition of oils, as shown above, allows to create biological products for the purpose in the future.

10 LABORATORY RESEARCH ABOUT OIL BIODEGRADATION BY STRAINS OF HYDROCARBON-OXIDIZING MICROORGANISMS

In the study of oil utilization activity, as noted above, 9 strains of HOM were involved in laboratory experiments. Series of experiments with oil was carried out at a temperature of 280C on the laboratory shaker for 12 days. This regime was conditioned by the time frame for research. Extraction conditions of post-experimental samples differed from the conditions for pre- experimental samples. Chloroform, as in post-experimental samples with diesel fuel, extracted residual oil and culture medium (containing microbial mass and intermediate products of bio-oxidation of oil). Then the chloroform extracts were combined and on full complex chemical bitumen analysis the total extract was coming, chloroform bitumoid (CHB), which is actually not recycled oil and the residual products of its oxidation. This allowed without preliminary calculations to immediately assess the loss of oil as a whole and its individual fractions, which, in fact, is provided by the objectives of the planned research (Nikulin et al., 2017).

Consideration of the results of the analysis of CHBDF and CHBCM of bio-oxidized diesel fuel showed that these data are of interest from the point of view of the physiology study of hydrocarbon-oxidizing microorganisms, the study of this direction is out of this research topic (Saitgaleev et al., 2019).

The selected mode of laboratory experiments and analytical data on oil utilization allow us to compare the tested strains of HOM on the ability to oil dispose under specified conditions and select the most active.

The main parameters of experiments on oil utilization by the studied strains: a charge of oil is 1.45–2.02 g/100 ml, or 14500-202000 mg/l. This is a fairly high oil contamination. HOM is in the range of (0.80-5.30) 108 cells/ml. After 12 days in post-experimental samples the pH of the culture medium remained at pre-experimental level or increased to 7.5 - 8.0. Decrease of pH was not recorded (Sukplanga et al., 1999).

Table 2 shows the change in qualitative composition of crude oil in post-experimental samples of studying the activity of utilization of the tested strains of HOM. As it follows from the table, there were some changes in the qualitative composition of oils within 12 days. In the initial experiments samples the content of oils was 69.98%. In the post-experimental samples the oil content varies from 63.76 to 70.67%, that is, in the qualitative composition of the post-experimental samples there is a decrease in the oil content (7 strains of HOM), and its increase (2 strains – 1-R and 99-T).

Table 2. Changes in oil composition (% rel.) in experiments on the study of the biodegradation activity of hydrocarbon-oxidizing microorganisms (the duration of experiments is 12 days).

	Group composition of bitumoid, %				Hydrocarbons oils composition, %					
						Aromatic hydrocarbons			$\frac{\text{Sat. HC}}{\text{Ar HC}}$	
Strain HOM in experiments	oils	benz. resins	sp./ benz. resins	asphaltene	saturated hydrocarbons	Ar I	Ar II	poly-Ar		HOM type
Initial oil	69,98	14,08	11,80	4,14	50,76	17,52	21,15	10,57	1,03	-
4-D	67,59	13,92	13,12	5,37	51,51	20,61	18,79	9,09	1,06	*Pseudomonas*
12-R	63,76	14,34	16,86	5,04	50,46	20,31	24,00	5,23	1,02	*Pseudomonas*
1-KP	68,66	13,57	12,38	5,39	54,71	12,76	28,27	4,26	1,21	*Rhodococcus*
1-R	70,65	11,96	13,04	4,35	47,63	23,66	14,20	14,51	0,91	*Pseudomonas*
2-V	69,40	13,80	11,40	5,40	51,34	19,76	16,22	12,68	1,05	*Pseudomonas*
99-T	70,67	11,81	13,19	4,33	47,73	22,16	17,04	13,07	0,91	*Pseudomonas*
4-G	66,14	13,94	13,35	6,57	48,15	25,00	16,36	10,49	0,93	*Mycobacterium*
1-SH	67,00	14,80	13,60	4,60	55,38	16,31	15,69	12,62	1,24	*Mycobacterium*
48-U	65,88	15,58	14,40	4,14	50,90	22,75	19,16	7,19	1,04	*Pseudomonas*

Similar changes occurred in the content of other fractions of post-experimental bitumoids, comparing with the original oil. It is almost impossible to make a certain predictability in the change of oils during biodegradation based on the results of the study of the qualitative composition (Nikulin et al., 2017).

Somewhat greater certainty in the characteristic of this process makes the ratio of saturated hydrocarbons to aromatic hydrocarbons. According to the deviation of the value of this ratio, comparing with that in the original oil, the tested strains can be divided into two groups. In case of oil biodegradation by one group of strains, the value of this ratio, in comparison with the original oil, it decreases, and in case of destruction by another group of strains – it increases (Dashko et al., 2016).

It is possible to evaluate and compare the activity of the tested strains of HOM only after carrying out the balance calculations of the processes of utilization in the conditions of laboratory experiments with oil and its specific fractions. Remaining oil in every experience and qualitative composition of post-experimental samples allowed to make balance calculations of the process of oil utilization by tested strains and to find loss of oil in whole and in its separate fractions in the weight % relatively to the content of their source in the sample (Table 3).

According to the table, oil losses in these experiments are 1.4-73.4% of its original components. The loss of specific fractions in the composition of the oil is the following: oil 5.0 to 75.8%, benzene resin 2.4-72.9%, alcohol benzene resin 9.0-62.0%, asphaltenes 17.0-67.6%. There were losses in the fractional composition of oils: the content of saturated hydrocarbons decreased by 2.8 – 75.9%, Ar I - 12.8 – 71.9%, Ar II - 14.1 – 72.5%, poly Ar - 1.0-88.0% relative to their initial content (Dashko et al., 2016).

The following fact is noteworthy. During oil biodegradation in the specified conditions of the experiments, a significant formation of intermediate products was recorded, which, according to their chemical characteristics, were analytically established in the fractions of oils (strain 1-R), resins and asphaltenes of the group composition of CHB and in the fractions of saturated hydrocarbons (strains 1-KP and 1-SH) and aromatic hydrocarbons in the oils. In the post-experimental samples of strains 48-U and 1-R the amount of remaining oil exceeds the initial sample weight.

Additionally, the calculations of oil losses in whole and oils fractions (strain 99-T) excluding new formations were carried out. In this case, as shown by calculations, the losses during the experiments of oil in whole and oil fractions increased. Based on the results of the study of the

Table 3. Loss of oil in experiments on the biodegration activity of hydrocarbon-oxidizing microorganisms (the duration of experiments is 12 days).

	Loss, weight % relative to the specific initial oil fraction									
						In oils				
Strain HOM	Oil in whole	Oils	benz. cm.	sp/ benz. cm.	Asph.	HC	Ar I	Ar II	poly Ar	HOM type
12-R	73,4	75,8	72,9	62,0	67,6	75,9	71,9	72,5	88,0	*Pseud.*
99-T	20,7	19,9/20,2	33,5	11,4	17,0	24,7	+ 1,3	35,5	1,0	*Pseud.*
4-D	5,6/7,1	8,9/10,1	6,7	+ 5,0	+22,5	7,5	+ 7,2	19,0	21,6	*Pseud.*
2-V	5,8/6,8	6,6/8,8	7,7	9,0	+22,9	5.6	+ 5,2	28,4	+11,9	*Pseud.*
1-SH	2,1/4,4	6,3/8,7	+ 2.9	+12,8	+8,7	+2.2	12,8	30,5	+11,9	*Myc.*
1-KP	3,1/4,4	5,0	6,7	+1,6	+26,2	+2,4	30,8	+27,0	61,7	*Rhod.*
4-G	1,4/5,1	6,8	2,4	+11,5	+56,5	11,6	+32,9	28,0	7,6	*Myc.*
48-U	±0,7/3,7	5,2	+11,4	+22,9	+,07	5,0	+23,1	14,1	25,5	*Pseud.*
1-R	±2,3/4,4	±3,6/11,4	12,9	+13,3	+7,8	2,8	+39,8	30,5	+42,2	*Pseud.*

activity of oil utilization in laboratory experiments, the most active strain is 12-R, the strain 99-T is noticeably worse in activity (Kotiukov et al., 2019).

Other tested strains did not show their activity in these experiment conditions. Disposal of oil in whole it amounted to 3.7-7.1%, oils 5.0 to 10.1 per cent (excluding new formations). But these strains showed quite high activity in the utilization of aromatic hydrocarbons in oils (up to 61.7% - strain 1-KP).

11 CONCLUSIONS

The degree of biodegradation of oil is evaluated by balance calculations under laboratory experiments. According to calculations, in general utilization makes 56.6 and 71.6%. Utilization of separate fractions of oil pollutant exceeds 80-90%. The theoretical substantiation of activity of hydrocarbon-oxidizing strains of microorganisms on utilization of oil and oil products is given.

REFERENCES

Bruheim P., Eimhjellen K. Chemically emulsified crude oil as substrate for bacterial oxidation: differences in species response // Canadian Journal of Microbiology. - 1998. -Vol. 44(2). - p. 195–204.

Dashko, R., Karpova, Y. Engineering geology and geotechnics of fractured clays as building base and surrounding medium (by the example as clayey bedrocks in Saint-Petersburg) (2016) *International Multidisciplinary Scientific GeoConference Surveying Geology and Mining Ecology Management, SGEM*, 3, pp. 85–92.

Dashko, R. E., Kotiukov, P.V. Fractured clay rocks as a surrounding medium of underground structures: The features of geotechnical and hydrogeological assessment (2018) *Geomechanics and Geodynamics of Rock Masses*, 1, pp. 241–248.

Nikulin, A., Nikulina, A.Y. 2017. Assessment of occupational health and safety effectiveness at a mining company. Ecology, Environment and Conservation, 23(1), pp. 351–355.

P. V. Kotiukov, I. Yu. Lange, Engineering Geological Analysis of the Landslide Causes During the Construction of Industrial Building, *International Journal of Civil Engineering and Technology* 10(4), 2019, pp. 316–323. http://www.iaeme.com/IJCIET/issues.asp?JType=IJCIET&VType=10&IType=4

Rueter P., Rabus R., Wilkest H., Aeckersberg F., Rainey Fred A., Holger W. Anaerobic oxidation of hydrocarbons in crude oil by new types of sulphate-reducing bacteria//Nature. - 1994. -Vol. 372. - p. 455–458.

Saitgaleev, M., Senchina, N., Sokolova, J. 2019. Application of the method of ion-selective electrodes in exploration work on the sea shelf. Marine Technologies 2019, Gelendzhik. DOI: 10.3997/2214-4609.201901811

Sukplanga P., Thongmeea A., Velaa G. Roland. Degradation of Linseed Oil Vapors by Soil Bacteria in Trickling Biofilters / / Bioremediation Journal. - 1999. -Vol. 3. - p. 189–200.

The study of the survival of microorganisms-oil destructors of Pseudomonas and Rhodococcus with different storage methods

K. V. Petrikov, T. V. Yakshina, E. P. Vlasova, etc. // Materials of worldwide conference “Current state and prospects of Microbiology and biotechnology”. Minsk, June 2-6, 2008. 223–225 pp.

Advances in Raw Material Industries for Sustainable Development Goals – Litvinenko (Ed)
© 2021 Taylor & Francis Group, London, ISBN 978-0-367-75881-3

The secondary dispersion halos of platinum group elements and rare elements in rocks of the Vysotsky ore occurrence, Svetloborsky massif, Middle Urals

V.S. Nikiforova
Engineer, Department of geology of oil and gas, Saint Petersburg, Mining University, Saint Petersburg, Russia

I.V. Talovina
Professor, Head of the Hystorical and dynamic geology department, Mining University, Saint-Petersburg, Russia

G. Heide
Professor, Institutsdirektor, Technische Universität Bergakademie Freiberg, Freiberg, Germany

ABSTRACT: Geological searches for secondary dispersion halos have important practical search value in areas with lack of exposure. In weakly exposed areas with a loose cover thickness of 0.2-10 m, testing is carried out using secondary dispersion halos - i.e. on the surface of eluvium, deluvium or the bottoms of a loose incision. The Svetloborsky dunite-clinopyroxenite zonal massif, like other massifs of the Ural Platinum belt, is characterized by a rather closed inaccessible territory, partially covered by a cover of quaternary sediments with a thickness of up to 10 m, in some areas - up to 25 m. Also, almost complete absence of chromite schlieres is characteristic of the Svetloborsky massif, which are usually a clear visual sign of the presence of platinum-metal mineralization. Therefore, when conducting search operations within the massif, in addition to direct ore testing of bedrock and weathering crust, a lithogeochemical survey was carried out and the contents of platinum, palladium, gold and rare elements in secondary dispersion halos were determined.

Keywords: secondary dispersion halos, platinum group elements, rare elements, lithogeochemical survey, dunite, vein rocks, the Svetloborsky massif, the Ural Platinum belt

1 INTRODUCTION

The territory of the Svetloborsky massif is almost completely covered by a continuous cover of quaternary sediments, the thickness of which is 2-10 m, and in some areas the weathering crusts of dunites up to 25 m thick are developed, which greatly complicates the exploration work. In addition, the dunites of the massif are characterized by an almost complete absence of chromite schlieres, which are in other massifs of the Platinum belt of the Urals, for example, in Nizhny Tagil massif, a clear visual sign of the presence of platinum metal mineralization (Ivanov, 1997). Therefore, in addition to direct ore testing of bedrock, on the territory of the Svetloborsky massif, a lithogeochemical survey was carried out for the first time for the platinum-bearing mineralization of the Urals for the search for radical platinum-ore mineralization, according to the results of which the mineralized occurrence zone of Vysotsky was identified (Tolstykh et al., 2011, 2015).

Lithogeochemical work on the Svetloborsky massif was carried out by CJSC Ural-MPG in the period 2006-2009 in order to determine the contents of platinum, palladium, gold and a number of related elements, testing was carried out on a exploration network.

2 METHODOLOGY

Within the central part of the Svetloborsky massif lithogeochemical survey using secondary halos showed only isolated abnormal samples, so it was necessary to identify anomalies extension exploration network and a re-sampling. In the central part of the Svetloborsky massif, the processes of recrystallization of dunites are developed, so the chromite formations and platinum are distributed extremely unevenly, therefore, lithogeochemistry can be effective only with a frequent sampling network.

During sampling, loose clay and sand-clay eluvial-deluvial material was selected from a subsoil layer weighing 200-300 g along a 200 × 40 m network with a network thickening in separate, most abnormal areas, to a cell size of 100 × 40 m. Separate profiles laid at a distance of 400 m from each other, they cross the massif, capturing not only the dunites of the massif core, but also the clinopyroxenites of the massif shell (Nikiforova et al., 2016).

During lithogeochemical survey, 1163 samples were obtained, of which 171 were taken directly at the Vysotsky ore occurrence. The sample processing process included drying the sampled material, sifting through an 80 mesh sieve, attritioning to 0.074 mm, quarrying of the sample to obtain two batches weighing about 100-150 g. These samples were analyzed for the content of Pt, Pd, Au by an assay in a Lakefield laboratory (South Africa) and spectral analysis for a number of rare elements in OJSC Ural Central Laboratory. In interpreting the sampling data for secondary halos for a more detailed study, the Vysotsky ore occurrence site was selected, characterized by the wide development of dike and vein rocks.

Processing and interpretation of the initial geochemical data was carried out by methods of mathematical statistics using modern software, including the programs Statistica 12.6 and Surfer 15.0. The data obtained as a result of the analyzes were used to study the distribution characteristics of precious metals and rare elements in eluvial and deluvial-eluvial deposits.

3 RESULTS AND DISCUSSION

Table 1 presents the average contents of Pt, Pd, Au and rare elements in eluvial and deluvial-eluvial deposits in comparison with the geochemical background calculated for the Svetloborsky massif. The geochemical background was calculated from 848 analyzes; the background concentrations of chemical elements were calculated as median values in the sample.

According to Table 1, for the eluvial and deluvial-eluvial deposits of the Vysotsky ore occurrence, elevated levels of platinum, palladium, chromium, manganese, nickel are characteristic, lower - barium, strontium and phosphorus, the content of other chemical elements (silver, cobalt, vanadium, titanium, copper, zinc, lead in the secondary halos of the Vysotsky ore occurrence are comparable with the geochemical background calculated for the Svetloborsky massif.

Among the group of precious metals, platinum has a maximum average content of 0.5 ppm, palladium - 0.08 ppm and gold - 0.06 ppm. The Pt/Pd ratio varies from 2 to 15, in some cases reaching 30-50, which is quite comparable with the data on the primary dunites of the Svetloborsky massif.

Most of the elements of the iron group are characterized by a relatively uniform distribution. Nickel contents vary from 7 to 150 ppm, cobalt from 2 to 70 ppm, manganese 70-600 ppm, with

Table 1. Average contents of Pt, Pd, Au and rare elements in eluvial and deluvial-eluvial deposits of the Vysotsky ore occurrence, ppm.

Element	Pt	Pd	Au	Ag	Cr	Mn	Ni	Co	V	Ti	Zn	Ba	Sr	Pb
Vysotsky ore occurrence	0,05	0,01	<0,02	0,01	600	250	60	10	17	600	7	50	1	0,9
Geochemical background	0,03	<0,02	<0,02	0,01	500	180	30	9	18	600	9	65	10	1

the exception of several samples with contents of 700-900 ppm, vanadium 18-50 ppm, in single samples - more than 200 ppm. Chromium in samples from Vysotsky ore occurrence is characterized by a less uniform distribution with a change in contents from 30 to 1000 ppm, on average 600 ppm. It should be noted that, unlike the whole array, samples with high chromium content do not always correspond to samples with high platinum content. Cobalt content also varies from 2 to 70 ppm, titanium - from 60 to 1000 ppm. Cobalt content also varies from 2 to 70 ppm, titanium - from 60 to 1000 ppm.

Transit elements in the eluvial-deluvial deposits of the Svetloborsky massif are characterized by an uneven distribution. Copper and phosphorus are contained in the initial samples in an amount of from 0.1 to 18 ppm and from 7 to 180 ppm, respectively. Lead and zinc are characterized by maximums of 4 and 20 ppm. The analyzed large-ion lithophilic elements reach maxima of 100 ppm (barium) and 60 ppm (strontium).

Based on the calculation results for all the studied chemical elements, maps were constructed with the image of the positive and negative anomalies of the element contents (Figures 1-4). Maps of anomalies of elements within the entire Svetloborsky massif are presented in (Gayfutdinova et al. 2015), and in this work refined detailed maps of

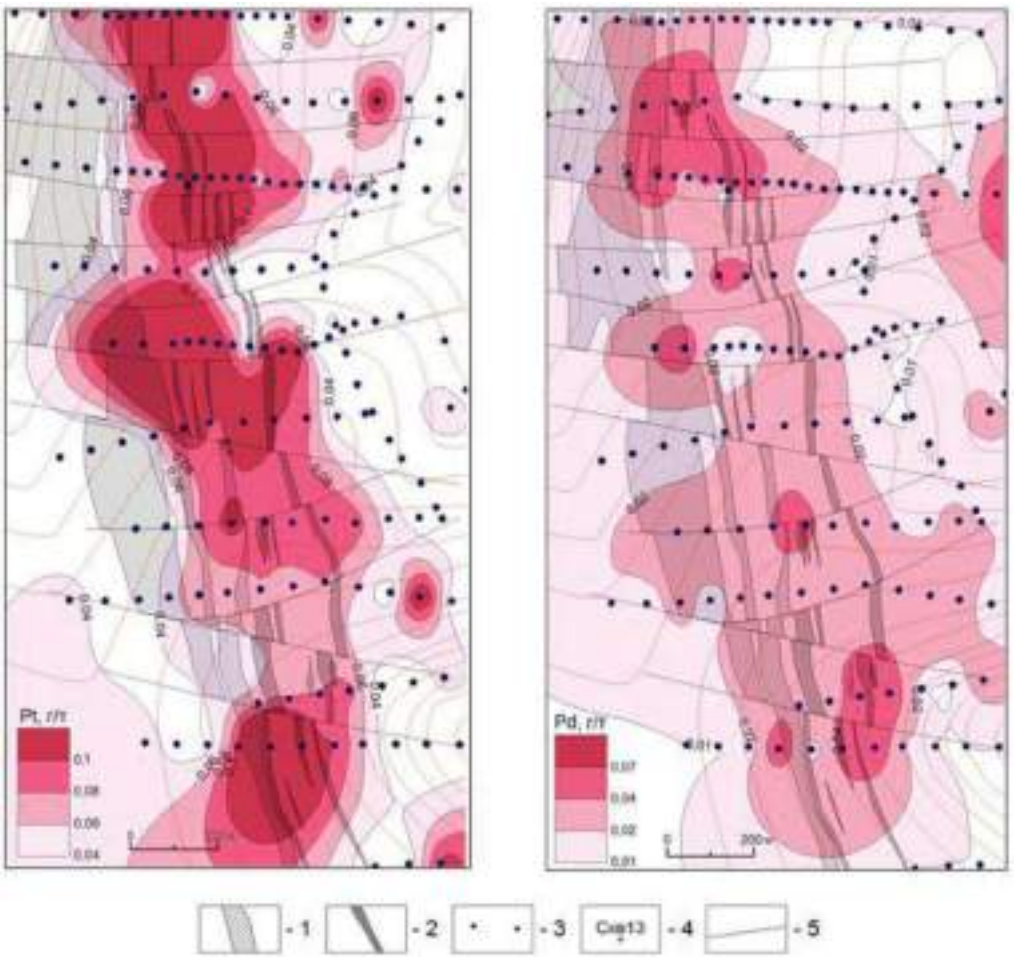

Figure 1. Secondary halos of dispersion of platinum and palladium.
1 - clinopyroxenite shell, 2 - hornblendite and diopside rock dikes, 3 - sampling points, 4 - wells, 5 - tectonic disturbances.

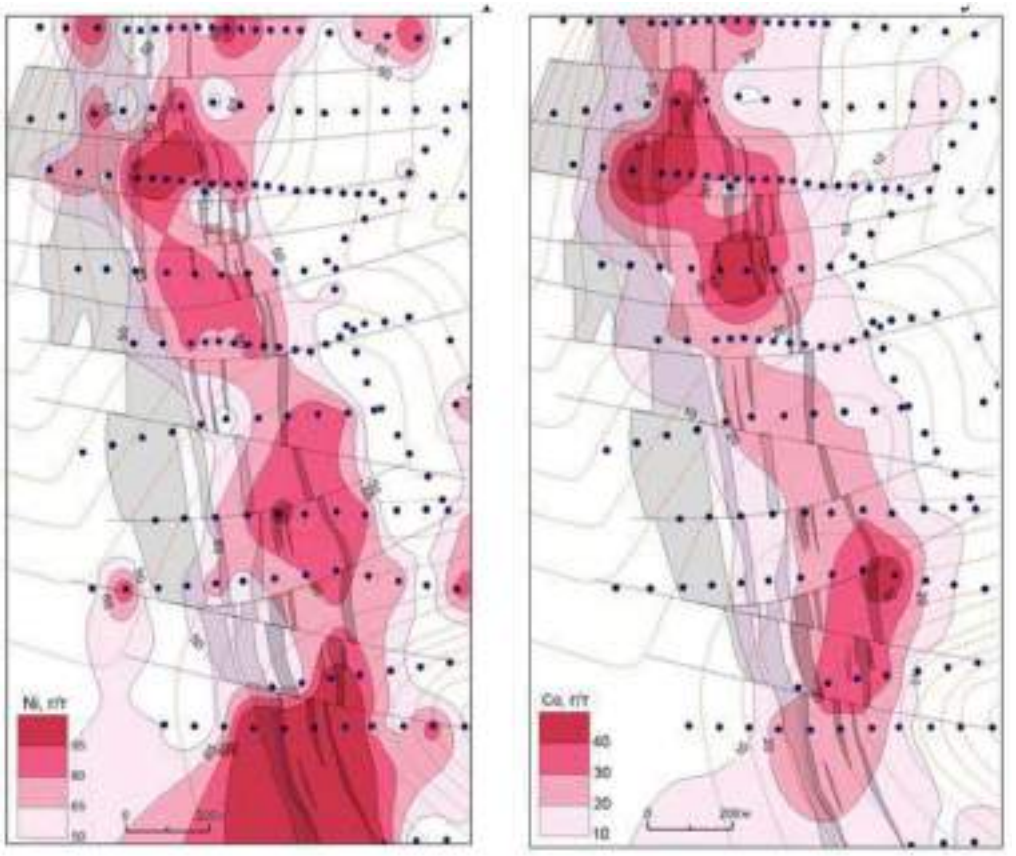

Figure 2. Secondary halos of dispersion of nickel and cobalt.

anomalies within the western contact of the massif, to which the Vysotsky ore occurrence is confined, are given.

3.1 *Platinum and palladium*

Within the Vysotsky ore occurrence platinum and palladium in secondary halos, several closely related positive elongated anomalies form (Figure 1).

The length of the platinum and palladium anomalies is from 400 to 900 m, with an average width of about 400 m. The platinum and palladium contents within the northern and southern positive anomalies exceed 0.23 ppm 0.04 ppm, respectively, which is higher than the platinum and palladium in anomalies within the entire array.

As was shown by us in (Gayfutdinova et al. 2015), the platinum anomalies are generally confined to the western boundary of the dunite core of the massif in the zone of contact with the clinopyroxenite shell in the region of development of recrystallized medium- and coarse-grained dunites of the core center and fine-grained peripheral dunites. The construction of anomaly maps on the scale of Vysotsky's ore occurrence also revealed the spatial confinement of platinum and palladium anomalies to the areas of development of vein hornblendites and diopsides and their conformity to each other.

Despite the fact that the level of platinum content in scattering halos is relatively low, the shape of the anomalies and their confinement to the fields of development of dyke rocks, as well as to certain petrographic varieties of primary dunites, suggests a regular nature of their

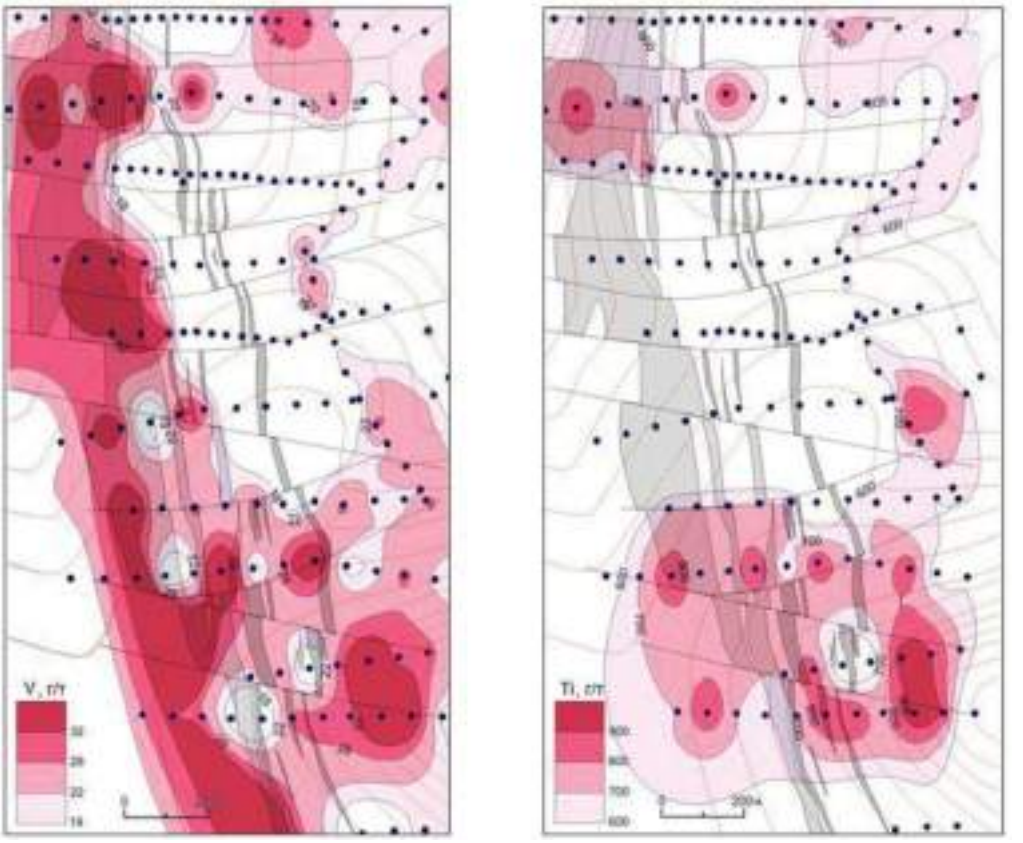

Figure 3. Secondary halos of dispersion of vanadium and titanium.

distribution, which is directly related to increased concentrations of platinum in the occurring under abnormalities of bedrock.

3.2 *Nickel and cobalt*

Among other rare elements, nickel and cobalt are distinguished by increased concentrations and contrasting anomalies (Figure 2). The positive anomalies of nickel and cobalt are partially spatially combined with the anomalies of platinum, but they are more widespread, while the promising positive anomalies of platinum (> 0.1 ppm) are characterized by a clear spatial confinement to the zones of vein rock development in the dunites of the Vysotsky ore occurrence.

A positive chromium anomaly is observed throughout the entire area of the ore occurrence, extending over more than 1.5 km in length with an average width of 400 m.

Anomalies of manganese within the Vysotsky ore occurrence are weakly manifested and small in size (no more than 300 m in width and 200 to 400 m in length), all observed anomalies are elongated in the submeridional direction. In the northern part of the ore occurrence, several close anomalies are observed (Pilyugin et al., 2015).

3.3 *Vanadium and titanium*

Vanadium and titanium (Figure 3) is characterized by positive anomalies elongated in the submeridional direction. The association of the positive anomalies of vanadium to the

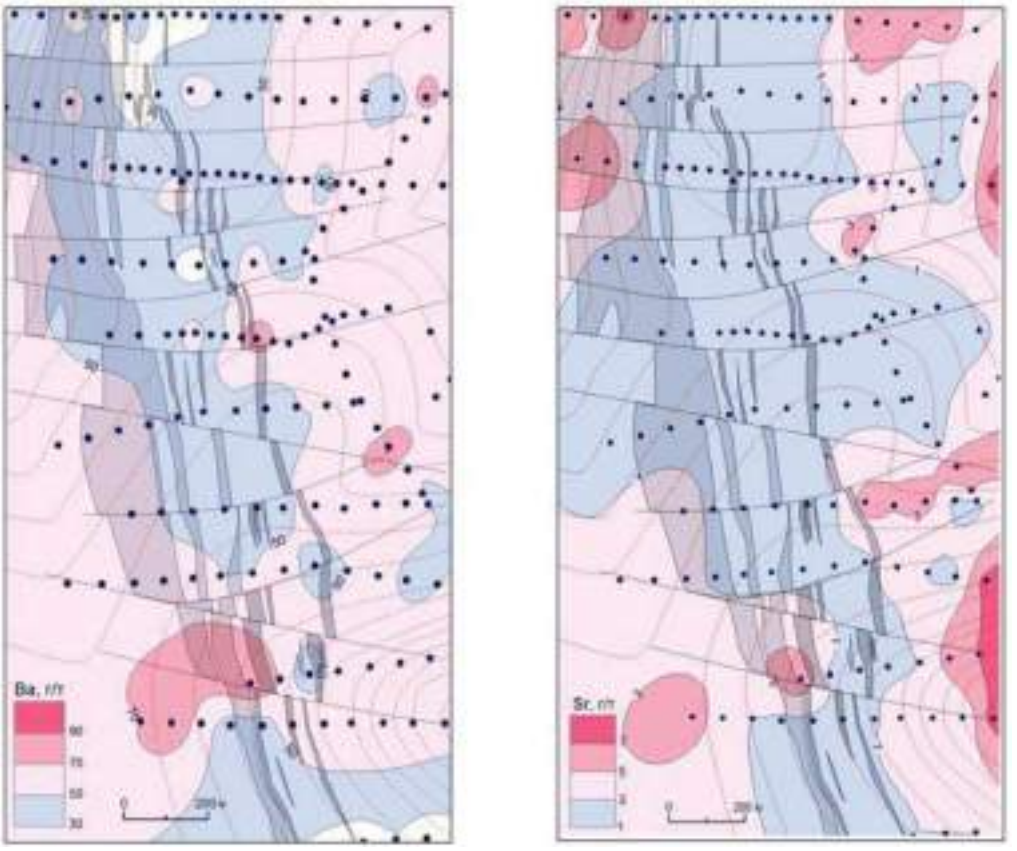

Figure 4. Secondary halos of dispersion of barium and strontium.

clinopyroxenite shell of the massif is noted, which is explained by the presence of vanadium in the composition of clinopyroxene (Lazarenkov et al., 2013).

Within the dunite core of the massif, the vanadium anomalies are less pronounced in the ore occurrence contour of the Vysotsky anomaly, but their confinement to dypsidite and gornblendite dikes is also noted.

3.4 *Barium and strontium*

Negative anomalies of barium and strontium spatially coincide with positive anomalies of platinum (Figure 4). Anomalies of barium are elongated in the submeridional direction, while there is a clear confinement of these anomalies to dikes of gornblendites and diopsides, but the reason for this is most likely the confinement of these concentrations to thick carbonate veins in the weathering crust of dunites, which in turn are confined to fracture zones at contacts by the rocks.

Negative anomalies of strontium are characterized by wider halos, while they are more manifested in the northern and central parts of the Vysotsky ore occurrence site.

Thus, in secondary scattering halos within the Vysotsky ore occurrence, positive anomalies of chromium, manganese, nickel and cobalt and negative anomalies of barium and strontium spatially coincide with positive anomalies of platinum and palladium. Anomalies of phosphorus, copper, zinc, lead and silver are less informative and cannot be used for search purposes. On the whole, the presence of sufficiently contrasting anomalies of chromium, manganese, nickel, and cobalt superimposed on each other allows us to recommend

lithogeochemical surveys to refine, identify and predict the indigenous platinum mineralization within the Svetloborsky massif, as well as other poorly studied massifs of the Ural Platinum belt with the known the number of dike and vein rocks, such as Veresovoborsky, Kamenushinsky and others massifs.

To clarify the relationships between platinum and individual rare elements in the eluvial-deluvial deposits of the Svetloborsky massif for samples taken at the Vysotsky ore occurrence, we performed statistical processing of the data obtained, including correlation analysis and factor analysis using the principal component method. The source data array consists of 171 samples. When statistical processing of the results of testing with the contents of chemical elements in samples below the detection limit of the device were replaced by 1/2 the detection limit. Since the contents of chemical elements are distributed lognormally, the prologarithmic values of the contents of elements were used for statistical analysis.

Based on the analysis of the matrix of correlation coefficients (r = 0.16, 95% probability, 171 samples), the following conclusions can be drawn about the relationship between the contents of chemical elements in the secondary dispersion halos of the Vysotsky ore occurrence:

- platinum has significant positive correlation coefficients with palladium, chromium, manganese, nickel and cobalt and significant negative correlation with silver and barium;
- palladium, unlike platinum, has positive correlation with only chromium (r = 0.18), nickel (r = 0.36), cobalt (r = 0.55) and negative with silver (r = -0.25)

Factor analysis carried out according to the logarithms of the contents of chemical elements in the overlying loose sediment massif allowed us to identify several elemental associations. Based on the results of factor analysis, we determined the main components of the indicator values, which were determined by the action of a particular factor, or a combination of both.

4 CONCLUSIONS

According to lithogeochemical surveys, the spatial distribution of anomalies of platinum and other rare metals, according to the results of correlation and factor analysis, the most informative from the point of view of searches for anomalies of platinum metals are data on Cr, Ni, Co, Mn, which can be considered indicator elements platinum-metal mineralization in eluvial-deluvial deposits of the Svetloborsky massif.

Thus, lithogeochemical surveys using secondary scattering halos are appropriate and can be recommended for other poorly studied massifs of the Platinum belt of the Urals with a developed platinum-dunite type of platinum-metal mineralization, for example, for Veresoborsky and Kamenushinskymassifs located a short distance from Svetloborsky massif.

The presence of secondary aureoles of platinum dispersion in the eluvial-deluvial deposits of the Svetloborsky massif serves as a reliable search sign of the indigenous platinum-metal mineralization.

1. Noble metal specialization in eluvial and deluvial-eluvial cover deposits monometallic platinum, inherited from indigenous sources.
2. In secondary scattering halos, the following associations of elements were distinguished: characteristic of dunites - Pt, Pd, Cr, Ni, Co, Mn, and characteristic of vein rocks - V, Ti, Cu, Zn, Pb, Ba, Sr.
3. It is noteworthy that the anomalies of individual elements are clearly confined to the areas of development of vein hornblendites and diopside rocks of the massif, as well as the anomalies of the elements themselves overlapping each other: within the Vysotsky ore occurrence, the positive anomalies of platinum and palladium spatially coincide with the positive anomalies of chromium, manganese, nickel and cobalt, as well as with negative anomalies of barium and strontium. Moreover, platinum has an average positive correlation coefficient with chromium, which indicates that platinum is associated not only with the platinum-chromite type of mineralization, but also with others.

4. Peculiarities of the distribution of elements found in the secondary halo identified within the Vysotsky ore occurrence can be used in searches for platinum ore occurrences both within the Svetloborsky massif itself and in other zonal clinopyroxenite-dunite massifs of the Platinum-bearing belt of the Urals.

REFERENCES

Gayfutdinova A.M., Telegin Yu.M., & Talovina I.V. 2015. Secondary dispersion halos of platinum group elements, gold and silver of the Svetloborsky dunite-clinopyroxenite massif, Platinum Belt of the Urals. *Mining informational and analytical bulletin* (1): 312–318.

Ivanov O.K. 1997. *Concentrically-zoned pyroxenite-dunite massifs of the Urals*, Ekaterinburg.

Lazarenkov V.G., Pilugin A.G., Vorontsova N.I. & Talovina I.V. 2013. Rare earth elements in platinum bearing vein chromitites of Nizhni Tagil pyroxenite-dunite massif, Central Urals. *Zapiski Gornogo instituta* (200): 222–225.

Nikiforova V.S., Vorontsova N.I., Duryagina A.M. & Talovina I.V. 2016. Vein rocks of the Svetloborsky massif and their petrochemical characteristics. *Mining informational and analytical bulletin* (2): 236–243.

Nikiforova V.S., Duryagina A.M., Telegin Yu.M. & Talovina I.V. 2016. Rare elements in veined rocks of the Svetloborsky dunite-clinopyroxenite massif of the Ural Platinum Belt. *Mining informational and analytical bulletin* (2): 244–252.

Pilyugin A.G., Talovina I.V., Duryagina A.M. & Nikiforova V.S. 2015. Geochemical features of platinum-bearing dunites of the Svetloborsky and Nizhny Tagil massifs of the Ural Platinum Belt. *Zapiski Gornogo instituta* (212): 50–61.

Tolstykh N.D, Kozlov A.P., Telegin Yu.M. 2015. Platinum mineralization of the Svetly bor and Nizhny Tagil intrusions, Ural Platinum belt. *Ore Geology Reviews* (67): 234–243.

Tolstykh N.D., Telegin Yu.M. & Kozlov A.P. 2011. Platinum mineralization of the Svetloborsky and Kamenushinsky massifs (Urals Platinum belt). *Russian Geology and Geophysics* (6): 603–619.

Advances in Raw Material Industries for Sustainable Development Goals – Litvinenko (Ed)
© 2021 Taylor & Francis Group, London, ISBN 978-0-367-75881-3

Hydrodynamic features of the formation and placement of thermal waters of the Eastern Ciscaucasia and their protection from surface pollution

M.M. Labazanov, Z.I. Gadaeva, P.U. Musaeva, T.Kh. Ozdieva & Z.M-E. Damzaev
Grozny State Oil Technical University named after Acad. M.D. Millionschikov, Grozny, Russia

ABSTRACT: Using the example of the Eastern Ciscaucasia, where there are extremely favorable and at the same time contrasting combinations of geological – tectonic, hydrodynamic, geothermal, and also hydro-hydrographic conditions, it seems possible to trace the main geological and physico-chemical processes that determine the formation and distribution of various types of groundwater associated with different zones and structural - hydrogeological floors and the dependence of the degree of their protection from surface pollution in connection with these especially features.

When considering this issue, first of all, it should be noted that all the main scientific hypotheses of the formation of groundwater are not groundless and depending on the geological conditions of the region, there are various options.

In particular, there is no doubt that the fresh and weakly mineralized warm groundwater of the Tersko-Kum artesian basin and groundwater of the aeration zone of the mountain-folded regions of Dagestan, in their overwhelming part, are waters of infiltration origin.

The processing of enormous factual material on hydrodynamics, hydrochemistry, gas geochemistry, geothermy, hydrological and climatic conditions, collected from the results of drilling about 3000 artesian wells, allowed us to conclude that the Tersko-Kum artesian basin of Pliocene and anthropogenic deposits is a hydrodynamically open flowing natural system with modern natural resources in the amount of 0.6 km³/year and potential resources of about 6.0 km³/year.

1 INTRODUCTION

The problem of groundwater formation is complex and multifaceted and, depending on specific environmental conditions, has common and specific features.

The results of comprehensive studies indicate that low-mineralized thermal waters of the structural-hydrogeological floor (Miocene complex) also relate to a large part to waters of infiltration origin with a certain proportion of sedimentation and elizion waters from below - and, in some cases, overlying horizons.

In the thickness of the Middle Miocene sediments, aquifers with a pore nature of groundwater circulation are distinguished, the formation of reserves of which occurs at the base by infiltration of atmospheric and surface waters, which is confirmed by actual material on the hydrodynamics of the aquifer. Actual hydrodynamic data make it possible to identify feeding, discharge and discharge areas for the Middle Miocene aquifer complex and, accordingly, areas more or less potentially susceptible to possible pollution.

The feeding areas are located within a fairly wide range of outcrops of Middle Miocene deposits to the surface, stretching from west to east along the Montenegrin monocline, the Narat-Tyubinsky zone; then the strip of exits turns in a southeast direction and stretches far south, where the Middle Miocene sediments overlap with the thickness of the Akchagyl deposits, which are mismatched on the underlying ones, down to the Jurassic (Andrushchuk,

Dubinsky, Hain, 1968). The yields of Middle Miocene sediments are located at hypsometric elevations from 200 to 800 m in places and more, with individual peaks up to 1000 m. The maximum elevations of 600 - 900 m, correspond to the Black Mountains, decrease to 200 - 400 m within the Narat-Tyubinskaya zone, slightly increase in Southern Dagestan is up to 300 - 500 m less often than 600 m.

In the north, northeast direction from the areas of exits there is a regional subsidence of the strata. The roof of the Middle Miocene deposits is located at depths: in Makhachkala - 800–1200 m, Ternair — 800–1000 m, Izberbash — 400–800 m, Karanai-Aul syncline — 1600 m, Bilgadi syncline — 400-600 m, in Derbent — 950 m. V the zone of maximum subsidence in the Tersko-Caspian trough, the roof of the Middle Miocene deposits is located at depths of 3,500 - 3,700 m (Kurush, Karamay) i.e. the water of these deposits is almost completely protected from surface pollution (Figure 1).

Thus, based on the classical representations of artesian basins, the difference in the hydrostatic sets of supply areas and wellheads in the transit areas reaches the first tens of atmospheres, which should practically ensure water self-discharge in the overwhelming part of the distribution area of the Middle Miocene aquifers, taking into account hydraulic resistance. In fact, self-draining waters are ubiquitous.

The exception may be some areas where deep erosion valleys drain the Middle Miocene deposits, because of which natural depression extends to aquifers within the first tens of kilometers (Andrushchuk, Dubinsky, Hain, 1968). Such conditions are available in areas adjacent to the river valley. Sulak and other foothill rivers that drain these deposits at elevations of 100 - 300 m, as well as near feeding areas.

In the areas of runoff and transit, which cover all the territories of the Forward Trough, the Kumskoy and Tersko-Sulak plains, the piezometric surface is characterized by a general drop in

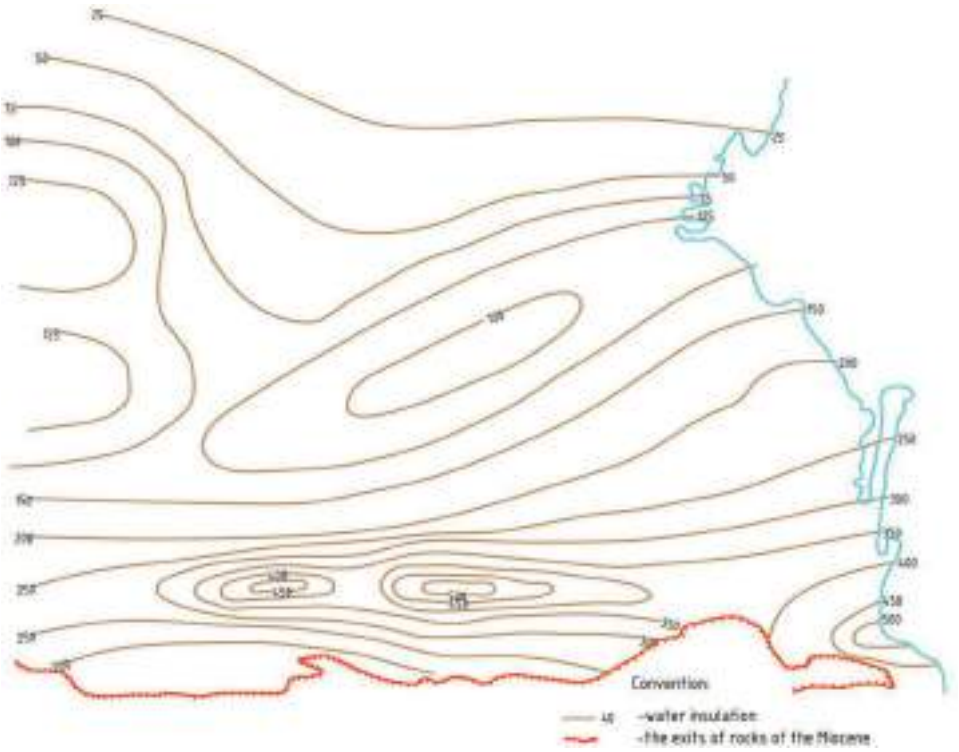

Figure 1. Schematic map of the conductivity of the Middle Miocene aquifer.

the pressure of water in the directions from the feeding areas to the north and northeast towards the Caspian Sea, consistent with the regional dip in the north - east and east.

Absolute elevations of piezometric levels vary from 200 - 500 m in areas directly adjacent to food areas, to 10 - 150 m in areas remote to significant distances from them. (Table 1). The relative elevation of the hydrostatic level increases from the first units of meters to 14-16 atmospheres in the Makhachkala, Kizlyar, Northeast of Kizlyar in the areas of Terekli-Mekteb – Chervlennye Buruns, hydrostatic pressure at the mouths drops to 10–8 atmospheres.

Actual material on the hydrodynamics and hydrochemistry of Middle Miocene deposits allows us to distinguish three hydrodynamic zones — active, slow and very slow water exchange, which therefore are logically subdivided into three zones of protection from surface pollution.

The zone of active water exchange includes the piedmont regions of the Eastern Ciscaucasia, composed of middle-price deposits entering the day surface with hypsometric marks 200-600 mine and deep erosion valleys, which serve as local erosion bases. This zone is characterized by maximum hydraulic slopes of 0.01-0.03, filtration coefficients (average) of 4.0-5.5 m/day, and filtration rates of 4-17 cm/day. or 15–62 m/year. In hydrochemical terms, this is the zone of maximum washing with fresh and slightly mineralized waters of hydrocarbonate, sulfate and mixed chemical composition.

Of the cations that determine the chemical composition, Ca and Mg prevail, and the anions are sulfates and bicarbonates.

The high hypsometric position, the presence of a rather dense river network, rugged terrain, and an abundance of precipitation with favorable lithological-facies and geomorphological-tectonic conditions contribute to intensive circulation and active groundwater exchange. In this case, the role of the distances from the supply area to the discharge area, which are minimal in this area, is significant. The upper hydrodynamic zone is represented by ground low-pressure and pressure fresh and low-mineralized waters. Numerous springs are confined to the Middle Miocene deposits in river valleys and natural relief depressions.

Numerous artesian and structural mapping wells have been drilled in the active water exchange zone, which reveal aquifers at depths from 50-60 m to 300-500 m and produce in most cases self-flowing waters with flow rates from fractions up to 2-15 l/s. The reservoir properties of the sandstones of the active exchange zone are quite high. The porosity in the Sulak basin is from 14 to 23.6%, an average of 18-20%, the permeability is very high from units to 8-10 darsi. (Mironenko, 2001).

In general, the zone of active water exchange is characterized by significant groundwater circulation rates, hydrogeological flushing of rocks and, as a result, low water salinity, the

Table 1. Absolute elevations of piezometric levels.

REGION	№№ well	Abs. Wellhead marks	Perforation interval	Deposits age	Abs. piezometric level marks
1	2	3	4	5	6
Agach aul	1	264,2	308-316	Karagan	210,5
Kaka-yurt	7	207,1	203-215	“	213,6
Ternair	20	2,25	1085-1110	“	92,2
Makhachkala	160	- 20	1487-1518	“	70,0
Bunaysk	1-56	557,0	77-93	“	558,65
Gerga	6-T	50,8	1388-1405	“	53,1
Manas Kent	10-T	36,18	1547-1561	Karanay	51,18
Manas Kultun	9-T	10,6	1414-1448	“	32,6
Kaspiysk	2-T	- 18,48	1482-1492	“	32,78
Derbent	11-T	- 14,77	1260-1278	“	24,43
Kizlyar	4-T	- 4,8	2786-2824	“	135,2
Kraynovka	1	- 20,0	2146-2148	“	60,0

predominance of calcium sulfates and bicarbonates, and a pronounced oxidative state. Flow rates, pressures, temperatures and composition of water, especially sources, are subject to seasonal fluctuations. The zone of active water exchange is the zone most susceptible to pollution.

The zone of delayed water exchange includes the water horizons of the Middle Miocene deposits located at depths from 400-500 to 2-3 thousand meters, which covers the vast majority of the study area. This zone includes the foothill and plain parts of the basin, which includes all thermal water deposits: Makhachkala, Izberbash, Kayakentsk, Kizlyarsk, Tarumovskoye, Terekli-Mektebskoye, Cherlennye Burun, Groznenskoye, Khankala and others. The regime of water horizons is characterized as a water head with estuary pressures 2-3 to 14-16 atm. Waters are self-draining throughout the territory, water flow rates are incomparably higher than in the first zone and reach up to 2-3 thousand m^3/day.

In general, for the southern part of the basin, filtration rates are 2-3 mm/day or 0.7-1.0 m/year.

The fall of piezometric levels occurs in the northern, northeastern and eastern directions, from 180-200 m. Near nutrition areas to 10-30 m in Southern Dagestan and 80-100 m in Northern Dagestan. The gradients of the piezometric levels are maximum in the foothills of Southern Dagestan from 0.007 to 0.24, in the foothill zone of Northern Dagestan from 0.012 to 0.05. As you move north in the platform part, minimum speeds are noted and hydraulic gradients here are 0.001 m or less (Ovcharova, 2009).

As aquifers sink, formation pressures, hydrostatic pressure and water temperature increase. The zone of delayed exchange is hydrochemically characterized by the presence of chloride-hydrocarbonate, chloride-sulfate sodium water. Mineralization of water gradually increases with depth to 10 g/l, and in some areas and formations to 30 g/l.

The zone of delayed water exchange is distinguished not only by the features of hydrodynamics and hydrochemistry of waters, but by the conditions of formation and regime of groundwater. The zone under consideration is characterized by relatively sustained thickness of aquifers, most often represented by small- and medium-grained sandstones of low cementation. As you move from the feeding areas deep into the flat part, the water regime gradually becomes stationary. Flow rates, pressures, chemical composition, temperatures are not subject to seasonal, annual and numerous fluctuations.

In general, the reserves and resources of this zone are incomparably large relative to the zone of active water exchange, which is explained by the maximum elastic reserves that can be exploited for apparently decades and are practically not subject to surface pollution.

The zone of a very slow water exchange includes the conditionally most submerged part of the Tersko-Caspian piedmont deflection, which is characterized by the presence of highly mineralized chlorine-sodium type in the Midiocene aquifer complex. Huge geostatic pressures contribute to a decrease in porosity, which determines the stagnant nature of the fluids. Unfortunately, this entire zone was not covered by drilling, and the only Karaman-I well drilled here in the southern geosynclinal board passed the very top of the Karagan Formation. This area is completely protected from surface contamination.

2 CONCLUSION

Thus, the underground waters of the Eastern Ciscaucasia according to their geological conditions of formation and occurrence are divided according to the degree of protection from surface pollution into 3 zones: unprotected; practically protected, but with the likelihood of contamination and fully protected.

The following tasks in the field of studying and developing the geothermal resources of the region, the authors consider:

- complex geological and geophysical, geochemical, geothermal, hydrogeological and experimental studies to prove and confirm the presence of depths of the hydrogeothermosphere, which should serve as a practically inexhaustible source of geothermal energy and valuable hydromineral raw materials;
- studies on practical confirmation and experimental proof of the possibility of implementing a self-circulating geothermal system and the growth of its effectiveness with depth.

It is known that there are “hot spots” on Earth that are hotbeds of fresh mantle jets; therefore, there should also be “cold spots” that should serve as large foci of infiltration of water resources to great depths. Perhaps they are decompressed zones of spreading in mountain - folded areas of land and ocean. In theoretical terms, the problem of heat and mass transfer of the upper horizons with deep bowels deserves attention the problem of finding “cold spots”, the existence of which is evidenced by a number of factors.

In the scientific, methodological and applied respect, the creation of a bank of geological and all parameters of gas-oil, geothermal and artesian wells of the basin, the creation of a hydrogeological balance model for managing geothermal resources of the East Ciscaucasia basin based on geoinformation modeling is of great importance.

In the matter of further rational development of geothermal energy and raw material resources, scientific and methodological studies on the development of multilayer geothermal deposits, improvement of the designs of geothermal production and injection wells, and the development of a model geothermal heat supply system, including underground and all ground circuits, as well as water treatment and pumping them back into the reservoir.

REFERENCES

Andrushchuk V. L., Dubinsky A.Ya., Hain V. E. 1968. *Geology of the USSR. Volume 9. Northern Caucasia Part 1*. Moscow: Geological description of the Subsoil

Borovikov A. A. Vasilieva N.V., Leiko D. M. 2018. *Engineering Geology and hydrology*. Moscow: BGCKHA chute.

Davis S. de Whist R. 1970. World. *Hydrogeology*. Moscow

Dvorov I.M., Dvorov V.I. 1976. Enlightenment. *Thermal waters and their use*. Moscow

Everett L.G. 2004. *Groundwater resources of the world and their use United Nations Educational Scientific and Cultural Organization*. Paris.

Kartsev A.A., Vagin S.B. Shurygin V.P. 1992. Subsoil. *Oil and gas hydrogeology*. Moscow.

Kovyatkin L.A., Matusevich V.M. 2010. *Oil and gas hydrogeology. Part 1. Theoretical foundations of oil and gas hydrogeology*. Tsogu, Tyumen.

Mironenko V. A. 2001. *Dynamics of underground waters*. Moscow: Moscow state mining University.

Ovcharova T. A. 2009. *Hydrogeology*. Ukhta: UGTU.

Cherkashin V. I., Mamaev S. A., Magomedov R. A., Isaeva N.A. 2015. *Geology and resources of Dagestan*. Makhachkala.

Vagin S.B., Kartsev A.A., Shugrin V.P. 1992. Nedra, *Oil and gas hydrogeology*. Moscow.

Vsevolzhsky V.A. 2007. Tutorial. 2nd ed. MSU Publishing House. Fundamentals of hydrogeology.

Vsevolozhsky V.A. 2007. Moscow State University. *Fundamentals of hydrogeology*. Moscow

Advances in Raw Material Industries for Sustainable Development Goals – Litvinenko (Ed)
© 2021 Taylor & Francis Group, London, ISBN 978-0-367-75881-3

Productive formations ranking methodology in order to select the optimal developing system

A.A. Farukshin
Postgraduate student, Saint-Petersburg Mining University, Saint-Petersburg, Russia

A.M. Zharkov
Doctor of geological and mineralogical Sciences, Saint-Petersburg Mining University, Saint-Petersburg, Russia

M.G. Ayrapetyan
Postgraduate student, Saint-Petersburg Mining University, Saint-Petersburg, Russia

ABSTRACT: The article describes the methodology for ranking the objects of development of the Lower Cretaceous deposits of Western Siberia for their further development. The ranking is based on the degree of knowledge assessment of oil and gas deposits and allows us to predict the degree of uncertainty in determining the amount of reserves, which directly affects the field development system. The technique is universal, and its criteria are flexible. This allows us to adjust the estimate for deposits with varying degrees of knowledge.

Keywords: geological modeling, multivariate formation evaluation, geological uncertainties, formations ranking, saturation modeling

1 INTRODUCTION

In recent years, the majority of oil-producing regions (Volga-Ural, Western Siberia, etc.) have been characterized by the entry of the main pool of deposits into the late stage of development, where the extraction of residual hydrocarbon (HC) reserves requires high unit costs. This, in turn, leads to a decrease in both the oil production rate and the efficiency of oil-producing enterprises. At the same time, the oil and gas industry still occupies one of the priority places in the Russian economy, contributing significantly to the development of other industries. One of the main ways to stabilize the rate of hydrocarbon production is to conduct exploratory work, the result of which is the discovery of new oil and gas fields.

However, in the "old" oil and gas producing regions, a decrease in the efficiency of prospecting is currently observed, which is associated with their relocation to areas with less prospects for oil and gas potential. In addition, work is being moved to areas with complex seismic and geological conditions with an increase in the number of small-scale deposits introduced into deep exploratory drilling. Obviously, drilling of unproductive facilities leads to economic losses. With this in mind, the task of prospecting for oil and gas is to obtain the most reliable information about the presence or absence of oil and gas-bearing object and its main characteristics.

This problem can be most rationally solved precisely by statistical methods based on a detailed study of the laws of structure and the criterion for evaluating small (1 to 5 million tonnes) and very small (less than 1 million ton) oil and gas deposits. Based on the analysis and systematization of factual material using multidimensional statistics, it is necessary to build geological models that provide the most rational choice of deposits for their input into further development. Ultimately, the effectiveness of prospecting will depend on the reliability of the economic planning of investment projects. The validity of the latter, first of all, is determined by the reliability

Figure 1. Research region.

of estimates of oil and gas reserves. The proposed approach allows even before significant investments to be made, to numerically assess the geological risks of exploration in Western Siberia, ensuring a reduction in the volume of exploration works by assessing uncertainties.

It is necessary either to discover new deposits, or to involve earlier discovered smaller deposits in the development, the commissioning of which is accompanied by large uncertainties in reserves, which causes concern when deciding on drilling or carrying out heavy geological and technical measures (GTM). Developers usually commission deposits from the bottom-up method; the choice is made according to the amount of residual recoverable reserves and the value of effective oil and gas saturated thicknesses. The same method accepts that, the value of reserves, this number is not fixed, but may vary within a certain interval.

Objects of research are undeveloped deposits of developed deposits and unexplored reserves of developed deposits of Lower Cretaceous deposits in Western Siberia (Figure 1).

2 VERIFICATION OF GEOLOGICAL MODELS

The goal of creating an algorithm for geological classification of formations was to create a unified scale for assessing the exploration of the hydrocarbon reservoir and forecasting the value of reserves with little exploration of hydrocarbon deposits. To compile a correctly working tool for ranking development objects, a geological analysis of all objects was carried out, as well as an analysis of their knowledge. For analysis, 12 deposits of the Snezhnoye field, which is at a late stage of development, were selected. All deposits are of the Lower Cretaceous age and are concentrated in the strata of the OK and AG groups. All deposits of the field are quite densely drilled by exploration and production wells. Detailed geological models were built for these deposits and hydrocarbon reserves (HC) were calculated. During the construction of geological models, data verification was carried out, which included: correlation of wells (Figure 2), construction of structural maps and thickness maps, derivation of the dependences of the permeability coefficient on the porosity coefficient, construction of a capillary model (Figure 3) for modeling oil saturation. Fluid contacts were also revised, because after drilling new wells the data were not updated. As a result, some substandard data were revealed, which were not taken into account when building dependencies and constructions.

The output was geological models that really reflected the structure of reserves, key uncertainties in their determination (Figure 4), as well as the distribution of hydrocarbon reserves.

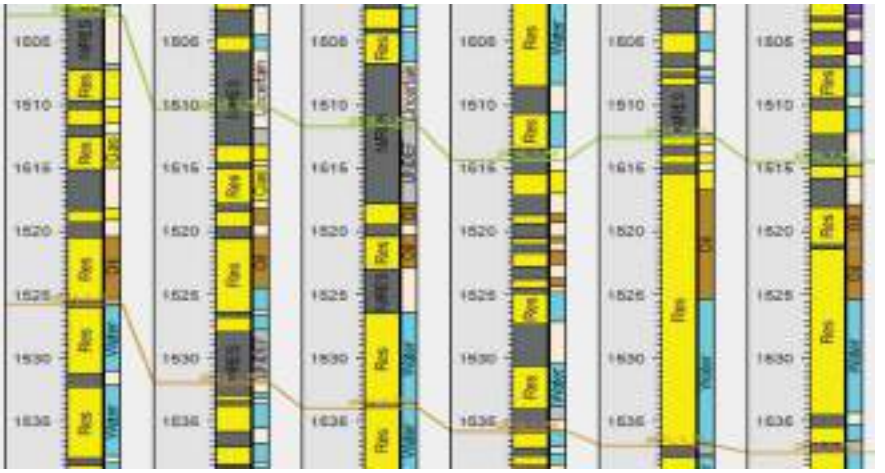

Figure 2. Correlation scheme of AK4 formation.

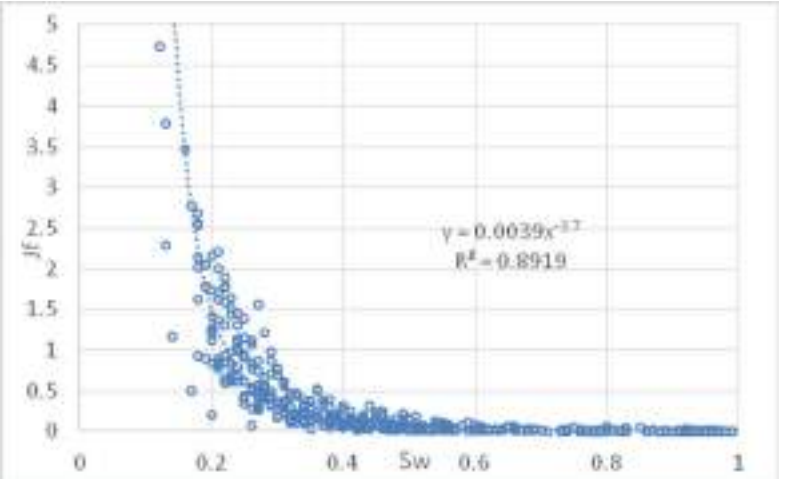

Figure 3. Capillary model (AK formations).

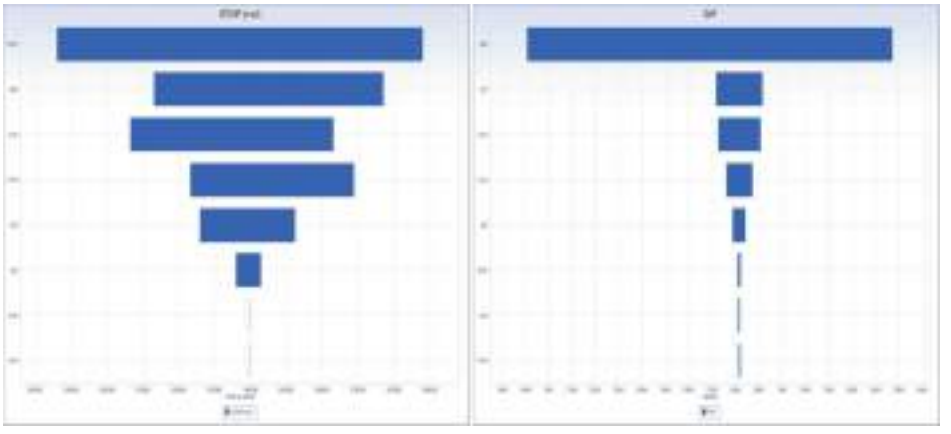

Figure 4. Sensitivity plot. OK2 formation reserves uncertainty decreases due to clarification of parameters. HC reserves more sensitive to varying of contacts and oil saturation.

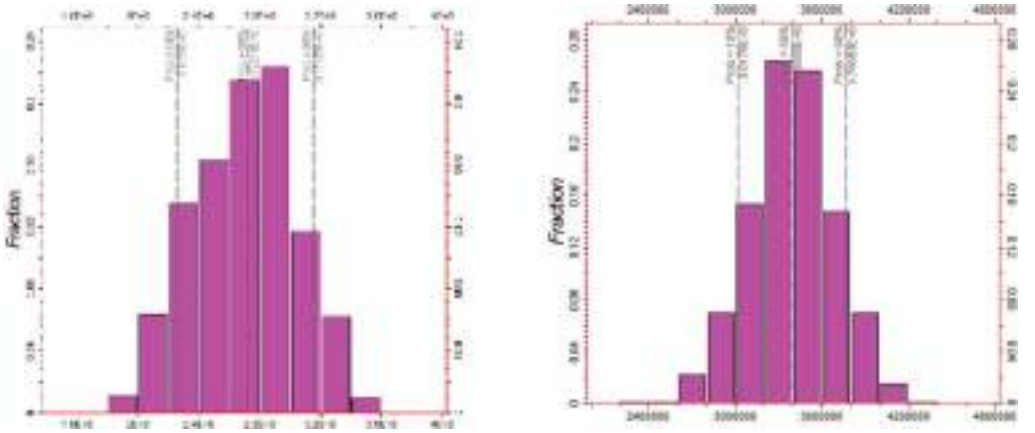

Figure 5. Clarification of initial oil reserves after remaking the geological model of OK2 formation.

The variability of reserves (Figure 5) was evaluated as a result of assessing the sensitivity of reserves to changes in the estimated parameters.

Thus, geological models were revised for all 12 sites. This was done to compile a reference sample that would allow us to develop a methodology for assessing the knowledge of development objects. Subsequently, all work was carried out on remade geological models with current data. For research, reserves of categories P10 (optimistic) and P90 (pessimistic) are useful.

3 METHODOLOGY FOR THE KNOWLEDGE ASSESSMENT

To assess the degree of knowledge of the development objects, a data pool was sorted, which somehow affects the uncertainties of hydrocarbon reserves. The study of deposits was considered as widely as possible and included:

1. Fluid studies
2. Petrophysical studies
3. Results of seismic data
4. Data from well tests and field geophysical data.

For each category of knowledge, parameters were described that describe the studies in detail. As a result, more than 80 parameters were collected that somehow contributed to the degree of knowledge of the reservoir. But it turned out that there are too many of these parameters to assess the degree of knowledge, since some of them strongly affect the calculated parameters, while others are not very. For example, the drilling density of a deposit affects the structure of the deposit, which in turn determines the area distribution and the size of reserves, and special geophysical studies, such as acoustic log data, do not affect the size of reserves so much.

Thus, directly related to the calculated parameters reservoir parameters were selected:

1. The structure of the deposits;
2. Fluid contact position;
3. Effective oil saturated thicknesses;
4. The coefficient of porosity (Kp);
5. The coefficient of fluid saturation (So);
6. The formation volume factor (B);

Parameters for convenience are encoded with letters from A to F

The data characterizing the knowledge were grouped into categories and encoded from 0 to 5:

1. Well stock;
2. Field geophysical surveys (FGS);

3. Seismic surveys;
4. Well log data;
5. Petrophysical core studies;
6. Reservoir Fluid Studies;

As a result, a summary table was obtained for assessing the degree of exploration of deposits, on which the influence of studies on the determination of a particular parameter was analyzed (Table 1).

After compiling a summary table, evaluation criteria for each of its cells are developed. Cell A0 - is determined by the degree of drilling density, A2 - by the correlation coefficient of the depth map with welltops. Cell B1 characterizes the knowledge of contacts by FGS, B3 - by well logs. C0 is determined by the drilling density (equal to A0), C2 is the correlation coefficient of the seismic data and thicknesses, C3 is the number of wells with a well logging. D2 - correlation coefficient of seismic data and Kp, D3 - correlation of core and well log data, D4 - presence of Kp core measurements. E3 - by correlation of the saturation parameter (Po) and So, E4 - by the presence of capillary studies and correlation of So with the capillary model.

To quantify the columns, the arithmetic mean for the parameters was calculated, but to take into account the weight of the studies, correction factors were also introduced:

$$I = ((aA0 + bA2) + \ldots)/N \tag{1}$$

where, I - knowledge, a and b - weighting factors.

All 12 deposits of the Snezhnoye field were estimated using this methodology (Figure 6).

Weight coefficients are independent.

Table 1. Criteria table for knowledge estimation. Green cells mean that study affects oil calculating parameters.

		Wells	Tests	Seismic data	Well log	Core	Fluids
Code	Parameter	0	1	2	3	4	5
A	Structure	+	-	+	+	-	-
B	Contacts	-	+	-	+	-	-
C	Net thickness	+	-	+	+	+	-
D	Porosity	-	-	+	+	+	-
E	Saturation	-	-	-	+	+	-
F	B	+	-	-	-	-	+

Figure 6. Formation knowledge.

4 RESULTS

The weight coefficients for the studied deposits were selected automatically by solving the problem of multidimensional regression, when the degree of influence of each study on a particular parameter is calculated. The purpose of the selection was to obtain the maximum correlation coefficient of the degree of study and the ratio of reserves in the categories P10/P90. This inventory ratio characterizes the uncertainty in the definition of reserves, that is, the wider the histogram of the distribution of reserves, the greater the uncertainty. As a result, a scattering diagram was obtained, the degree of correlation of which was 92% (Figure 7). For 12 Snezhnoye deposits, the maximum weight factor was introduced for the So parameter and the contact position. Thus, all deposits are characterized by a strong sensitivity of the reserve uncertainty structure to these parameters.

5 DISCUSSION

This pattern of assessment of the degree of knowledge is universal for deposits. Depending on the degree of knowledge of the deposit for each cell in the table, you can set arbitrary numerical criteria, for example, for one field, the seismic data can describe the geological structure more detailed than for others.

This technique is designed to help the geologist in a number of tasks: the selection of the object of development from a variety of deposits for the purpose of priority, higher priority for further input into development, planning GTM; assessment the state of deposits knowledge allows assessing risks and uncertainties.

GTM planning on deposits with small and very small reserves is characterized by the presence of economic risk due to the possibility of a small economic effect.

The relevance of the method at the moment is that it allows the geologist to consider and type a new object in 1-2 hours. It can also be used for further studies of the object-timely update information in special checklists and get updated results instantly.

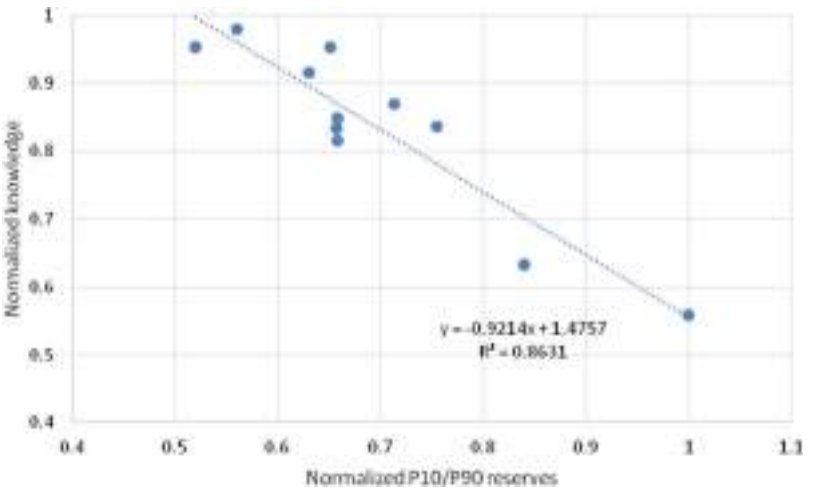

Figure 7. Normalized knowledge to P10/P90 reserves cross-plot.

6 CONCLUSIONS

A method was developed for rapid assessment of the degree of knowledge of oil and gas deposits. The working tool is a table, which is a universal template for differentiating deposits depending on the availability, sufficiency, reliability and quality of input information. For a more accurate correlation of the study with the uncertainty in reserves, weight coefficients were automatically selected to determine the study that most affects them. The method was tested on 12 layers of the OK and AG group of the Snezhnoye field, the geological models of which were detailed in advance and the reserves of which were calculated by the probabilistic method. A high correlation coefficient (92%) showed that the developed template accurately reflects the structure of uncertainty in hydrocarbon reserves. This means that after assessing the uncertainty of several deposits in detail, you can choose such criteria that can predict with high confidence the uncertainty of other deposits of the field of interest.

REFERENCES

Ababkov, K. (2010). Fundamentals of three-dimensional digital geological modeling. Ufa: "Oil and Gas business".

Bolshakov, M., Meynarands R., Naugunov M. V. "A new approach to the assessment of the index of complexity of development of deposits in Western Siberia". SPE-187780-RU

Disposal of the Ministry of Russia from 01.02.2016N 3-R (edition of 19. 04.2018) "On approval of methodological recommendations on application of Classification of reserves and resources of oil and combustible gases, approved by order of the Ministry of natural resources and ecology of the Russian Federation on 01.11.2013 N 477"

Gutman, I., Kuznetsova G. P. Classification of correlation of geological sections of wells in connection with the degree of study of oil and gas objects. Features of performance of comparison of geological sections of wells with use of the latest computer technologies. - Moscow: Gubkin Russian state University of oil and gas, 2006.

Matveev, V.P., Tarasenko, A.B. 2019. The study of the Berkha Island reef massif (Novaya Zemlya), based on lithological and geochemical data. - Chemie der Erde.

Prishchepa, O., Nefedov, Y., & Grokhotov, E. 2019. Geochemical and petrophysical studies of hydrocarbon potential of domanic shale formation (Timan-Pechora petroleum province). EAGE/SPE Workshop on Shale Science 2019 - Shale Sciences: Theory and Practice

Rose, P. "Risk Analysis and management of oil and gas exploration projects" // SIC "RCD", "Izhevsk Institute of computer research", - Moscow-Izhevsk, 2011, - 304 p.

Sirotkin, A.N., Talovina, I.V., Duryagina, A.M. 2019. Mineralogy and geochemistry of alkaline lamprophyres of north-western Spitsbergen (Svalbard) - Chemie der Erde.

Zakrevsky, K. (2009). Geological 3D modeling. Moscow: LLC CPI Mask.

Advances in Raw Material Industries for Sustainable Development Goals – Litvinenko (Ed)
© 2021 Taylor & Francis Group, London, ISBN 978-0-367-75881-3

Prospective petroleum accumulation areas in the non-structural traps in the Upper Permian sequences of the southern part of the Vilyuy Syneclise (Eastern Siberia)

G.A. Cherdancev
Postgraduate student, Saint-Petersburg Mining University, Russia

V.P. Semenov
Candidate of Geological and Mineralogical sciences, leading researcher, Joint-Stock company «All-Russia Petroleum Research Exploration Institute» («VNIGRI»), Russia

I.A. Kushmar
Candidate of Geological and Mineralogical sciences, head of department, Joint-Stock company «All-Russia Petroleum Research Exploration Institute» («VNIGRI»), Russia

ABSTRACT: The article provides the updating of the petroleum potential forecast of the Permian formations in the southern part of the Vilyuy Syneclise, which is a promising territory for the petroleum exploration. Article includes a brief description of the Upper Permian sequences and justification of the oil and gas prospects of the Upper Permian Taragay Formation. Authors have performed updated scheme of the oil and gas potential prospects of the Permian section based on the data of new geological and geophysical studies carried out in the southern part of the syneclise.

1 INTRODUCTION

The current issue in the east of Russia - in Yakutia - is certain risks associated with the provision and refill of the energy and industrial sectors of the national economy with petroleum resources (Sivtsev, Chalaya et al., 2016). One solution to this problem is exploration of new accumulation areas in Central Yakutia.

Vilyuy Syneclise is one of the areas in Eastern Siberia, where researchers expect discovery of new petroleum accumulations in the Upper Paleozoic formations.

Vilyuy Syneclise is the largest depression in the east of the Siberian Platform. The syneclise is located on a large territory between the Anabar Anteclise in the north and Aldan Anteclise in the south; in the east the syneclise borders on the Pre-Verkhoyansk Trough. The geological structure of the sedimentary cover includes formations from the Upper Proterozoic to Cenozoic systems.

The petroleum potential of the Permian section of the Vilyuy Syneclise is confirmed by the presence of accumulations in the Upper Permian formations (gas and gas condensate fields in the central part of the syneclise - within the Khapchagay Uplift Area), as well as oil and gas occurrences within the syneclise.

Different researchers have repeatedly pointed out the possible oil and gas prospects of the Permian section in the south of the Khapchagay Uplift Area (Sitnikov et al., 2014, Vasiliev et al, 2018). The geological and geophysical studies recently conducted by JSC "Yakutskgeofizika" and JSC "VNIGRI" in the southern part of the syneclise confirm the prospects of Permian formations in this area.

2 BRIEF GEOLOGICAL CHARACTERISTICS OF THE STUDIED AREA AND UPPER PERMIAN FORMATIONS

The studied area is about 12 thousand km^2. In general, the Permian structural plan of this territory is the southern monoclinal slope of the Vilyuy Syneclise. It is complicated mainly by structural elements such as structural noses, flexures, etc. In the northeast of the territory there is the Tangnaryn Depression adjacent to the Khapchagay Uplift Area from the south. In the southwest of the studied area there are Ygyattin and Kempendyay depressions, which are separated by the Suntar Arch. The Arbaysk-Sinsk Uplift Area is located to the southeast from the Kempendyay Depression; from the southeast it is limited by the Sarsan Depression. To the east there is a northwest side of the Aldan Anteclise (Figure 1).

The Permian formations are widespread throughout the studied territory. Their thickness varies from 3.6 km in the central part of the Tangnaryn Depression to wedging-out closer to the sides of the syneclise. The subdivision of the Permian sequences is based on the presence or absence of coal layers.

The terrigenous-coal-bearing Permian section in the south and in the center of the syneclise is divided into the Lower Permian Mohsogolokh Formation and the Upper Permian Khomustah, Kharyass, Kyundey, and Taragay formations. A comparison of the time of their formation with the international stratigraphic chart and the general stratigraphic chart, used in the period of time when they were described, is presented in Figure 2. These formations are dominantly composed of sandstones, layers of interbedded siltstones and mudstones (Frolov et al, 2019). They were formed in continental sedimentation environments.

Gas-bearing reservoir rocks of the Upper Permian formations in the central part of the syneclise are confined to the Taragay Formation of the Tatarian series of the Permian system. The main type of deposits is lithologically screened roof deposit.

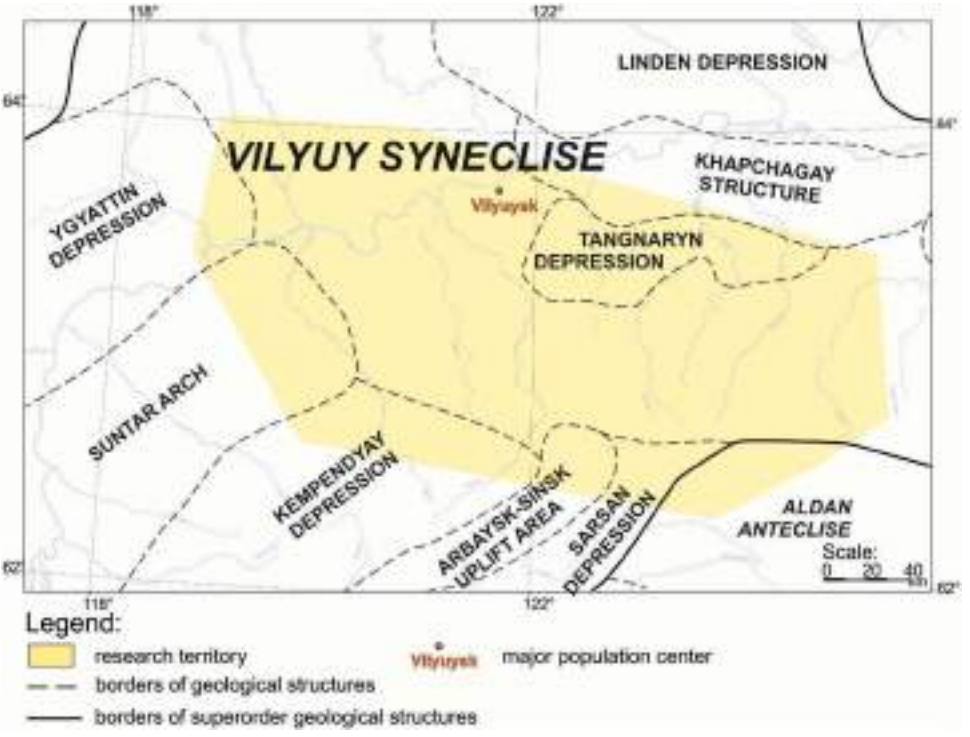

Figure 1. Structural and tectonic schematic view of the research territory.

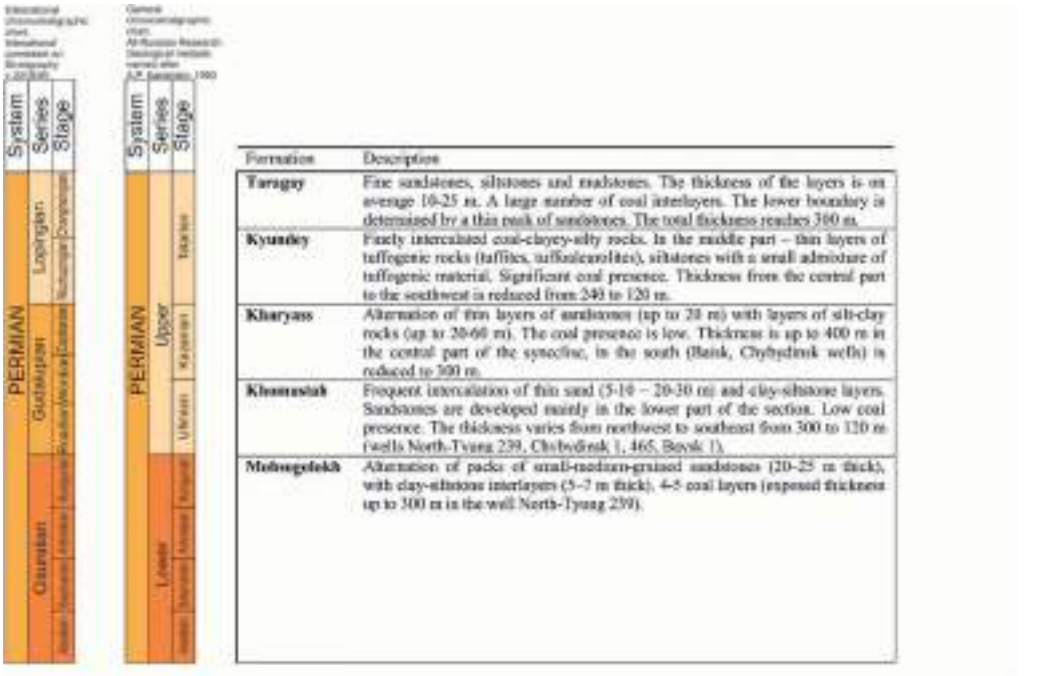

Formation	Description
Taragay	Fine sandstones, siltstones and mudstones. The thickness of the layers is on average 10-25 m. A large number of coal interlayers. The lower boundary is determined by a thin rock of sandstones. The total thickness reaches 300 m.
Kyundey	Finely intercalated coal-clayey-silty rocks. In the middle part – thin layers of tuffogenic rocks (tuffites, tuffolavarolites), siltstones with a small admixture of tuffogenic material. Significant coal presence. Thickness from the central part to the southwest is reduced from 240 to 120 m.
Kharyass	Alternation of thin layers of sandstones (up to 20 m) with layers of silt-clay rocks (up to 20-60 m). The coal presence is low. Thickness is up to 400 m in the central part of the syncline, in the south (Baink, Chybydinsk wells) is reduced to 300 m.
Khamnsiah	Frequent intercalation of thin sand (5-10 – 20-30 m) and clay-siltstone layers. Sandstones are developed mainly in the lower part of the section. Low coal presence. The thickness varies from northwest to southeast from 300 to 120 m (wells North-Tyung 239, Chybydinsk 1, 465, Baysk 1).
Mohugolokh	Alternation of packs of small-medium-grained sandstones (20-25 m thick), with clay-siltstone interlayers (5–7 m thick), 4-5 coal layers (exposed thickness up to 300 m in the well North-Tyung 239).

Figure 2. Description of the Permian formations of the southern part of the Vilyuy Syneclise.

The Taragay Formation was drilled by 26 wells within the studied territory; however, its full section was exposed only in wells of the Khapchagay Uplift Area. The formation is composed by thin layers of sandstones and carbon-bearing-clayey-siltstone rocks with thickness up to 10-15 m. Thin layers of tuffogenic rocks are exposed in the top of the formation. Taragay Formation on the southern side of the Vilyuy Syneclise was formed in the continental sedimentation environments. The section formed in the beds of meandering rivers, their floodplains, lakes and swamps, are widespread within the territory. The thickness of the formation within the site decreases from 304 m on the south (Middle Vilyuy 27 well (27_Sr-Vil)) to 85.9 m (Bappagay 1 well (1_Bapp)).

Permeable rocks of the upper part of the Permian section were discovered in the South Byrakan area (Byrakan wells (1184_Byr, 3_Byr, 2_Byr)). The porosity of the reservoirs reaches 14.2%.

Satisfactory pore reservoirs are also discovered in Baysk 1 well (1_Bays) with a porosity of 14-15.8%; during the tests the water inflow of 14.25 m^3/day was reached.

In the South Nedzhelinsk well (251_Y-Nedj) the natural gas inflow up to 1000 m^3/day was obtained from Permian formations (Sitnikov et al., 2017).

During tests in Hailakh 1213 well (1213_Hayl) the inflows of water with dissolved gas were obtained; core porosity of the reservoir rocks of the Taragay Formation was up to 9.4%. The reservoir properties are also confirmed by the results of re-interpretation of well logs carried out by specialists of JSC "VNIGRI".

Reliable impermeable rocks for the potential Taragay Formation are the Lower Triassic Nedzhelinsk Formation, regionally developed on the territory of the Vilyuy Syneclise (Vasiliev et al, 2018). The Nedzhelinsk Formation is not distributed throughout the whole territory. On the remaining territory, the lower part of the Lower Jurassic Kyzylsyr Formation, which overlaps the Permian formations in the south where Triassic formations are absent, may serve as possible reservoir caprock due to its impermeable properties. In addition, there are impermeable layers of clay rocks within the Taragay Formation that can serve as local reservoir caprocks.

3 PERMIAN SOURCE ROCKS OF THE VILYUY SYNECLISE

The Permian terrigenous structure is the main oil and gas producing formation for the Upper Paleozoic-Mesozoic sedimentary sequences of the basin (Zueva et al., 2014). Due to the high bio-productivity of the continental Permian landscapes, the large masses of organic matter are accumulated in this section.

The dispersed organic matter (DOM) of the Permian sequences has a mixed genetic nature with a different ratio of sapropelic and humic components, but is mainly represented by sapropelic and humic types (Zueva et al., 2014).

By the beginning of the Triassic, the Permian sequences entered the initial stage of the main phase of oil formation in the depressions in the south of syneclise. On the territory of the Linden Depression and the present-day Khapchagay Uplift Zone, they approached the main stage of gas generation. In subsequent eras, the Permian sequence continued to plunge unevenly. Subsidence depths were determined by the thickness of the overlying sections, which created various conditions for the generation and migration of hydrocarbons.

To the end of the Lower Cretaceous, the Permian sequences in most of the territory were located at the levels of the main gas generation zone, corresponding to the stage of maximum migration of gas hydrocarbons, while in the Linden Depression - to the stage of gas process attenuation.

At the present stage, corresponding to the depths of maximum deposits subsidence, the Permian formations are located almost throughout the territory within the gas generation zone. In the deepest parts of the depressions, the Permian section could have exhausted their gas-producing properties.

Thus, starting from the Triassic time, the hydrocarbon migration could occur from the most deepened part of the syneclise to its sides, where they could be accumulated in traps.

4 OIL AND GAS PROSPECTS

There are not many typical anticlinal traps in the studied area. They were identified earlier (Byrakan, Hailakh sites); wells were drilled within them, in which gas inflows were received during well tests. No other large anticlinal traps have been identified; therefore, the oil and gas accumulation zones within the studied area can be primarily confined to non-anticlinal traps. Favorable factors for their formation are the presence of interbedded sand and clay rocks, large regional Pre-Triassic and Pre-Jurassic erosion, on the surfaces of which the porous and impermeable rocks come into contact, the development of facial substitution areas and regional wedging out of sequences that are characterized by oil and gas potential. The positive impact of such factors on the oil and gas potential is also known in other oil and gas basins in Russia (Prishchepa et al, 2019; Borovikov and Volchenkova, 2018).

The identification of promising zones of oil and gas accumulation was preceded by a detailed correlation of productive levels, structural and tectonic studies based on seismic, electrical, and gravimetric surveys, which allow us to clarify the structural plans for prospective petroleum bearing areas within the territory and to update the pinch-out line of the Permian sequences.

As an example, the fragment of seismic survey interpretation performed by JSC «Yakutskgeofizika» specialists is provided in Figure 3, where the pinching out of the Permian sedimentary complex is presented.

Figure 4 shows the same seismic section with a possible petroleum prospect in the Upper Permian sedimentary rocks.

As a result of research, promising oil and gas zones were localized in the upper part of the Permian section (Figure 5).

In the eastern part of the research area, a promising prospecting object is limited from the northwest by tectonic fault traced along seismic sections. The level of oil and gas content was

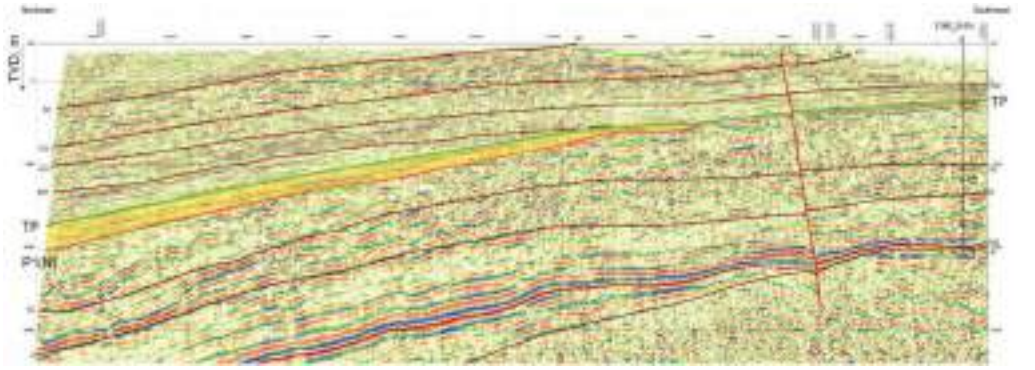

Figure 3. Fragment of the seismic section. TP (green) –top of the Upper Permian formation (Taragay Fm); P1(N) (orange) – bottom of the Upper Permian formations; the interval of the Upper Permian section is shown in yellow.

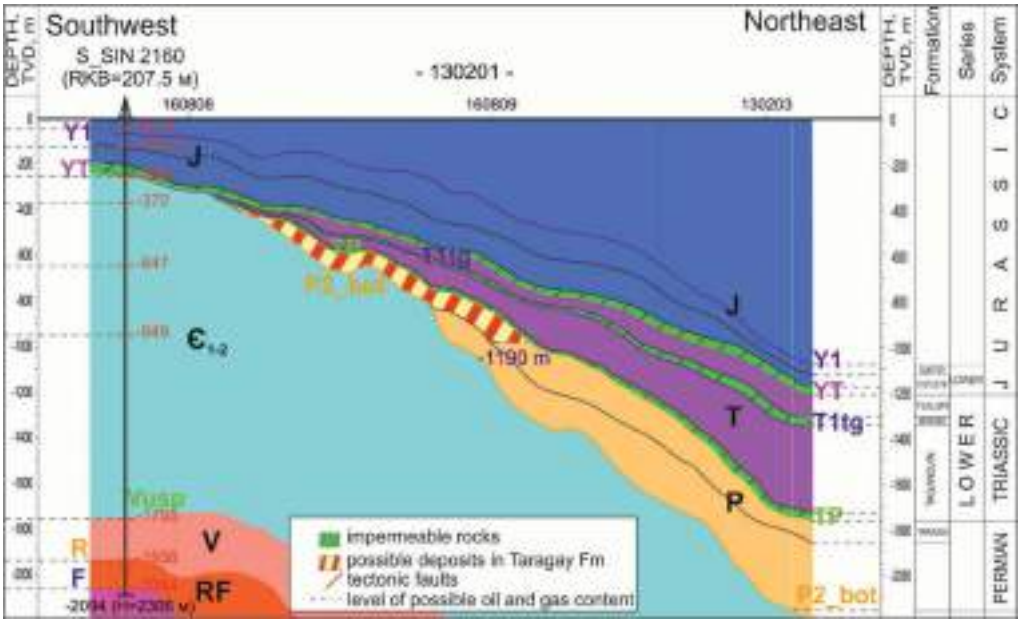

Figure 4. Fragment of the geological section.
Seismic horizons: Y1- top of Suntar Fm (J1sun); YT- top of Tulur Fm (T1tl); T1tg- top of Tagandjin Fm (T1tg); TP- top of Taragay (P2tr); P2_bot - bottom of Upper Permian formations; R- top of Riphean sequences; F - top of basement rocks

taken at an absolute depth (TVD) of -1190 m, corresponding to the top of water-saturated reservoirs according to well log data in Andreevsk 2 well (2_Andr) located nearby. In the south the perspective zone is limited by the wedging line of the Taragay Formation, traced on seismic surveys sections and deep well drilling data.

In the western part of the site, the prospecting object is bounded from the southwest by the pinch-out line of the Permian sequences, and by tectonic faults that limit the Suntar Arch from neighboring depressions. The probable oil and gas content level has an absolute depth -1300 m, which corresponds to the top of the water-saturated reservoir in the Nizhnetyukyan 311 well (311_N-Tuk).

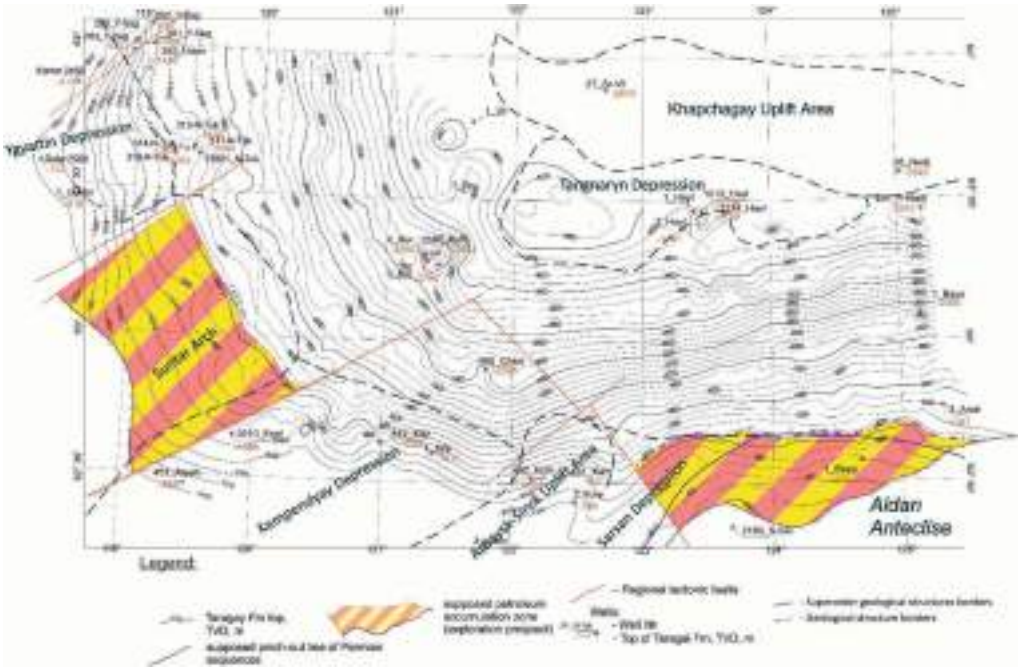

Figure 5. Scheme of oil and gas prospects of the Permian section in the southern part of the Vilyuy Syneclise.

5 CONCLUSIONS

The Permian oil and gas structure is associated with certain prospects for the discovery of hydrocarbon accumulations in the southern part of the Vilyuy Syneclise. Non-anticlinal traps are expected there. They are controlled by the surfaces of erosion, limiting the Permian sequence from below and above, as well as by the development of weakly permeable or impermeable rocks below the surface of the Pre-Permian erosion. Other factors are the distribution of clay rocks above the Triassic erosion surface and facial variability within the Permian section.

As a result of the studies conducted by VNIGRI specialists on the basis of complex geological and geophysical surveys, the perspective objects in the Upper Permian were localized within the research object and the pinching out boundaries of the Permian formations were clarified.

The traps in the selected zones are assumed to be of non-structural type and will be confined to the zones of pinch-out of productive reservoir rocks and controlled by regional lithological screens.

The types of deposits associated with these traps are stratigraphic, lithological and stratigraphic with elements of tectonic shielding.

The obtained geological results indicate the need for further study of this territory.

REFERENCES

Borovikov I.S., Volchenkova T.B. 2018. Model of forming hydrocarbon pools in the west of Melekess depression. *Conference Proceedings, Innovations in Geosciences. Time for Breakthrough*, Saint *Petersburg*, *Apr 2018*, (2018): 1–6. EAGE.

Frolov S.V., Karnyushina E.E., Korobova N.I., Bakay E.A., Kurdina N.S., Krylov O.V., Tarasenko A. A. 2019. Features of the structure, sedimentary complexes and hydrocarbon systems of the Leno-Vilyuisky oil and gas basin. *Georesources* 21(2): 13–30.

Prishchepa, O., Nefedov, Y., & Grokhotov, E. 2019. Geochemical and petrophysical studies of hydrocarbon potential of domanic shale formation (the timan-pechora petroleum province). *Conference Proceedings, EAGE/SPE Workshop on Shale Science 2019*, *Apr 2019*, (2019): 1–5. EAGE.

Sitnikov V.S., Alekseev N.N., Pavlova K.A., Pogodaev A.V., Sleptsova M.I. 2017. Newest forecast and development updating of Vilyuy Syneclise petroleum objects. *Petroleum Geology - Theoretical and Applied Studies* 12 (1).

Sitnikov V.S., Prishchepa O.M., Kushmar I.A., Pogodaev A.V. 2014. Petroleum potential prospects of southern part of Vilyusky syneclise. *Prospect and protection of mineral resources* 7: 22–28.

Sivcev A.I., Chalaya O.N., Zueva I.N. 2016. Prospects of oil and gas in the Central Yakutia as resource of energy security. *Oil and Gas Business* 2: 71–82.

Vasiliev S.A., Sobolev P.N., Taffarel E.S., Golovanova M.P., Garifullin I.I. 2018. Oil and gas potential of Vilyuiskaya syneclise and prospects of hydrocarbon deposits searching. *Geology, geophysics and development of oil and gas fields* 12: 14–26.

Zueva I.N., Chalaya O.N., Safronov A.F., Kashircev V.A. 2014. Oil Generated Potential of the Permian Deposits of the Vilyui Basin. *Science and Education* 2: 110–117.

Advances in Raw Material Industries for Sustainable Development Goals – Litvinenko (Ed)
© 2021 Taylor & Francis Group, London, ISBN 978-0-367-75881-3

Bituminous sandstones of the Chechen Republic

Sh.Sh. Zaurbekov
Doctor of Economics, Professor, Vice-Rector, Grozny State Oil Technical University named after Acad. M.D. Millionschikov, Grozny, Russia

M.M. Labazanov
Ph.D., Head of Scientific and Technical Center "Nedra", Grozny State Oil Technical University named after Acad. M.D. Millionschikov, Grozny, Russia

T.Kh. Ozdieva
Head of the laboratory "ILGEM" NTC "Nedra", Grozny State Oil Technical University named after Acad. M.D. Millionschikov, Grozny, Russia

P.U. Musaeva
Laboratory Assistant, ILGGP Scientific and Technical Center Nedra, Grozny State Oil Technical University named after Acad. M.D Millionshchikov, Grozny, Russia

Z.I. Gadaeva
Head of the laboratory "ILGGP" NTC "Nedra", Grozny State Oil Technical University named after Acad. M.D. Millionschikov, Grozny, Russia

A.A. Batukaev
Laboratory Assistant, Ecology and Nature Management, Grozny State Oil Technical University named after Acad. M.D. Millionschikov, Grozny, Russia

Z.M-E. Damzaev
Junior Researcher, Scientific and Technical Center "Nedra", Grozny State Oil Technical University named after Acad. M.D. Millionschikov, Grozny, Russia

ABSTRACT: The article gives a general description of tar sandstone deposits in the Chechen Republic. In total, nine areas of outcrops of sand and sandstones of the Karagansky and Chokraksky stages of the Neogene system, which are confined to two structural zones, are the zone of the Advanced Ranges and the zone of the Montenegrin monocline. Four zones were identified in each area.

All deposits of the Advanced Ridge zone are small, due to their local distribution of bituminosity and a steep occurrence of the host reservoirs. In addition to the volume of reserves, the deposits of the Montenegrin monocline are unpromising due to their remoteness from the main transport and energy highways.

When studying the bituminous strata of the promising sections, the following problems were solved: the geological structure of the section was studied; layers with industrial significance are highlighted in the context of the tar layers; bitumen content and the nature of its change are determined; the physicochemical characteristics of bituminous rocks and interposition with the host rocks are specified; qualitatively evaluated and determined technological parameters of bitumen; estimated mineral reserves are estimated.

The general characteristics of bituminous rocks include - the uneven distribution of bituminous in both individual intersections and in areas as a whole; are classified as - from low

bitumen to medium bitumen. By particle size distribution and particle size modulus, finely and medium-grained, by mineralogical composition, quartz sand.

All described areas of bituminous rocks can be attributed to promising development at the local regional level.

1 INTRODUCTION

Currently, the task has arisen of searching for additional resources of organic binders and developing methods for their rational use in the construction of roads. The source of reducing the deficit in oil bitumen is natural bituminous rocks, the deposits of which are widespread, including in the Chechen Republic.The conditions for the formation of natural bitumen in the host sedimentary formations are migration processes of fluids consisting of water and hydrocarbons with the obligatory access of air and specific microorganisms. In the process of this, this fluid mixture is differentiated on the fractured-pore surfaces of the rocks according to the fractional basis, i.e. heavy hydrocarbons, aspaltenes and resins.

An analysis of the available material obtained during geological exploration from the 30s of the XX century, which includes specialized geological studies for oil and gas in the Grozny and Nozhay-Yurt districts, to the present (expedition of Chechenneftekhimprom OJSC) indicates that manifestations of bituminous rocks occur almost everywhere in the strip of outcrops on the surface of Karagan-Chokrak deposits. (Mitchin, 1992)

Deposits of the Jurassic, Cretaceous, Paleogene, Neogene, and Quaternary systems take part in the geological structure of the territory of the Chechen Republic. (Orel, Raspopov, Skripkin, 2001) Because bituminous sandstones have a clear stratigraphic and lithological confinement; in practice, we will only dwell on the characterization of these deposits only to the sandstones of the Chokrak and Karagans. (Khasanov, Shaipov, Zaurbekov, 2010)

The deposition of the Chokrak and Karagan strata together with the overlying layer of the Miocene and Pliocene belong to the Neogene system (N)

According to the scheme of N.A. Kozlova distinguishes 11 strata of sandstones of the Chokrak deposits (E1 - E11) of various thicknesses and lithology, including strike. The layers are separated by clays and marls of various thicknesses and lithology. (Orel, Raspopov, Skripkin, 2001) The lower boundary is drawn along the roof of the marls in accordance with the presented fauna. The thickness of the entire Chokrak tier reaches 1068 m.

The rocks of the Karaganskian layer, according to the overlap of the deposits of the Chokrak layer and are represented by interbedded horizons of sandstones and packs of clay. The section of Karagan deposits is similar to the section of the Chokrak and differs from the latter only in fauna.

In total, 13 layers of sandstones, some of which are largely bituminized, were noted in the Karagan section. (Khasanov, Shaipov, Zaurbekov, 2010) These deposits are confined to the Grozny manifestation of tar stoves and some others (Bulgat-Irzu). The total thickness of the Karagansk deposits varies between 150-200 m.

Miocene sediments are undivided, according to overlap the formation of the Karagansian stage and are represented mainly by clays, with the appearance of sandstones, marls, shells and conglomerates in the upper part of the section.

Pliocene sediments are characterized by a wide range of lithological differences in rocks: sands, clays, sandstones, limestone, marls, and limestone.

The deposits of the Quaternary system (Q) are represented by clays, loams, sands, and pebbles.

In tectonic terms, the described region belongs to the zone of the Advanced Ranges and the Montenegrin monocline of the Northern slope of the Greater Caucasus.

In the zone of the Advanced Ranges, Tersky, Sunzhensky, Grozny, Bragunsky and Gudermes anticlinoria, as well as the Sunzhensky and Alkhanchurt synclinoria are distinguished. (Khasanov, Shaipov, Zaurbekov, 2010)

He anticlinoria are composed of a series of anticlinal brachisculides elongated in the sublatitudinal direction and complicated by a series of longitudinal reverse faults. As a rule, in the

nuclei of these structures the rocks have a steep occurrence, noticeably flattening towards the northern and southern wings. In the zone of the Montenegrin monocline, the rocks have a stable northern fall at angles of 20-40. The eastern part of the Montenegrin anticline is complicated by the Benoic anticlinal ledge of sub-latitudinal strike with steep northern and flatter southern wings. The central part of the Benoy ledge is complicated by a series of transverse discontinuities. A significant gap was noted along the line of the village of Gilyana - Mount Eli Baving, called the Gilyansky reverse fault. There is an opinion that according to the throw-up in the area with. The Gilans are brought into contact with the Maykop and Karagan-Chokrak deposits, and oil flows from the former to the latter.

Within the described area there are a number of oil and gas fields. (Kerimov, Daukaev, 2003) In hydrological terms, the area can be divided into three zones: the zone of the Advanced Ranges, the lowland zone and the Black Mountains zone. In the zone of the Advanced Ranges, formation-fractured waters confined to the cover are developed. In the lowland zone, aquifers of the Pliocene, Pleistocene, and also underground waters of the terrace complex are noted. The Black Mountains zone is hydrologically poorly understood. Potentially aquifers are sandstones of Karaganchokrak deposits.

When studying promising areas of bituminous strata in the Chechen Republic, only 9 sites were covered: Grozny, Sernovodsky, Simsirsky, hkendatenn-Kort, Bulchat-Irzu, Kuren-Benoy, Gudermes, Bragunsky. (Mitchin, 1992) (Figure 1).

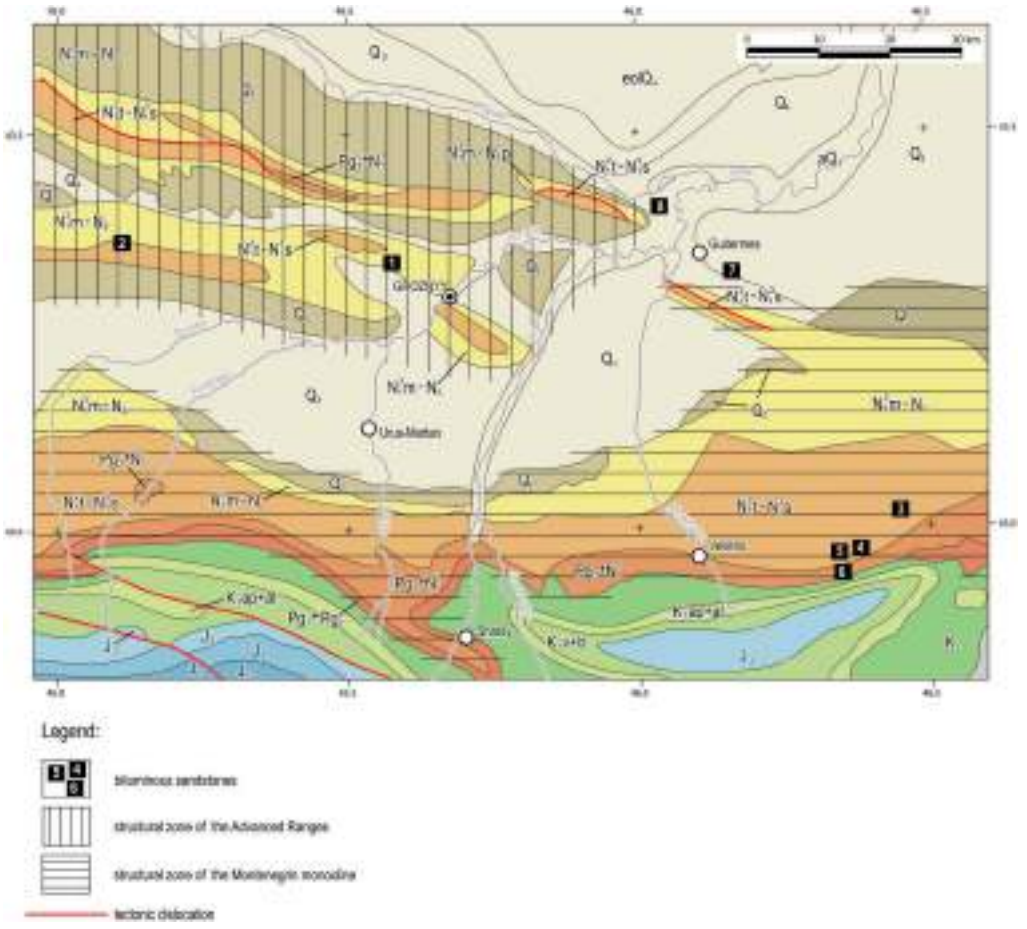

Figure 1. Schematic map of the manifestations of tar sandstones.

The numbers on the map indicate

№	Name	Location
1	Grozny site	Starogroznensky ridge, Mamakaevskaya beam
2	Sernovodsky site	On the southern slope of the Sunzhensky ridge, between the villages of Sernovodsk and Sleptsovskaya
3	Simsirsky district	District of the village of Simsir, the confluence of the Yaryk-Su and small Yaryk-Su
4	Section Mahkendatten	Court 2.5 km east of the village. Bulgat Irzu
5	Plot Bulgat-Irzu	Western outskirts with. Bulgat Irzu
6	6 Section Kuren-Benoy	Northern outskirts of the village
7	Gudermes	section 4-5 km Southeast of Gudermes on the northern slope of the Gudermes ridge
8	Bragunsky site	4-5 km. west of s. Braguns, on the northern slope of the Bragun range

In these studies, the following tasks were solved:

- study of the geological structure of the site;
- the allocation in the context of tar packs, layers of "industrial" intervals;
- determination of the contour of productive intervals and assessment of their mining and geological conditions;
- determination of bitumen content and the nature of its change;
- clarification of the physico-chemical characteristics of bitumen-containing rocks and their interposition with the host rocks;
- a qualitative assessment of the mineral;
- determination of technological parameters and their compliance with the requirements for road construction.

The remaining sites were studied in less detail.

Grozny site. It is located on the northwestern outskirts of Grozny in the Mamakayevskaya beam (the Starogroznensky ridge is a spur of the Sunzhensky ridge). The size of the surveyed area is 1.1 x 0.7 km2. Only part of the selected promising area measuring 100x300 m2 was subjected to detailed examination.

The orographically studied site occupies the valley of the Mamakayevskaya beam, which has sides 30-40 m high, composed of sandstone layers. By age, sandstones belong to the Sarmatian and Karagansk layers. Overlap loams of Quaternary age, low power.

The mineral is confined to the Karagansky bituminous sandstones, which form an anticlinal fold, the core of which is opened by the Mamakayevsky beam incision.

Sandstones are heterogeneous, with a predominance of fine-grained and silty differences of massive texture, gray to black, depending on the intensity of bitumen saturation. In the absence of bitumen, sandstones are light gray to white in color with a slight yellowish tint. Visually, the bituminous intensity is heterogeneous, and it was not possible to establish any regularities in its distribution.

Productive sandstones are overlain by weak interbedded clays and marls of the Sarmatian stage, which reach up to 30 m in thickness to the north and south from the outcrops of the studied layers at a distance of 50-60 m.The Grozny site was studied by routes and five clearing, of which 65 laboratory and 1 laboratory and technological samples were selected. (Table 1.)

The table shows an extremely uneven distribution of bituminousness in the Grozny manifestation - from a practical absence to a high content. In general, according to the manifestation of bituminosity, sandstones and sands are characterized as having a low bitumen content.

According to the mineralogical composition, sands are essentially quartz; the silica content in them varies from 96.14% to 98.01%.

Based on the ratio between water saturation and strength of water-saturated samples at 2000 ° C, the optimum values of the amount of bitumen in the asphalt-concrete mixture were

Table 1. Characterization of bituminous sandstones of the Grozny site.

№	№ workings	Number of samples	Bitumen content,%		
			from	to	from to weighted average
1	Clearing 1	9	3,17	39,4	9,46
2	Clearing 2	17	0,19	3,66	1,61
3	Clearing 3	13	0,08	2,43	0,74
4	Clearing 4	11	0,89	3,08	2,15
5	Clearing 5	15	1,79	8,59	0,39
6	Manifestation	65	0,08	39,4	2,95
7	Regulations	Not less 2 %			

determined, which are 54% for the sample. The knowledge of the manifestations allows us to classify reserves by C2.

The expected reserves of the Grozny manifestation with a deposit width of 100 m, a length of 300 m and an optimal thickness of 6 m are: 100x300x6 = 180 thousand m3.

Simsirsky site. Located 0.5 km north of the village of Sim-Sir Nozhai-Yurt district at the confluence of the rivers Yaryk-Su and Malaya Yaryk-Su. Erosion processes here formed an isolated isometric area, armored with a layer of tar sandstones. The size of the site is 500x100 m2. In geomorphological terms, it is an inclined plane in the northwest direction cut off from the north, west and east by a river cut.

Exceeding the maximum values of the site above the confluence of the rivers reaches 120 m. The sides of the river valleys are gorges formed by cuts into sandstone packs.

The geological structure of the site is simple. It is composed of a rather powerful (up to 15 m) pack of sandstones of the Chokrak stage, covered by an alluvial-deluvial cover of loam with detrital material and underlain by shaley argillite-like clays. The fall of bedrock (sandstones and shale clay) is measured in the north-western rumbas, the angle of incidence is 200.

The mineral is represented by tar sandstone. Its thickness varies within 8-15 m. The section of the sandstone layer from the roof to the bottom is presented in the following form:

- loose sandstone light gray to white - up to 4 m,
- weakly bituminous banded sandstone - up to 4 m,
- medium-bituminous banded sandstone - up to 6 m,
- strongly bituminous banded sandstone - up to 2 m.

Visually, the bituminous content of the rocks is uneven.

The upper part of the sandstones, especially in exposed areas, washed and sandstones become white with no signs of bitumen. Down the section of the sandstone formation, the degree of bituminousness increases, reaching its maximum at the bottom. (Table 2). Bitumen and crusts of bitumen are formed in this part, especially with the development of fracturing.

Table 2. Characterization of bituminous sandstones of Simsirsky site.

№	Clearings	Number of samples	Bitum contains, %		
			from	to	average
1	Clearing 20	10	0,91	6,57	4,39
2	Clearing 21	8	0,58	3,81	1,37
3	Clearing 23	12	3,72	6,61	4,82
4	Clearing 24	14	1,98	3,05	2,42
5	Clearing 25	13	2,28	6,05	4,60
6	Clearing 26	10	3,43	7,11	6,22
7	On site	67	0,58	6,61	3,86
8	Regulations	Not least 2 %			

Table 3. Characteristics of bituminous sandstones of the Mahkendatten Cort.

№	Clearings	Number of samples	Bitum contains, %		
			from	to	average
1	Clearings 27	4	2,67	3,72	3,38
2	Clearings 28	5	0,01	4,30	2,41
3	Clearings 29	5	1,08	1,54	1,34
4	Clearings 30	5	0,72	2,01	1,59
5	Clearings 31	5	0,09	1,14	0,52
6	Clearings 32	5	0,83	1,43	1,18
7	Clearings 33	5	1,34	1,68	1,56
8	ON the site	34	0,01	4,3	1,62
9	Regulations	Not least 2 %			

In hot weather, drops and streams of bitumen form on the surface of the rocks and a characteristic "asphalt" smell is felt at a considerable distance

It follows from the table that, as for individual intersections, and for the site as a whole, the distribution of bitumen saturation is heterogeneous and is classified from low contents (p. 21, 24) to medium (p. 20,23,25,26), average bitumen content in the site characterized as low, close to average.

According to the grain size and size modulus, the sands are fine-grained, with a clear predominance of the 0.14 fraction.

By mineralogical composition - quartz sands, with silica content of 96, 34-98, 37%.

The studied area has forecast reserves of categories C2 in accordance with the sizes 500x100x10 m3 -500 thousand m3, i.e. the deposit is small.

Section Mahkendatten - Court. It is located 2.5 km east of the village of Bulgut - Irzu in Nozhai - Yurt district and is confined to a gentle hill with a mark of 1008.7 m. On the northern and southern slopes, erosion processes in the form of a 10-15 meter ledge reveal tar sands of the Chokrak stage, which object of search work.

Judging by the elements of occurrence, two layers are recorded here, separated by a 10-15 meter pack of clay rocks. The bedding of the strata is north-western at angles of 200. An optimized section of sandstones, compiled from clearing, is presented as follows:

- uneven-grained sandstone - 1-4 m,
- fine-grained sandstone, silty - 4-7 m,
- uneven-grained sandstone - 7-11 m.

The observed bitumen saturation of the host rocks varies. More saturated rocks, exposed on the southern slope (clearing 28). In hot weather, a hydrocarbon consistency flows out of the formations, which is quite liquid and oily with the smell of oil.

The site is contoured along the perimeter by seven clearing sites (p. 27-33), of which 34 samples were taken. Bituminous rocks are characterized as follows (Table 3).

The table shows that this site is characterized by a fairly uniform, albeit low bitumen content.

The mineralogical composition of the sands is quartz, with a silica content of 97.28%.

The Makhkendatten-Kort section has reserves of up to 325 thousand m3, in accordance with the dimensions 250x130x10 m, which is characterized as a small field, in the presence of the likelihood of continuation of productive formations of the considered section along strike. Although the geomorphology of the region does not fully confirm these assumptions.

2 CONCLUSION

Thus, the available geological materials on the outputs of the bituminous sites allow us to say the following: all deposits promising for bituminousness are confined to two structural

zones — the zone of the Advanced Ranges and the zone of the Montenegrin monocline. (Ganieva, Polovnyak, 2012)

The zone of advanced ranges (Tersky, Sunzhensky, Gudermes and Bragunsky) is represented by anticlinoria, folded brachiskladas of various orders and complicated by numerous fractures of the thrust nature. (Mitchin, 1992) The bedding here is mostly steep, productive horizons of bituminous rocks quickly "dive" under the deposits overlapping them. In this zone, the Grozny, Sernovodsky, Gudermes and Bragunsky sites were studied. In general, the zone of the Advanced Ranges should be classified as unpromising for the identification of deposits of bituminous rocks. (Zaurbekov, Mintsaev, Cherkasov, Labazanov M.M., Shaipov,Damzaev, 2015)

The zone of the Montenegrin monocline is composed of monoclinically falling to the north at angles of 20-400 rock strata, including bituminous. Theoretically, in this zone it is possible to identify deposits of bituminous rocks.

Within the Montenegrin monocline, the sections Simsirsky, Mahkendatten-Kort, Bugat-Irzu, Kuren-Benoi were studied. Only the Simsirsktä and Mahkendatten-Kort sections have certain prospects.

REFERENCES

Ganieva T.F., Polovnyak V.K. 2012 High viscosity oils, natural bitumen and bituminous rocks. Kazan: Kazan National Research Technological University

Kerimov I.A., Daukaev A.N. 2003 Minerals of the Chechen Republic. Terrible: GGNI

Khasanov M.A., Shaipov A.A., Zaurbekov Sh.Sh. 2010 Geology and oil and gas bearing Phanerozia of the Eastern Ciscaucasia. Terrible: GSTU named after Acad. M.D. Millionschikova; Stavropol: Sev-KavSTU; Service School

Mitchin A.D. 1992 Report on the results of prospecting for tar sands in the Chechen Republic. The terrible

Orel V.E., Raspopov Yu.V., Skripkin A.P. 2001 Geology and oil and gas potential of the Ciscaucasia. Moscow: GEOS

Zaurbekov Sh. Sh., Mintsaev M.Sh., Cherkasov S.V., Labazanov M.M., Shaipov A.A., Damzaev Z.M. E. 2015. Prospects for oil and gas potential and further areas of geological exploration within the Tersko-Sunzhenskoye oil and gas region. Moscow. Territory Neftegaz.

Advances in Raw Material Industries for Sustainable Development Goals – Litvinenko (Ed)

The method of multivariate geological modeling and wells correlation of pashiysky horizon

M.G. Ayrapetyan
Postgraduate student, St. Petersburg mining University, St. Petersburg, Russia

A.A. Farukshin
Postgraduate student, St. Petersburg mining University, St. Petersburg, Russia

Y.V. Nefedov
PhD, Associate professor, St. Petersburg mining University, St. Petersburg, Russia

ABSTRACT: This article describes the method of multivariate calculation of geological uncertainties and the first stage of the geological model construction - well correlation of the pashiysky horizon of Novosergievsky and Perevolotsky districts of the Orenburg region in the domestic tNavigator software product of RockFlowDynamics. This technique allows to construct geological models of the pashiysky horizon on variants P10 (optimistic), P50 (realistic), P90 (pessimistic), thereby to estimate risks and to carry out quality control of geological model. This method is used to construct structural maps of the roof and bottom of the pashiysky horizon.

1 INTRODUCTION

Against the background of the decrease in recoverable oil reserves of large deposits in the world and in Russia, the intensification of hydrocarbon production at current assets is a very urgent problem. One of the forced approaches to increase the production of hydrocarbons is the involvement in the development of small reserves and complex formations. A characteristic feature of field development in the oil and gas industry is the emphasis on the main object of development, while secondary layers may actually be no less profitable. Insufficient attention to secondary objects of development of oil and gas fields today is a challenge for oil and gas companies not only in Russia but also around the world.

One of such perspective layers is the pashiysky horizon of the Orenburg region. In the fields of the territory of Novosergievsky and Perevolotsky districts, the pashiysky horizon is a secondary potential object of development with a rather complex geological structure.

The problem of the object of research is the insufficiency of studying the formation, complex facies and tectonic structure, which leads to the impossibility of in-depth analysis of the filtration-capacitive properties of the horizon and its oil and gas potential. The interest to the object is caused by single wells producing oil from the pashiysky horizon, which indicates the confirmed oil and gas potential of the reservoir in the studied area. Thus, the identification of inhomogeneities and patterns of distribution of the filtration-capacitive properties of the pashiysky horizon will help to increase the understanding of the structure and geometry of the formation for further development.

This problem can be solved most rationally by methods of geological and hydrodynamic modeling on the basis of a detailed study of the regularities of the structure and properties of the formation. On the basis of data of geophysical researches of wells, their interpretation, core material, and also data on development it is possible to construct conceptual facies, structural and, as a result, geological model of a layer, as much as possible reflecting actual

distribution of properties in a reservoir. And the first stage of the formation study is one of the tasks of this article – well correlation of the formation.

The second important task of the current article is the technique of multivariate modeling. The geologist's ideas about the geological structure of a deposit or formation are never exhaustive. Further decisions on field development depend on the reliability of the geological model. Due to the large number of uncertainties, the simulation will take place in a multivariate mode. In other words, each parameter or property of the formation and fluid will vary within certain boundaries already accepted by core studies and other data. At the final stage, this will determine the most likely model to make a decision and recommendations on drilling, geological and technical measures and production.

2 WELL-TO-WELL CORRELATION

In terms of petroleum Geology, the study area belongs to the East Orenburg oil and gas bearing area, which corresponds to the East Orenburg uplift in tectonic terms. The industrial oil-bearing capacity of the area is associated with deposits of the pashiysky horizon, the Kolgan strata and the Tournai tier.

The Geology of Orenburg and the Orenburg region (Figure 1) includes sedimentary formations of the upper Proterozoic, Paleozoic and Mesozoic, which lie on igneous and metamorphic deposits of the Archean-early Proterozoic crystalline basement (Figure 2).

In the studied area, the main object of development is the Kolgan strata. However, a considerable number of vertical and directional wells opened pashiysky horizon (Figure 3)

Well-to-well correlation was carried out in the following stages (Figure 4, Figure 5):

1. The choice of the reference line, i.e., the reference horizon which can be traced in all the wells.
2. Selection of the reference section, that is, the most representative section, on which all reference layers are clearly well distinguished, sufficient power of the section is presented, a full complex of GIS is performed.
3. Comparison of well sections with reference section.
4. Well-to-well correlation according to different correlation schemes.

Well descriptions and core photos are attached to wells in the software simulator (Figure 6).

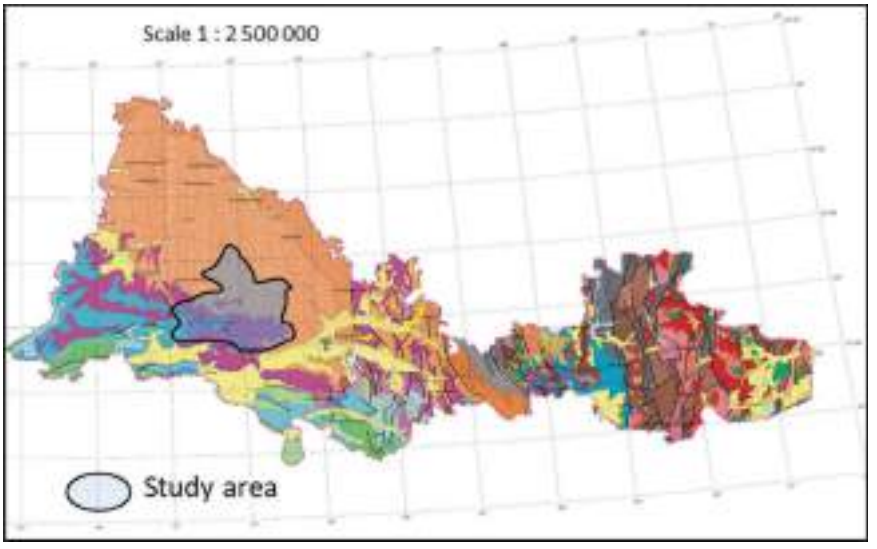

Figure 1. Map of pre-Quaternary formations of Orenburg region.

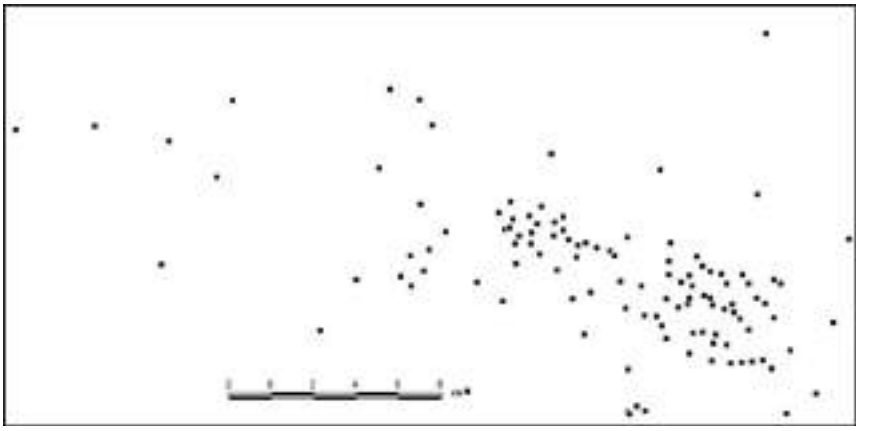

Figure 2. Wells, opening the main object of development in the study area.

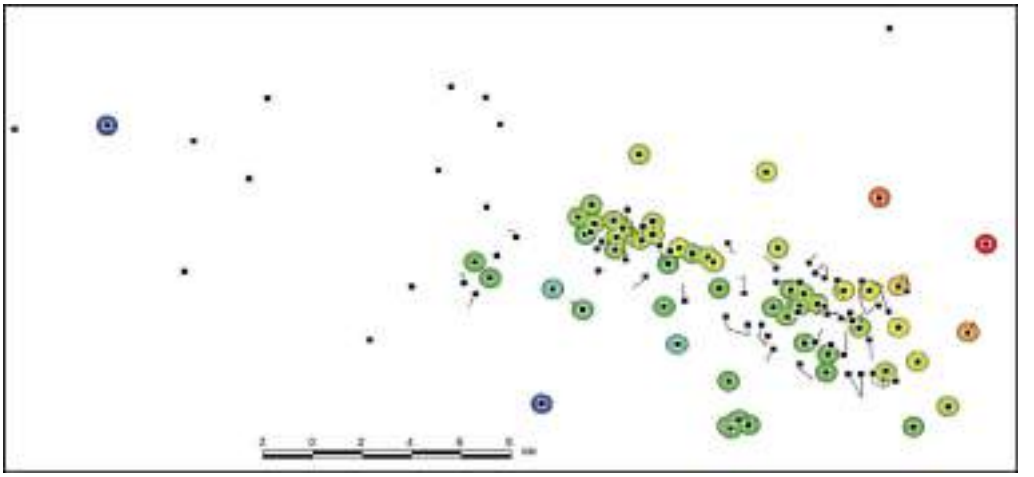

Figure 3. Wells that opened the roof of the pashiysky horizon.

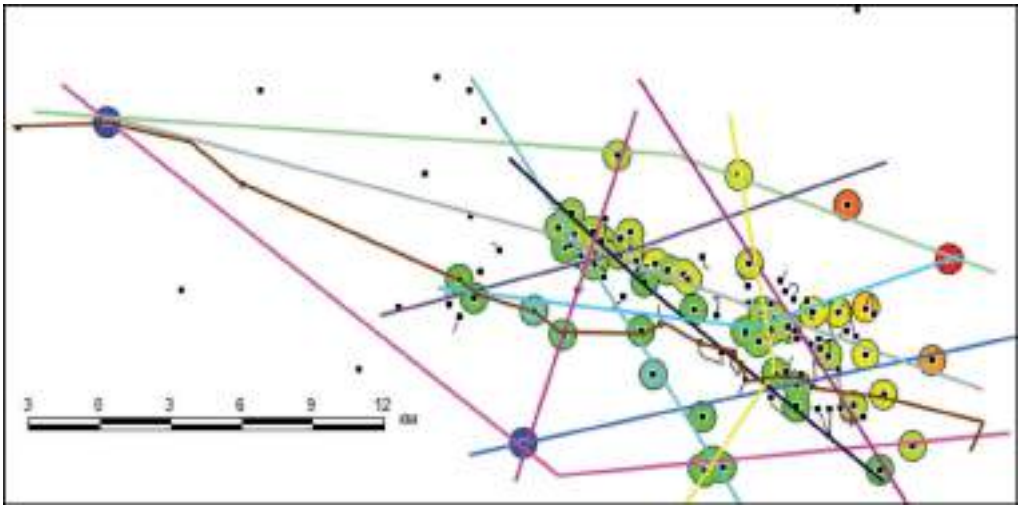

Figure 4. Correlation schemes.

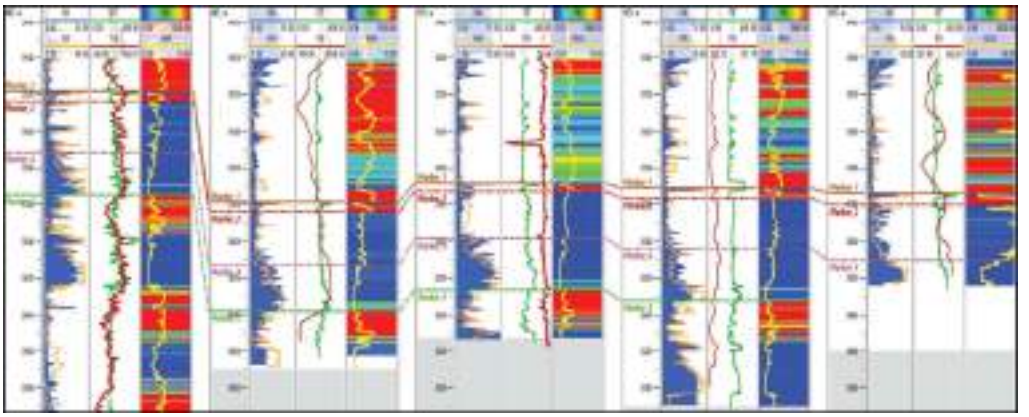

Figure 5. The correlation of the wells penetrated pashiysky horizon.

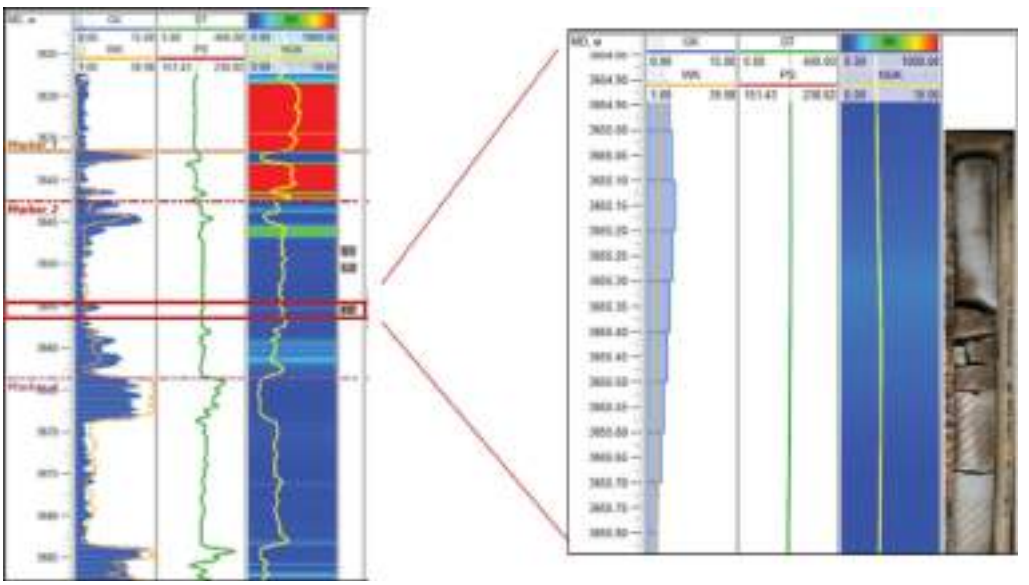

Figure 6. Snap photos and description of the core in the correlation scheme.

The peculiarity of the correlation of the pashiysky horizon was the inhomogeneous structure, which often causes difficulties when comparing well-logs curves. The lack of well data has become the reason for the interpolation of a formation over long distances. The pashiysky horizon is relatively constant in power in the area under study.

The pashiysky horizon is composed of fine - and fine-grained siltstone sandstones, with thin layers of siltstone and mudstone.

Reservoir rocks are sandstones light gray, light gray with a brownish tinge, quartz, porous, strong and medium strength, massive, lenticular-indistinctly layered, obliquely layered texture areas.

Dense clay sandstones, siltstones gray, dark gray, indistinctly layered, lenticular-layered and mudstones dark gray, thinly layered are common in the inefficient part of the formation.

The seal rock is a pack of mudstones of the roof part of the horizon, dark gray, dense, calcareous, with an uneven admixture of sand-silt material, thin-layered.

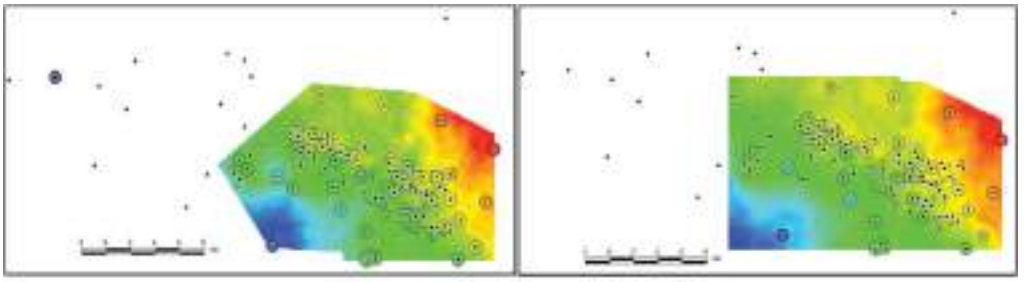

Figure 7. Map of the roof (A) and bottom (B) of the pashiysky horizon.

The deposits of the pashiysky horizon were formed in the conditions of the sea coast with mixed wave and river activity.

3 MULTIVARIATE MODELING TECHNIQUE

The technique of multivariate geological modeling is to vary the parameters and properties of the reservoir and fluid, in which there is no absolute value or there are doubts about their reliability. As a rule, dependencies and studies that are obtained in the process of processing the initial data, give a cloud of values and a significant spread with some trend.

As practice shows, deterministic methods of geological modeling give a figure of reserves, which can change during the development and updating of geological information.

The most important source of uncertainty in the construction of a geological model is the ambiguity of structural simulations.

Stages of multivariate modeling:

1. Estimation of the most probable depths of structural horizons in the inter-well space. The definition of the standard deviation of the depth.
2. Construction of structural horizons of the roof and the sole of the formation in the model.
3. Determination of lithological and genetic types of rocks and probability of distribution of sedimentary body morphology.
4. Filling of the structural framework with lithotypes based on borehole data, given forms of sedimentary body and probabilities of its size.
5. Reservoir filling with petrophysical properties based on probabilistic estimates of rock properties variability.
6. Calculation of hydrocarbon reserves by volumetric method for all possible variants of the geological model.
7. Choice of options P10 (optimistic), P50 (realistic), P90 (pessimistic)

Multivariate structural maps of the roof and sole of the formation were constructed on the basis of this technique and the correlation of the pashiysky horizon. Below are maps of the sole and roof of the pashiysky horizon according to the P50 variant (Figure 7).

4 CONCLUSION

As a result, the following conclusions were obtained:

- Correlation of the pashiysky horizon was carried out
- Snap photos and description of the core to the wells.
- Defines the uncertainty in the spacing layers
- The technique of multivariate geological modeling is proposed
- Maps of the roof and sole layers are constructed.

It is important to use the multivariate approach in geological modeling, when a large amount of information is approximated.

The work showed an approach at the well correlation level. However, this approach is expected to be used at all stages of oil and gas field development.

REFERENCES

Ababkov K. V. (2010). Fundamentals of three-dimensional digital geological modeling. Ufa: *"Oil and Gas business"*.

Bulgakov S. A. Investigation of layers of the pashiysky horizon by probabilistic-statistical Express method. *Samara state technical University. "Oil and gas business"* - Samara, 2011, 75 p.

Dudchenko, O.L., Fedorov, G.B., Andreev, A.A. (2018). Innovative method for the classification of coal slurries. *"Ugol"*.

Gospodarikov, A.P., Zatsepin, M.A. (2019). Mathematical modeling of boundary problems in geomechanics. *"Gornyi Zhurnal"*.

Gutman I. S., Balaban I. Yu., Isyangulova N. R., Potemkin G. N., et al. Modeling of complex oil and gas objects on the basis of detailed correlation of well sections in automatic and interactive modes// *Neft.Gas.Innovations, No. 12*, 2014. - Pp. 16–23.

Gutman I. S., Kuznetsova G. P. Classification of correlation of geological sections of wells in connection with the degree of study of oil and gas objects. *Features of performance of comparison of geological sections of wells with use of the latest computer technologies*. - Moscow: Gubkin Russian state University of oil and gas, 2006.

Zakrevsky K. E. (2009). Geological 3D modeling. Moscow: LLC CPI Mask.

Losheva Z. A., Magdeev M. sh., Agafonov S. G., Fedotov M. V., Magdeeva O. V. a New look at the geological structure of the pashiysky horizon (D3ps) of the Aznakaevskaya area of the Romashkinskoye oil field. *Georesources*. 2017. T.19. No. 1. Pp. 21–26.

Lyadsky P. V., Kvasnyuk L. N., Zhdanov A.V., Chechulina O. V. and others. State geological map of the Russian Federation. Scale 1:1,000,000 (third generation). *A Series Of The Ural. Sheet M-40 (Orenburg) with valve M-41. Explanatory note.* – SPb.: Map factory VSEGEI, 2013. 392 p. + 1 incl.

Potemkin G. N. Features of geological structure and optimization of development of oil and gas potential of Devonian terrigenous deposits of the southern part of the Volga-Ural oil and gas province. Moscow: Gubkin Russian state University of oil and gas, 2016. - 137 c.

Prischepa, O., Nefedov, Y., Grokhotov, E. Geochemical and petrophysical studies of hydrocarbon potential of domanic shale formation (Timan-Pechora petroleum Province) EAGE/SPE Workshop on Shale Science 2019 - Shale Sciences: Theory and Practice DOI: 10.3997/2214-4609.201900475 ISBN: 978-946282281-8

Sinitsyn I. M., Sinitsyna G. I. State geological map of the Russian Federation. Scale 1: 200000. Series The Middle. Sheet O-40-XXXII (kuyeda). Explanatory note. - Moscow: Moscow branch of fsbi "VSEGEI", 2017. 81 PP.

Technical guide simulator "tnavigator". (2017). The Company "Rock Flow Dynamics". Moscow.

Advances in Raw Material Industries for Sustainable Development Goals – Litvinenko (Ed)
© 2021 Taylor & Francis Group, London, ISBN 978-0-367-75881-3

Geological and economic assessment of resources of oil field of the West-Siberian oil and gas province

A.Kh. Ibatullin
Postgraduate student, Saint-Petersburg Mining University, Saint-Petersburg, Russia

A.M. Zharkov
Doctor of geological and mineralogical Sciences, Saint-Petersburg Mining University, Saint-Petersburg, Russia

O.E. Kochneva
PhD in Geology and Mineralogy, Associate Professor, Saint-Petersburg Mining University, Saint-Petersburg, Russia

ABSTRACT: The presence of a geological structure partially determines the formation of the field. In addition, experts need to analyze other parameters that affect the accumulation of hydrocarbons in prospective traps. In this article a feasibility study of geological exploration of West-Siberian deposit was carried out, within which structural maps were built for 24 layers and the profitability of the proposed project was estimated. This article describes different methods (geological and economic) of identifying prospective oil and gas zones and deciding whether to involve the territory in the geological study project.

1 INTRODUCTION

The oil field is geographically located in the Yamalo-Nenets Autonomous District of the Tyumen Region. In the northeast corner of the license area, structures are identified that could potentially contain hydrocarbon fields. Based on the calculation of the resource potential and the analysis of geological risks, an appraisal was made of the feasibility of prospecting work, a tree of scenarios was built, and an analysis of VOI (value of information) was executed.

Tasks:

1. Construction of 1D-2D geological model, which will be used to evaluate and analyze information;
2. Answer the question about the need for geological prospecting;
3. Assess the resources of field;
4. Assess the appropriateness of conducting geological prospecting in the north-eastern section.

2 CHOICE OF RESEARCH FACILITIES

The first stage of the study is the determination of reservoirs. Of the 31 strata of the Cretaceous age, available on the territory of the field, 24 are selected. They are presented in Table 1. The criterion for the selection of strata is a change in isohypses to lower depths in the northeastern part, which leads to the presence of promising positive dome-shaped structures. The main factor in the study of this area was the location of the tectonic structure of

Table 1. Reservoirs with promising structures in the north-eastern part of the field.

	Age of collectors		
№	Sukhududinskaya suite	Malohetskaya suite	Pokurskaya suite
1	BU6-3	MH1	PC1-3
2	BU7	MH3	PC12-1
3	BU8	MH4	PC15
4	BU9	MH5	PC19
5	BU10-1	MH71	PC20-1
6	BU10-2	MH8-9	PC20-2
7	BU11-1		PC21-1
8	BU12-2		PC21-2
9			PC22-1
10			PC22-2

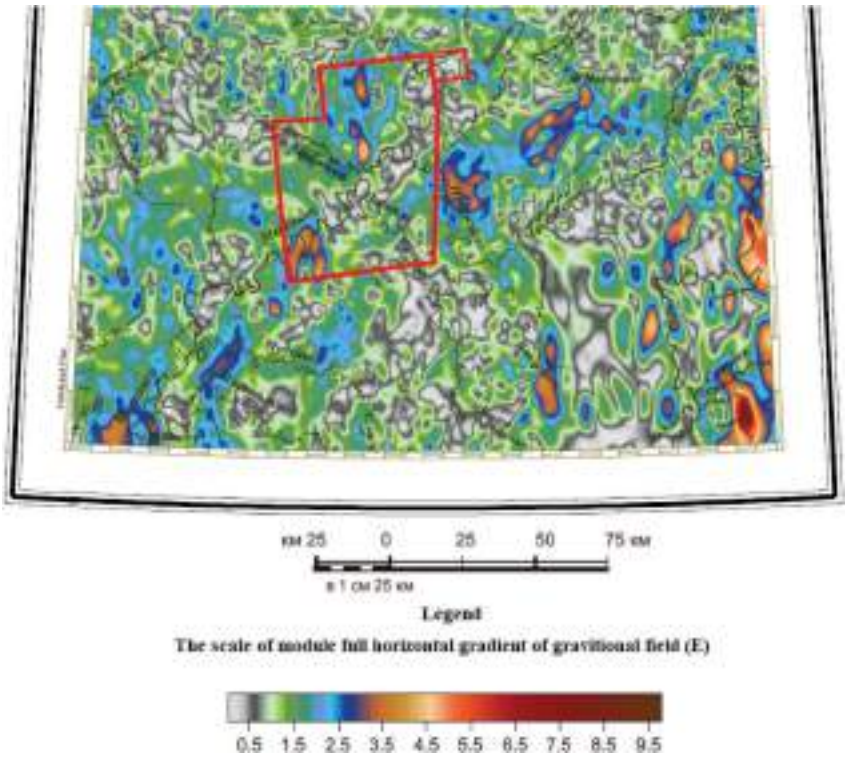

Figure 1. Fragment of map of full horizontal gradient module of gravitational field (Egorov T.N.).

the 3rd order (Figure 2) at the Ust-Port megaswell, adjacent to the Messoyakha megaswell (Egorov et al, 2016). Confirmation of the presence of hydrocarbons at the object of interest is a map of the module of the full horizontal gradient of the gravitational field (Figure 1), which shows abnormally low values in the north-eastern part of the field. When comparing detailed gravitational anomalies constructed from high-precision gravimetric measurements in oil and gas fields, it was found that oil and gas fields are displayed with relatively negative anomalies.

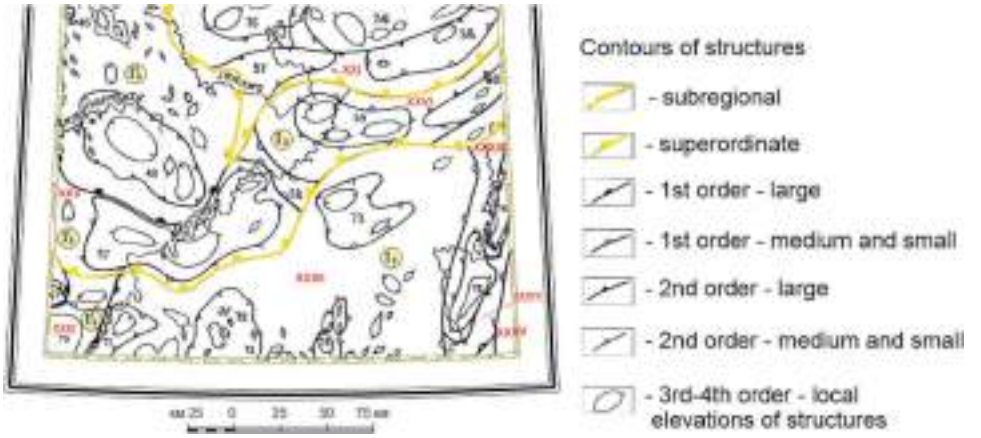

Figure 2. Fragment of tectonic map. I_3 – Messoyakh-Antipayutin zone of liner structure; I^2_3 – Messoyakha Belt magavals.

3 CALCULATION AND SELECTION GEOLOGICAL PARAMETERS OF OBJECTS

After selecting the reservoirs of interest, resources were calculated and the geometrical parameters of the fields were specified. As noted earlier, there are no seismic and borehole data outside the licensed area, which significantly complicates further calculations (Prishepa & Nefedov, 2018; Cherepovitsyn et al, 2018). Using bicubic extrapolation, in Schlumberger Petrel software, structural maps were plotted for all collectors in the area of interest. Bicubic extrapolation is a method of calculating a parameter from two others beyond the area of available data (Gospodarikov & Zatsepin, 2019). From a geological point of view, this means determining depths from coordinates outside the licensed area. The result was the allocation of 24 traps outside the license area, which are located on the area of 12.5 km × 10 km.

As a result, the geometrical parameters of promising traps were obtained, which are presented in Table 2 with the geological volumes of the traps.

4 EVALUATION OF INITIAL RECOVERABLE RESOURCES

Monte-Carlo simulation is a random selection method. The algorithm consists in selecting values from the indicated intervals, substituting them in the necessary formula. The advantage of this method is that it can be used by Microsoft Excel.

Initially, distribution type for each parameter should be specified. Two types of distribution were used in the work:

1. Uniform (GRV, NTG, density, conversion factor, oil recovery factor);
2. Normal (Kporo, Ko).

As a result of work, 8000 realizations were generated for each parameter and 1,344,000 values were obtained at the output. The parameters were taken according to the data of wells drilled at the field earlier (Table 4). The calculation of resources was carried out by the volumetric method according to the formula (1) (Gutman & Sahakyan, 2017, Nedosekin et al, 2019):

$$Q = GRV \times NTG \times Kporo \times Ko \times \rho \times \theta \times ORF \quad (1)$$

where GRV - gross rock volume; NTG – net to gross; Kporo - porosity factor; Ko - oil saturation factor; ρ – density; Θ - the recalculation factor; ORF - oil recovery factor. Using

Table 2. Geometric parameters of perspective traps.

Horizon	Gross rock volume	
	Max (P10), thous. m^3	Min (P90), thous. m^3
BU12-2	406887.000	2202.130
BU11-1	398479.000	91846.400
BU10-2	422400.000	18160.800
BU10-1	423940.000	2643.580
BU9	442589.000	25475.300
BU8	289241.000	3510.220
BU7	333590.000	1329.390
BU6-3	392238.000	1994.120
MH8-9	415825.000	18481.500
MH7-1	82445.000	42239.000
MH5	96548.000	151.769
MH4	119869.000	22137.200
MH3	168850.000	47274.400
MH1	288077.000	26938.200
PC22-2	262542.000	88.335
PC22-1	305907.000	46030.300
PC21-2	192563.000	4930.790
PC21-1	160561.000	3417.710
PC20-2	118530.000	891.833
PC20-1	124591.000	42.546
PC19	91821.800	738.545
PC15	129476.000	4613.470
PC12-1	139719.000	13031.400
PC1-3	930820.000	4651.910

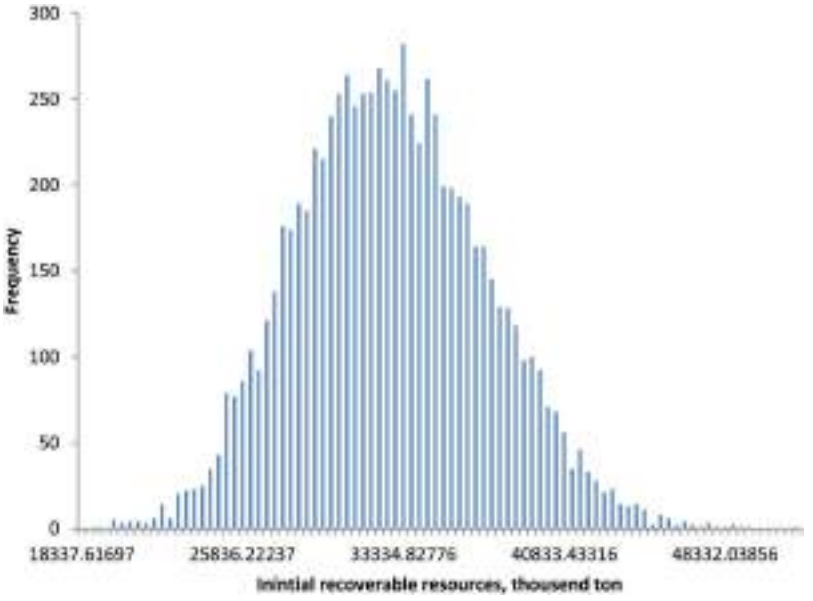

Figure 3. The distribution of resources in the north-eastern part of field No. 1 constructed by Monte-Carlo method.

Table 3. Initial recoverable resources calculated by the Monte Carlo method.

Probability	Resources, million tons
P90	26,97
P50	32,42
P10	38,29

the Monte-Carlo method, we obtained the normal distribution of resources (Figure 3) calculated in Microsoft Excel and the volumes of initial recoverable resources presented in Table 3.

Additionally, the calculation was performed in the Oracle Crystal Ball software package, which allows to process large amounts of data than the mathematical apparatus of Microsoft Excel al-lows. The methodology for selecting a random distribution is similar to that described above. A feature of the Oracle Crystal Ball software package is that it allows to perform more than 40,000 realization at a time. At the end of the calculation, the distributions of the initial recoverable re-sources were obtained (Figure 4), descriptive statistics (Table 5) and the values of probable re-sources (Table 6).

Analysis of the obtained values of probable resources and descriptive distribution statistics showed similar calculation results, which indicates the reliability of the work performed. The result is also confirmed by the sensitivity value, in which the main contribution to the distribution is made by the values of the geological volume of the rocks (75.9%).

5 DETERMINING THE PROBABILITY OF GEOLOGICAL SUCCESS

Geological Chance of Success (gCos, probability of geological success) - the probability which the discovery of an oil field will occur, estimated taking into account all existing uncertainties (Glebov, 2016).

This parameter is directly related to conditions for formation of hydrocarbon fields. The main probabilities reflect the result of a particular type of process, which form an accumulation of oil and gas in the reservoir (Shatrov, 2015). Depending on the method, the number of variables can vary from 4 to 6 (Gorbovskaya, 2017). In this work, five parameters were used that reflect the entire process of formation of the field and take into account the necessary conditions for this: Formation of the oil source reservoir (Posr); Migration of hydrocarbons (Pm); The presence of a collector for the accumulation of hydrocarbons (Pc); The presence of traps (Pt); Safety (Ps).

The total probability of occurrence of independent events is equal to their product (2):

$$gCos = Posr \times \mathrm{P}m \times \mathrm{P}c \times \mathrm{P}t \times \mathrm{P}s \tag{2}$$

Probabilities of geological success for each formation are given in Table 7.

6 BUILDING A DECISION TREE

The decision tree is a graphical method of information analysis that displays the process of taking managerial decisions in the form of a set of sequential alternative actions and the realization of scenarios characterized by the presence of risks and uncertainties, combinations of which, at given probabilities, lead to the achievement of goals (Figure 5).

After the construction of the Decision Tree, information value (VOI) was estimated including NPV and probability for each outcome (Alekseeva et al, 2019), as well as EMV for all branches separated by probable events (Efimov & Tashlitskaya, 2013). NPV (Net Present Value): net present value of free cash flow (calculated by formula (3)):

Table 4. Estimated parameters by horizons.

	Geological volume of rocks, thousand, m3		NTG, fractions		Kporo, fractions		Ko, fractions		Density, g/cm3		Correction factor, fractions		ORF, fractions	
Horizone	Min	Max	Min	Max	Min	Max	Min	Max	Min	Max	Min	Max	Min	Max
BU12-2	2202.130	406887.000	0.300	0.700	0.163	0.209	0.439	0.631	0.816	0.865	0.554	0.870	0.210	0.290
BU11-1	91846.400	398479.000	0.200	0.400	0.187	0.188	0.532	0.538	0.839	0.842	0.702	0.718	0.210	0.290
BU10-2	18160.800	422400.000	0.500	0.800	0.164	0.210	0.440	0.633	0.816	0.865	0.553	0.868	0.210	0.290
BU10-1	2643.580	423940.000	0.400	0.800	0.164	0.210	0.438	0.632	0.816	0.865	0.552	0.872	0.210	0.290
BU9	25475.300	442589.000	0.300	0.700	0.164	0.210	0.580	0.617	0.816	0.865	0.553	0.872	0.210	0.290
BU8	3510.220	289241.000	0.300	0.700	0.164	0.210	0.442	0.633	0.816	0.865	0.551	0.870	0.210	0.290
BU7	1329.390	333590.000	0.300	0.700	0.164	0.209	0.440	0.632	0.816	0.865	0.553	0.868	0.210	0.290
BU6-3	1994.120	392238.000	0.300	0.700	0.164	0.210	0.580	0.617	0.816	0.865	0.553	0.872	0.210	0.290
MH8-9	18481.500	415825.000	0.400	0.800	0.212	0.252	0.409	0.545	0.830	0.910	0.829	0.910	0.210	0.290
MH7-1	42239.000	82445.000	0.400	0.800	0.211	0.252	0.409	0.543	0.848	0.907	0.830	0.910	0.210	0.290
MH5	151.769	96548.000	0.500	0.900	0.212	0.252	0.409	0.543	0.848	0.907	0.829	0.910	0.210	0.290
MH4	22137.200	119869.000	0.400	0.800	0.211	0.252	0.407	0.543	0.848	0.907	0.829	0.910	0.210	0.290
MH3	47274.400	168850.000	0.300	0.600	0.212	0.252	0.408	0.541	0.847	0.908	0.830	0.910	0.210	0.290
MH1	26938.200	288077.000	0.600	0.800	0.212	0.252	0.408	0.541	0.847	0.908	0.830	0.910	0.210	0.290
PC22-2	88.335	262542.000	0.200	0.600	0.233	0.289	0.421	0.617	0.873	0.923	0.875	0.918	0.210	0.290
PC22-1	46030.300	305907.000	0.200	0.700	0.233	0.289	0.420	0.618	0.873	0.923	0.875	0.918	0.210	0.290
PC21-2	4930.790	192563.000	0.200	0.700	0.233	0.288	0.421	0.617	0.873	0.923	0.876	0.918	0.210	0.290
PC21-1	3417.710	160561.000	0.300	0.700	0.233	0.289	0.420	0.619	0.873	0.923	0.876	0.918	0.210	0.290
PC20-2	891.833	118530.000	0.200	0.700	0.233	0.289	0.420	0.618	0.873	0.922	0.875	0.918	0.210	0.290
PC20-1	42.546	124591.000	0.300	0.700	0.233	0.290	0.420	0.617	0.873	0.923	0.876	0.917	0.210	0.290
PC19	738.545	91821.800	0.200	0.700	0.233	0.288	0.420	0.617	0.873	0.923	0.875	0.918	0.210	0.290
PC15	4613.470	129476.000	0.300	0.700	0.233	0.289	0.422	0.619	0.873	0.923	0.876	0.918	0.210	0.290
PC12-1	13031.400	139719.000	0.300	0.700	0.233	0.289	0.420	0.619	0.873	0.923	0.876	0.917	0.210	0.290
PC1/3	4651.910	930820.000	0.400	0.900	0.272	0.317	0.564	0.681	0.945	0.950	0.970	0.975	0.250	0.300

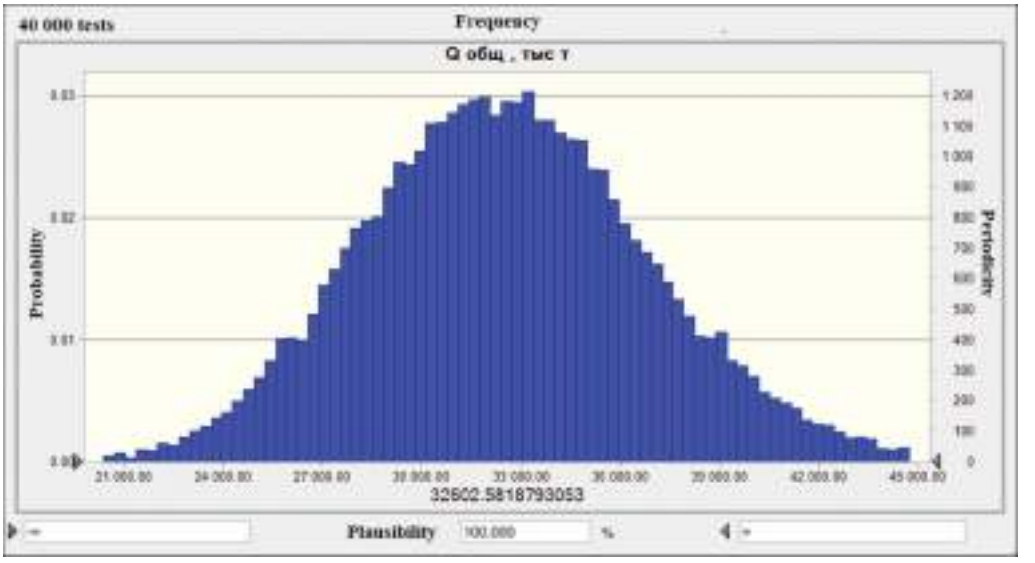

Figure 4. Calculation of the distribution of resources in the north-eastern part of field per-formed in the Oracle Crystal Ball software package.

Table 5. Descriptive statistics of resource allocation.

Statistics	Forecast values
Test	40 000
Base value	32 602,58
Mean	32 550,68
Average	32 439,68
Standard deviation	4 342,53
Discrepancy	18 857 562,34
Asymmetry ratio	0,1797
Excess ratio	3,03
Coefficient. Variations	0,1334
Minimum	16 195,62
Maximum	51 952,11
Average square error	21,71

$$NPV = Income_I - Consumption_I \tag{3}$$

EMV (Expected Monetary Value): expected cash value (calculated by formula (4)).

$$EMV = \sum (NPV_i \times p_i) \tag{4}$$

VOI (Value of Information): The value of Information (DI or VOI) is the increase or decrease in the value of an asset after acquiring information on its further study (Warren, 1983; Reidar, 2009; Whitney, 2010). The Value of Information is calculated by the formula (5):

$$VOI = EMV_1 - EMV_2 \tag{5}$$

Table 6. Probability resources.

Percentile	Forecast values, thousand tons
P100	16 195,62
P90	27 078,05
P80	28 860,11
P70	30 190,54
P60	31 338,40
P50	32 439,56
P40	33 521,78
P30	34 728,50
P20	36 133,22
P10	38 207,28
P0	51 952,11

Table 7. Probability of geological success in studied formations.

Horizon	Oil	Migration	Collector	Trap	Safety	gCos
PC1-3	1.00	1.00	0.64	0.4	0.7	0.182
PC12-1	1.00	1.00	0.64	0.4	0.7	0.182
PC15	1.00	1.00	0.65	0.4	0.68	0.178
PC19	1.00	1.00	0.63	0.4	0.67	0.171
PC20-1	1.00	1.00	0.67	0.4	0.71	0.19
PC20-2	1.00	1.00	0.67	0.4	0.69	0.186
PC21-1	1.00	1.00	0.65	0.4	0.68	0.178
PC21-2	1.00	1.00	0.66	0.4	0.71	0.189
PC22-1	1.00	1.00	0.63	0.4	0.69	0.174
PC22-2	1.00	1.00	0.64	0.4	0.72	0.182
MH1	1.00	1.00	0.66	0.4	0.71	0.186
MH3	1.00	1.00	0.64	0.4	0.71	0.181
MH4	1.00	1.00	0.68	0.4	0.7	0.191
MH5	1.00	1.00	0.67	0.4	0.69	0.185
MH7-1	1.00	1.00	0.66	0.4	0.7	0.185
MH8-9	1.00	1.00	0.65	0.4	0.69	0.18
BU6-3	1.00	1.00	0.64	0.4	0.69	0.18
BU7	1.00	1.00	0.66	0.4	0.69	0.184
BU8	1.00	1.00	0.65	0.4	0.71	0.185
BU9	1.00	1.00	0.63	0.4	0.69	0.177
BU10-1	1.00	1.00	0.64	0.4	0.69	0.175
BU10-2	1.00	1.00	0.65	0.4	0.69	0.181
BU11-1	1.00	1.00	0.66	0.4	0.71	0.189
BU12-2	1.00	1.00	0.64	0.4	0.68	0.173

Having analyzed the "Decision Tree", three values of EMV were calculated:

- In the case of the purchase of area (EMV1 = 9.989 billion rubles)
- In the case of leasing of medical facilities and carrying out of construction and installation works (EMV2 = 9.934 billion rubles)
- In the case of a leased asset rental without carrying out of construction works (EMV3 = 4.219 billion rubles)

Next, an EMV must be selected, which will be used to evaluate the value of the information. Priorities for further evaluation are EMV2 and EMV3. Since EMV2> EMV1, it is able to provide greater risk reduction.

VOI = EMV2 - EMV3 = 9.934-4 4.219 = 5.714 billion rubles

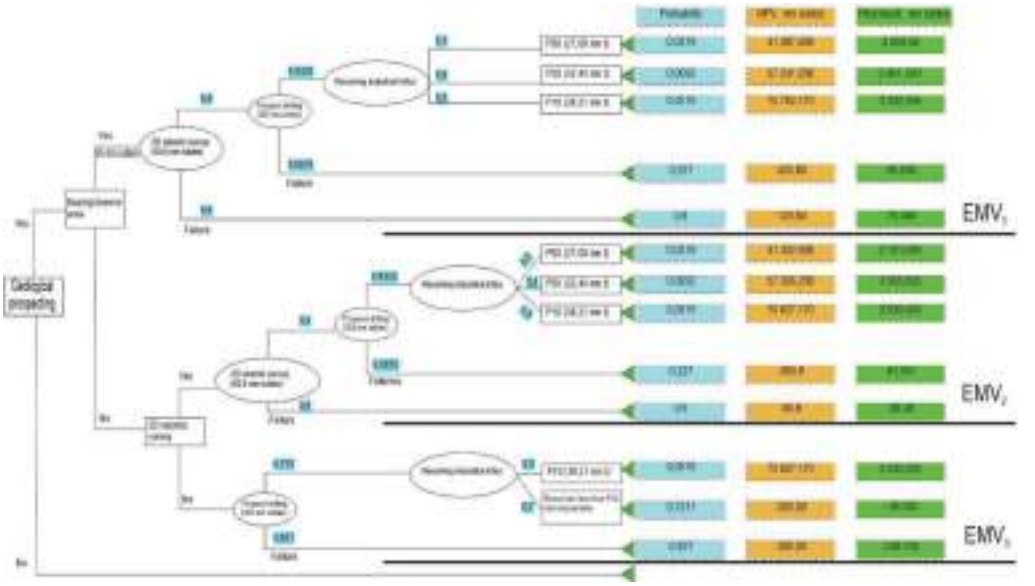

Figure 5. The decision tree.

A positive VOI determines the planning of a solution for 2D seismic survey and reduces our costs and risks when choosing this scenario by 5.714 billion rubles.

7 DISCUSSION

The described methodology for assessing resources allows to study the investigated object from two perspectives: geological and economic. The basis for this analysis is a geological model that defines all the factors and parameters designed to calculate resources and economic indicators. Calculation of the cost of information allows to assess the risks that are always present in the work of specialists. This technique is intended to help the geologist in choosing a priority object for further exploration and to assess risks and uncertainties in the study area. The relevance of the method lies in the fact that the specialist forms a decision on the work, which allows to explore the area with minimal cost and maximum profit.

8 CONCLUSIONS

A study of the available data on the area of the field was carried out, a 1D-2D geological model was built, a decision tree was built, an assessment and analysis of the value of information was performed. A feasibility study has been drawn up for geological prospecting. Design solutions for the placement of prospecting work are presented. An assessment of the initial recoverable resources was made, which showed that with a probability of 90% oil resources will be confirmed in the amount of 26.97 million tons, with a probability of 50% - 32.42 million tons, and a probability of 10% - 38.29 million tons. Value of Information, amounting to 5.714 billion rubles. The project profitability calculation was estimated at 9.934 billion rubles. An assessment of the value of information, calculated on the basis of the constructed geological model, showed that the geological prospecting with 2D seismic surveys at the area is a reasonable option for choosing a company strategy in order to increase resource potential.

REFERENCES

Alekseeva M.B., Bogachev V.F., Gorenburgov M.A. Systemic Diagnostics of the Arctic Industry Development Strategy.Journal of Mining Institute. 2019. Vol.238,p.450-458. DOI 10.31897/PMI.2019.4.450

Cherepovitsyn, A.E., Larichkin, F.D., Vorobiev, A.G., Ibrokhim, A., 2018. Economical prospects of advancement in liquefied natural gas production, *Gornyi Zhurnal*.

Efimov, A.V. & Tashlitskaya, A.M. 2013. An example of economic evaluation of projects at the stage of geological prospecting taking into account risks and uncertainties, *Oil industry* (11): 94–96.

Egorov, A.S., Vinokurov, I.Y., Kalenich, A.P., Belevskaya, E.S., Ageev, A.S. 2016. Deep structure of the Barents-Kara region according to geophysical investigations along 1-AR and 2-AR geotravers, *7th EAGE Saint Petersburg International Conference and Exhibition: Understanding the Harmony of the Earth's Resources Through Integration of Geosciences:* 728–732.

Glebov, A.F. 2016. Factor analysis of the geological and technological success and risks of oil and gas seismic survey in modern Russia for 20 years, *Seismic survey technologies* (4): 5–12.

Gorbovskaya, O.A. 2017. Probability Assessment of Geological Uncertainties: Lessons Learned, *SPE Journal*.

Gospodarikov, A.P., Zatsepin, M.A., 2019. Mathematical modeling of boundary problems in geomechanics, *Gornyi Zhurnal*.

Gutman, I.S. & Sahakyan, M. I. 2017. Methods for calculating reserves and estimating oil and gas resources: textbook, Moscow: Nedra.

Nedosekin A.O., Rejshahrit E.I., Kozlovskij A.N. Strategic Approach to Assessing Economic Sustainability Objects of Mineral Resources Sector of Russia. Journal of Mining Institute. 2019. Vol.237, p.354–360. DOI: 10.31897/PMI.2019.3.354

Prischepa, O., Nefedov, Y., Grokhotov, E. 2019. Geochemical and petrophysical studies of hydrocarbon potential of domanic shale formation (Timan-Pechora petroleum Province), *EAGE/SPE Workshop on Shale Science 2019 - Shale Sciences: Theory and Practice*. DOI: 10.3997/2214-4609.201900475 ISBN: 978-946282281-8

Prishepa, O.M., Nefedov, Y.V., 2018. Methodical approaches to the allocation of oil and gas accumulation zones on the example of the timan-pechora OGP, *Geomodel 2018-20th Conference on Oil and Gas Geological Exploration and Development*.

Reidar, B. 2009. Value of Information in the Oil and Gas Industry: Past, Present, and Future, *SPE Reservoir Evaluation & Engineering*.

Shatrov, S.V. 2015. Calculation of the probability of discovery of a field taking into account the mutual dependence of the parameters within the estimated formations and structures, *Oil and gas geology. Theory and Practice*.

Warren, J.E. 1983. The Development Decision: Value of Information, *SPE Hydrocarbon Economics and Evaluation Symposium, Dallas, 3–4 March . DOI: 10.2118/11312-MS*: SPE.

Whitney, J. T. 2010. On the value of information for spatial problems in the earth sciences.

Advances in Raw Material Industries for Sustainable Development Goals – Litvinenko (Ed)
© 2021 Taylor & Francis Group, London, ISBN 978-0-367-75881-3

Mineral formation sequence in the hyperbasites of the Serovsko-Maukski ophiolite belt (the Northern Urals)

R.K. Ilalova
PhD in Geology and Mineralogy, assistant of the hystorical and dynamic geology Department, Mining university, Saint-Petersburg, Russia

I.V. Talovina
Professor in Geology and Mineralogy, head of the hystorical and dynamic geology Department, Mining university, Saint-Petersburg, Russia

I.V. Vorontsovac
PhD in Geology and Mineralogy, associate Professor of the geology and exploration of mineral deposits Department, Mining university, Saint-Petersburg, Russia

ABSTRACT: a comprehensive research of the geological structure and mineral composition features of the hyperbasites of the Serovsko-Maukski ophiolite belt and the weathering crust along them was carried out. Due to the complex geological history of formation of the weathering crust, a wide range of precision methods of investigation was used - optical-microscopic, X-ray diffraction, thermal, micro-ray spectral and Raman methods. As a result, the sequence of mineral formation was revealed and the modern genetic classification of hyperbasite minerals and weathering crust was compiled. In the presented classification, all minerals of the weathering crust and hyperbasites of the Serovsko-Maukski ophiolite belt are divided into endogenous and exogenous ones. Among the endogenous ones there are four groups - magmatogenic-relikt minerals, oceanic weathering minerals, low-grade metamorphogenic-relikt and hydrothermal-relikt minerals; among the exogenous ones there are residual and infiltration-overlaid minerals. Residual minerals are divided into two subgroups - diffusion and infiltration. Thus, the results obtained allow us to identify the most important geological processes associated with the evolution of hyperbasite massifs of the Serovsko-Maukski ophiolite belt and the weathering crust along them. Moreover, the conclusions prove the appearance of hydrothermal processes and low-grade metamorphism in the history of massifs development and the weathering crust of the Serovsko-Maukski ophiolite belt, and can also be used for prediction and search for new ore nickel deposits.

1 INTRODUCTION

This study seems to be a topical subject because it allows us to identify the most important geological processes associated with the evolution of hyperbasite massifs of the Serovsko-Maukski ophiolite belt and the weathering crust along them. And geological processes, in turn, are associated with the prediction and search for ore deposits, which also emphasize the importance of the research topic.

Aim of the research is complication of the modern genetic classification of minerals of the hyperbasites and weathering crust. Tasks of the research are: 1) to study the geological structure of hyperbasite massifs and weathering crust along them; 2) to study the mineral composition of rocks of the weathering crust and hyperbasites; 3) to establish the zonation of the weathering profile; 4) to correlate the mineral composition of rocks and geological processes.

The issue of the sequence of mineral formation of hyperbasites was first considered in the works of Ginzburg (1946, 1947, 1953, 1963). Later, some data on this issue were published by Nikitina (1956), Kukovsky (1961, 1963, 1966), Zhuravleva et al. (1971). The most recent data on the mineral composition of the weathering crust were presented in the works of Mezentseva (2011), Talovina (2012) &Vorontsova (2013).

2 METHODOLOGY

During the 2015-2018 field seasons, the authors of this article carried out field work, collection of stone material, description and documentation of outcrops, ditch and well cores. A total of 150 geological sections and 500 samples of petrological differences in rocks were studied. The study of the material composition of rocks was conducted using digital technologies, which now occupy a special place in the world of science (Litvinenko, 2020; Zubov, 2017). Such as, Detection of altered rocks was carried out by means of petrographic study of transparent thin rock sections on the Leica DM2700 P microscope using domestic methods of studying these formations (400 pieces). In order to refine the diagnosis of minerals, micro-rays and Raman methods (300 definitions) were used - on the JSM-6510LA raster electron microscope with energy dispersive spectrometer JED-2200 (JEOL) in IGGD RAS (analyst O.L. Galankina) and ReactRaman 785 spectrometer (analyst E.A. Vasiliev), X-ray method (60 definitions) - on XRD 3000 TT and URD-6 X-ray diffractometers in the laboratory of the Freiberg Mining Academy (analyst R. Kleeberg), thermal method (40 definitions) - on the STA 429CD+QMS (ISC RAS, V.L. Ugolkov).

3 RESULTS AND DISCUSSION

The Kolskij, Ustaiskiy and Vagranskiy hyperbasite massifs (O_{1-2}) are located on the eastern slope of the Northern Urals and are a part of the Serovsko-Maukski ophiolite belt - the northern branch of the belt of the Urals ophiolite massifs (Vtorushin, 1969; Kononova, 1974; Vershinin, 1966). They are stretched in the meridional direction and occur among volcanogenic-sedimentary formations of Middle Palaeozoic age - diabase porphyrites, tuff shales and tuff sandstones, contacting in the southwest with intrusive formations of porphyrites and quartz diorites. In the course of the Mesozoic-Cenozoic tectonic movements, the massifs were divided into large blocks and were covered by platform sediments of the Jurassic, Cretaceous and Paleogene ages. (Figure 1).

The ultramafic rocks of the massifs are almost completely serpentinized and bear the traces of intensive tectonic processing. Serpentinites are broken through by numerous dykes of basic and intermediate composition, in contact with which they are talked, chloritized and carbonated. Under the cover of the Meso-Cenozoic sediments are preserved aposerpentin rocks, which compose the ancient (T-J) weathering crust of the hyperbasites. The latter belongs to the linear-platform type and is divided into residual and transformed infiltration-metasomatic (chamosite) by genetic features. The residual crust is relict; initially it could form the lower horizons of a rather powerful primary weathering crust. During the Albian-Cenomanian period, the upper horizons of the latter were partially eroded, partially re-deposited, and underwent changes in the conditions of the recovery environment when the area was swamped and affected the laterites of H_2S и CO_2 (Talovina et al., 2010; Mezentseva et al., 2011).

In the section (from bottom to top) the following zones are alternating (Table 1): 1) the zone of disintegrated serpentinite, chloritized and carbonated, weakly affected by weathering processes, 2) the zone of leached serpentinite (subjected to kerolitization, carbonation, siliconization, nontronitization, oxidation), 3) the hydration zone, 4) the oxidation zone and 5) the chamosite zone.

The mineral composition of the weathering crust of hyperbasites in the Serovsko-Maukski ophiolite belt is very complex and diverse due to the complex geological history of their formation (Stepanov et al., 2019; Aleksandrova et al., 2019; ElDeeb et al., 2019; Popov et al.,

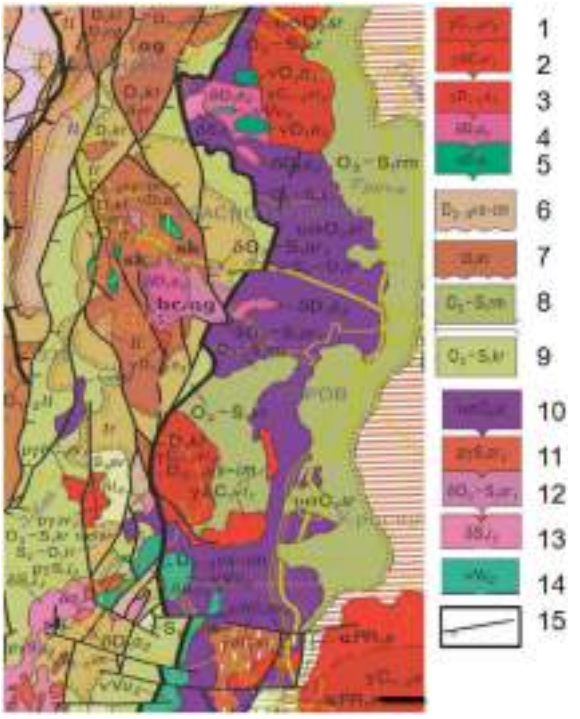

Figure 1. Geological map of the Daurian formations of the Northern Urals (A.P. Karpinsky Russian geological research institute, Uralian geological survey expedition. Map scale 1:1 000 000. Drawer: T.A. Petrova) 1-2 – Verhisetsky complex granodiorite-granite; 3-5 – Auerbach complex gabbro-diorite granite; 6 – undivided Wysotinsk and Limkin formations; 7 – Krasnoturyinsk formation; 8 – Romahinsk thick; 9 – Krasnouralsk formations; 10 – Serov complex dunite-harzburgite; 11-12 – Arbatsk complex diorite-plagiogranite; 13 – Levinsk complex gabbro-tonalit-plagiogranite; 14 – Usteysk complex dunite-verlite-clinopyroxenite-gabbro; 15 – dislocations.

Table 1. Weathering profiles zoning.

Weathering zone	Ongoing process	Rock varieties	Mineral varieties
Shamosite	Shamositization	Chamosite rocks	Chamosite, millerite-brindleyite-chamosite, clinochloro-bertierine-chamosite, chamosite-lizardite
Oxide-iron	Oxidation	Goethite rocks	Goethite, quartz goethite, clinochloro goethite
Nontronite	Hydration	Nontronite rocks	Nontronite, talc-chlorite-nontronite
Serpentinite	Leaching	Lysardite rocks	Clinochlore-talk-lizardite, nepuite-quartz-lizardite, clinochlore-pennine lizardite
	Disintegration	Chrysotile rocks	Clinochlore-chrysotile, talc-chrysotile, diabantite-brunsvigite-picnochlore-chrysotile

2020). Despite this fact, the authors have compiled a detailed genetic classification of weathering crust minerals and hyperbasites (Table 2). Moreover, the sequence of mineral formation was noted (Table 3).

In the presented genetic classification all minerals of the weathering crust of hyperbasites of the Serovsko-Maukski ophiolite belt are divided into endogenous and exogenous (Ilalova, 2019). Four groups are distinguished among the endogenous ones: magmatogenic-relict

Table 2. Genetic classification of the basic minerals of the weathering crust of the hyperbasites of the Serovsko-Maukski ophiolite belt.

Endogenous			
Magmatogenic-relict minerals	Oceanic weathering minerals	Low-grade metamorphogenic-relict	Hydrothermal relict minerals
Olivine, pyroxene, chromspinelide	Lysardite, chrysotile, pecoraite, amphibole, bastis, magnetite	Chlorite, talc	Millerite, pyrite, chalcopyrite, pyrrhotite, chlorite, talc
Exogenous			
Residual			
Diffusion	Infiltration	Infiltration-overlay minerals	
Nontronite, montmorillonite, hydrochlorite, halloysite, kaolinite	Goethite, hydrogetite, hematite, nontronite, talc, quartz, opal, chalcedony, calcite, magnesite, dolomite, hydrargillite	Shamosite, siderite, rhodochrosite, pyrite	

Table 3. Genetic classification of the basic minerals of the weathering crust of the hyperbasites of the Serovsko-Maukski ophiolite belt.

Minerals of the hyperbasites	Profile zones of the weathering crust			
	Disintegration	Leaching	Nontronite	Ochre
Olivine	Iron hydroxides		Nontronite	Iron hydroxides
Serpentine	Initial stage of nontronite formation			Nontronite Quartz, chalcedony, opal Oxides and hydroxides of iron
Chlorite	Hydrochlorite		Hydro mica	Kaolinite, quartz, chalcedony, opal
	Hydrochlorite	Montmorillonite, halloysite, kaolinite		Hydrargillite, iron hydroxides
Piroxene	Hydrated piroxene		Nontronite	Iron hydroxides, silica minerals
Amphibole	Hydrochlorite	Montmorillonite		Kaolinite, iron hydroxides, hydrargillite
Bastite	Hydrated bastite		Nontronite	Iron hydroxides, silica minerals
Magnetite	Maghemit, hematite			Iron hydroxides
Chromspinelids	Magnetite	Hematite		Iron hydroxides

Note. The table does not include minerals of infiltration-overlaid genesis.

minerals, minerals of oceanic weathering, low-grade metamorphogenic and hydrothermal relict minerals; among the exogenous ones - residual and infiltration-overlay minerals. Residual minerals are divided into two subgroups - diffusion and infiltration minerals.

The following rock-forming minerals of hyperbasites are referred to as magmatogenic-relict minerals: olivine, pyroxene and chromspinelide. Minerals of oceanic weathering (at the spreading stage) are chrysotile, lysardite, pecoraite, bastite, amphiboles and magnetite. Olivine is transformed into serpentine, pyroxene into bastite and chromspinelide into

magnetite. Chromspinelide and magnetite are found in all areas of the crust, and in the ochre zone, compared to the lower zones, the content of magnetite and chromspinelide is much higher. Low-grade metamorphogenic-relict minerals are formed at low-grade metamorphism of the hyperbasites at the stage of early Mesozoic tectonic-magmatic activation of the region, which appeared as a result of transregional riftogenesis and trap magmatism (Rapoport, 1998; Spiridonov, 2008). Serpentine, bastite, amphibole forms chlorite and talc. Chlorite in the weathering crust by composition belongs mainly to the iron-magnesia series. At microscopic study of thin section from zones of disintegration and leaching full or partial replacement of serpentine, bastite, amphiboles by chlorite is clearly visible. Talc forms pseudomorphoses over the chlorite and other earlier minerals. Iron, released from olivine and pyroxene, forms in serpentinite thin rash or chain-shaped clusters of tiny grains of magnetite. Hydrothermal relict minerals found in the cracks of chrysotile-lysardite metasomatites from the zone of disintegrated serpentinite, are formed in hydrothermal processes. Low-temperature hydrothermal solutions separated from the magmatic hearth and containing copper, nickel, iron and sulphur have deposited sulfide minerals such as pyrite, millerite, chalcopyrite and pyrrhotite in the tectonically disturbed serpentinite zones. Since these minerals are localized in the cracks of disintegrated serpentinite, their formation due to the serpentinization process is excluded. Chalcopyrite, pyrite, pirrotine in the form of grains up to 1 mm in irregular and cubic shape are associated with millerites, which have the form of needle crystals, often collected in radial-beam aggregates. In the ochre zone, sulfide minerals are hardly preserved, except for pyrite, which is formed here by infiltration. These sulfides quite often contain nickel, which is reflected in their chemical compositions.

Thus, at this stage, the transformation of relict minerals and the formation of new minerals occurring during low-grade metamorphism and hydrothermal processes are being completed. Subsequent transformations of minerals are the result of exogenous processes.

Residual minerals can occur in two ways:

1) as a result of direct metasomatic substitution of serpentinites during their weathering (diffusion);
2) as a result of deposition of cold solutions during their infiltration into the depths of tectonic disturbance zones and cracks in serpentinite (infiltration).

Depending on this, the residual minerals are subdivided into diffusion and infiltration minerals. Often the same mineral can be formed in different ways. Nontronite, montmorillonite, hydrochlorite, halloysite, and kaolinite are classified as diffusion residual minerals. Serpentine, being exposed to weathering agents (oxygen, carbon dioxide, humus acids and ground water) undergoes a complex successive process of changes. Weathering of serpentine minerals occurs under conditions of humid climate and strong cracking of rocks. In the disintegration zone, serpentine, absorbing water moving through the cracks or rock pores, begins to hydrate and partially turn into nontronite. Further removal of cations from serpentine minerals leads to destruction of the crystal lattice, reduction of volume weight, increase of porosity and change of other physical and optical properties, in particular the refractive index. If relict olivine remains in serpentinite, then in the disintegration zone, mainly in its upper part, it is destroyed with the formation of a residual grid, consisting of brown iron hydroxides.

Piroxene and amphibole in the upper horizons of the disintegration zone and in the lower horizons of the leaching zone turn into hydrogetite (as a fine mesh) and nontronite. Under the microscope it can be seen that this process begins with microcracks and gradually spreads to all grains.

There are several ways of chlorite weathering in the weathering crust, but the end products of their decomposition are the same minerals: halloysite, kaolinite and iron hydroxides (Lazarenkov et al., 2011; Ilalova et al., 2018). The stage of chlorite change can be represented by the following schemes:

1. Chlorite → hydrochlorite → hydromica → halloysite → kaolinite →
   → quartz, opal, chalcedony
   → iron hydroxides
   → hydrargillite
2. Chlorite → hydrochlorite → montmorillonite → halloysite → kaolinite →
   → hydrargillite → iron hydroxides

During weathering, chlorite is converted to hydrochlorite, which is particularly characteristic of the upper crust areas of the weathering. Hydrochlorite under a microscope is usually observed as scaly grains or earthy masses of green, pale green color. During weathering of chlorite there is oxidation of FeO and hydrolysis of silicate, accompanied by silica release, and partial removal of MgO. During MgO leaching, the coloration of the mineral turns pale and the refractive index decreases. If there are high concentrations of nickel in descending waters, it replaces Mg^{2+} and Fe^{2+} equivalent. Montmorillonite, in turn, decomposes to form kaolinite or halloysite and iron hydroxides.

Magnetite, maghemite and hematite occur as a result of oxidation of magmatogenic-relict chromspinelids, magnetite. Change of chromspinelids begins at the periphery of grains, then spreads through cracks, gradually covering the entire area of the grain. Magnetite formed during oceanic weathering (at the stage of spreading) during subsequent weathering also turns into magnetite, then into hematite.

Infiltration-resistant minerals are the most interesting and numerous. Goethite, hydrogethyte, hematite are formed as a result of the release of iron from iron-containing minerals at their destruction in various zones of the weathering crust. Thus, when magnetite, maghemite and other iron-containing minerals change further, iron is transferred from the crystal lattice to cold solutions as a result of the release of these minerals. These solutions seep into the loose ochre mass of the upper crust zone and move along the cracks of leached and disintegrated serpentinite and as the corresponding concentrations are reached, iron falls out of the solutions in the form of goethite, hydrogetite and hematite. When other chemical elements, such as Mg, Al, Si and Ni, were introduced into the solutions together with iron, the formation of nontronite occurred.

Silicon entering the crust solutions due to the destruction of diorite minerals was used to form sedimentary quartz, chalcedony and opal. Some part of silicon precipitated together with magnesium, iron, aluminum and sometimes nickel to form talc, nontronite and other minerals. Calcite, magnesite and dolomite, as well as other minerals of this group, are sediment-newly formed. Magnesium and calcium were introduced into crust solutions as a result of plagioclases and pyroxenes destruction from dikes, serpentine and chlorites. Carbonate minerals were mostly precipitated in cracks of disintegrated and leached serpentinite, where pH>11 and environment was reductive.

Infiltration-overlay minerals appeared after the formation of the weathering crust and its overlapping by precipitation from the Jurassic and Cretaceous periods. They are not connected with the destruction of hyperbasite massifs and dike rocks. Mineralized waters from lake and marsh water bodies penetrated downwards (into the upper zones of the weathering crust) and as a result of infiltration and overlaying replaced some previously formed minerals. In addition to metasomatic substitution, the minerals of this group were precipitated from cold solutions of cracks and rocks in the weathering crust. Infiltration-metasomatic chamosite was found in the weathering crust of serpentinite, which partially replaced both exogenous newly formed and endogenous relic minerals. Infiltration chamosite is distinguished by cracks and voids and belongs to the later generation. This group also includes pyrite, siderite and rhodochrosite. Pyritization and sideritization as infiltrationally superimposed processes are weaker in the weathering crust than chamositization. Pyrite in the form of crystals 0.5 mm in size is often found in the ochreous hydrogethyte mass of the upper area of the weathering crust. Siderite is in close paragenetic association with chamosite, rhodochrosite. It is observed in the form of rounded spherolite grains and clear crystalline aggregates in loose clayey chamosite rocks, cementing them.

4 CONCLUSIONS

The sequence of mineral formation in the weathering crust does not have to be a fully developing process with inevitable and always defined transition minerals. It depends on physical and chemical conditions of the environment. Under favorable conditions this process occurs very quickly, in adverse conditions - slowly or even stops at some stage, not giving "final" products of rock decomposition. The "final" products are minerals resistant in the uppermost horizons of the weathering crust; most often these are hydro-oxides and oxides of iron, quartz, opal.

Thus, the weathering crust of the hyperbasite massifs of the Serovsko-Maukski ophiolite belt contains a large number of minerals of various genesis and carries the traces of various processes - oceanic weathering, low-grade metamorphism, hydrothermal and metasomatic processes. The obtained results allowed the authors provide evidence of the appearance of hydrothermal processes and lowgrade metamorphism in the history of development of massifs and weathering crust of the Serovsko-Maukski ophiolite belt.

The particular importance of this study is that the obtained knowledge allows reconstructing the processes of redistribution and accumulation of ore components in the weathering crust rocks, in particular, the results can be used in forecasting estimates of the territory for nickel.

It should be noted that rich nickel-rich weathering crusts occur due to overlapping processes of endogenous, thermal and eluvial origin (otherwise - a combination of hypergenic and hypogenic factors), which results in the formation of polychronous and polygenic formations. This suggests that surface eluvial formations can continue to the depth, especially in the zones of faults, contacts of intrusive bodies, wide development of dyke complex rocks and other tectonically weakened zones. Comprehensive geological data analysis shows that such deposits can be found on poorly studied areas of overlapping serpentinite melange of deep faults with a platform cover, in particular in the fracture zones framing the Tagilo-Magnitogorsky deflection and the East Ural Rise.

The study was performed as part of the Joint German-Russian Project No 20-55-12002 of the Russian Foundation for Basic Research.

REFERENCES

Aleksandrova, T.N., Talovina, I.V., Duryagina, A.M. 2019. Gold–sulphide deposits of the Russian Arctic zone: Mineralogical features and prospects of ore benefication. *Chemie der Erde (144)*. DOI: 10.1016/j.chemer.2019.04.006.

ElDeeb A.B., Brichkin V.N., Kurtenkov R.V., Bormotov I.S. 2019. Extraction of alumina from kaolin by a combination of pyro- and hydro-metallurgical processes. *Applied Clay Science (172):* 146–154.

Ilalova R. K. 2019. Geological structure, composition and conditions of formation of nickel-bared weathering crust of hyperbasites of the eastern slope of the Northern Ural: dissertation [*Geologicheskoe stroenie, sostav i usloviya formirovaniya nikelenosnoj kory vyvetrivaniya: dis. … kand. geol.-min. nauk*], St. Petersburg: 173 p.

Ilalova R. K. & Gulbin Y. L. 2018. Thermometry of nickel chlorites of the Kolskii massif (the Northern Urals). *Proceedings of RMS* (147): 1–17.

Lazarenkov V.G., Talovina I.V., Vorontsova N.I., Mezentseva O.P. & Ryzhkova S.O. 2011. Nickel chlorites of oxide-silicate nickel deposits of the Urals. *Lithology and mineral resources* (3): 1–10.

Litvinenko V.S. 2020. Digital Economy as a Factor in the Technological Development of the Mineral Sector. *Natural Resources Research (29):* 1521–1541.

Mezenceva O. P. & Talovina I. V. 2011. The value of δ^{34}S in millerite and the genesis of chamosite nickel ores of the Elovsky deposit, the Northern Ural. *Journal of Mining Institute* (189): 58–61.

Popov O., Talovina I., Lieberwirth H., Duryagina A. 2020. Quantitative microstructural analysis and x-ray computed tomography of ores and rocks—comparison of results. *Minerals 10 (2),129*. https://doi.org/10.3390/min10020129.

Talovina I. V., Lazarenkov V. G., U. Kempe, Voroncova N. I., Mezenceva O. P., Ryzhkova S. O. & Ugolkov V. L. 2010. Nickel serpentines of the lysardite – nepuit and karyopilite series in hypergene nickel deposits of the Urals. *Proceedings of RMS* (4): 80–94.

Spiridonov E. M. 2008. In development of the idea of F.V. Chukhrova about late hydrothermal formations: low-grade metamorphism as ore preparation, ore-forming and ore-transforming processes. *Institute of Geology of Ore Deposits, Petrography, Mineralogy and Geochemistry RAS:* 206–209.

Stepanov S. Y., Palamarchuk R. S., Kozlov A. V., Khanin D. A., Varlamov D. A., Kiseleva D. V. 2019. Platinum-group minerals of Pt-placer deposits associated with the svetloborsky Ural-Alaskan type massif, middle urals, Russia. *Minerals 9(2)*. https://doi.org/10.3390/min9020077.

Voroncova N. I., Talovina I. V., Lazarenkov V. G., Gajfutdinova A. M. & Tihomirova M. 2013. $^{87}Sr/^{86}Sr$ isotopic ratios in the rocks and ores of the Sakharin and Ufaleysky hypergene nickel deposits of the Urals. *Journal of Mining Institute (200):* 179–185.

Zubov V.P. 2017. Status and directions of improvement of development systems of coal seams onperspective kuzbass coal mines. *Journal of Mining Institute (225):* 292–297.

Advances in Raw Material Industries for Sustainable Development Goals – Litvinenko (Ed)

Granulite from the Bunger Hills, Eastern Antarctica: Mineral parageneses and terms of metamorphism

I.A. Abdrakhmanov
Postgraduate student, Saint-Petersburg Mining University, St. Petersburg, Russia

Yu.L. Gulbin
Doctor of geological and mineralogical Sciences, Saint-Petersburg Mining University, St. Petersburg, Russia

ABSTRACT: The article presents the results of mineral thermobarometry and physicochemical modeling of mineral parageneses in garnet-sillimanite-cordierite gneiss from the Mesoproterozoic metamorphic unit of the Bunger Hills, East Antarctica. Therefore, a clockwise R-T path was inferred using petrograthic and mineralogical data. It is shown that peak temperature of metamorphism could exceed 900 °C. Such temperature conditions in combination with post-peak decompression records the collision-related tectonic evolution of the studied area.

Keywords: thermobarometry, granulites, Bunger Hills, East Antarctica

1 INTRODUCTION

The problem of the generation of the continental crust in Precambrian is one of the leading ones in modern geology. Therefore, the reconstruction of processes of sedimentation magmatism, and subsequent metamorphism during the formation of Precambrian complexes are the most important tasks of the petrological study of the folded basement of the East Antarctic shield. The relevance of this kind of research is all the more undeniable in the light of the discussion of the evolution of the supercontinent Rodinia. One of the key sites capable for understanding the geological history is the Bunger Hills in the eastern part of the Antarctic Shield.

2 GEOLOGICAL SETTING

The Bunger Hills is a narrow strip of a land, free from ice, stretching along the Antarctic coast in the area of Wilkes Land. The geological structure of this territory was studied by Soviet and Australian geologists (Ravich et al., 1965; Sheraton et al., 1995).

A variety of plagiogneisses and crystalline gneisses, which are largely granitized and migmatized, take part in the geological structure of the Bunger Hill (Figure 1).

In the thickness of these rocks, there are concordant intrusions of metabasites and layers of silicate marbles and calciphyres, bored and weakly granitized. In addition to the most diverse migmatites, shadow granites and numerous veins of granite composition arise. Massifs of charnockites also occur among migmatites. Dolerite dikes cut through all other rocks. The thickness of migmatized plagiogneisses and crystalline gneisses are deformed into large folds, whose wings are complicated by smaller folds of higher orders. Three fault systems, along which there are zones of milonites and diaphthoritic schists, broke this section of the crystalline basement into separate blocks, mostly slightly moved relative to each other.

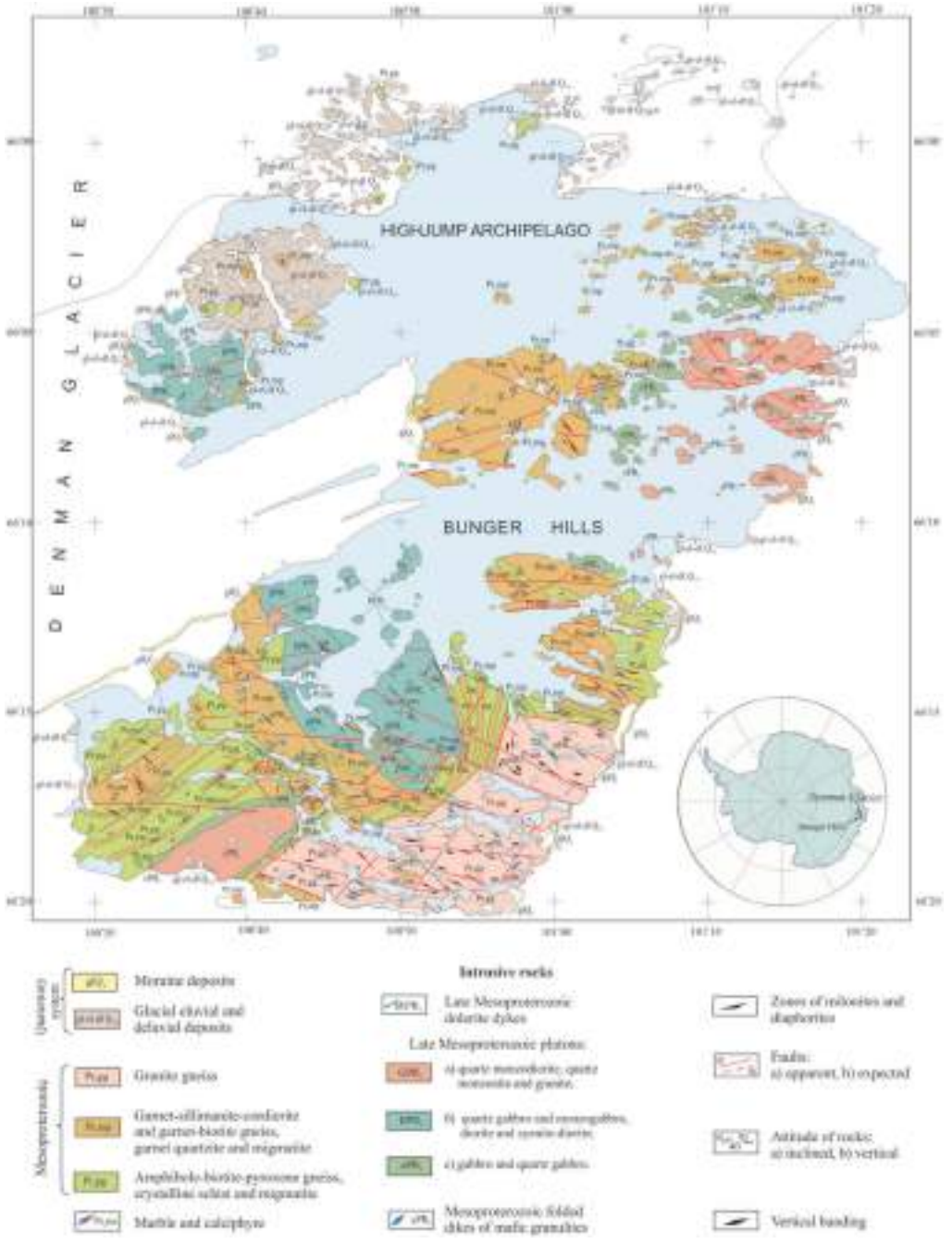

Figure 1. Geological map of the Bunger Hills, East Antarctica (Ravich et al., 1965).

According to the U–Pb dating of syngenetic zircon, the igneous protolith of orthogneisses formed in the interval 1700–1500 Ma, while the appearance of plutons took place at the turn of 1170–1150 Ma (Sheraton et al., 1995). The age of metamorphism, according to in situ U-Pb dating of monazite from paragneisses, is 1240–1150 Ma (Tucker et al., 2016, 2017, 2018) and closely coincides with the formation of the Albany–Fraser orogenic belt (southwestern Australia) during the amalgamation of Rodinia.

3 SAMPLE DESCRIPTION AND ANALITICAL METHODS

Samples utilized in this study were collected during the 2nd Soviet Antarctic Expedition of 1956-57. Sample 651a (from the Krylatyy peninsula) contains quartz (30 vol.%), alkali feldspar (25), cordierite (20), garnet (10), biotite (7), sillimanite (5), ilmenite (2), albite (1), spinel (hercinite) <1, rutile, zircon ≪ 1. The rock has a medium-fine-grained texture and banded structure due to the alternation of lenticular quartz layers with cordierite-garnet-sillimanite-biotite sections.

The bulk chemical composition of the rock was determined with the XRF method in VNNII-Okeangeologiya. Chemical compositions of minerals were obtained using JSM-6510LA elec-tron microprobe equipped with EDS JED-2200 (JEOL) at the Institute of Precambrian Geology and Geochronology of the Russian Academy of Sciences (Saint Petersburg, Russia).

The method of isochemical diagrams (pseudosection modeling) was applied to retrieve P-T history of the rock. This method implements the fundamental principle of metamorphic fa-cies. By this method, P-T phase diagrams are calculated that show which mineral assemblage stability field takes place for the rock of a given chemical composition under given temperature and pressure conditions. The modeling was done in the system NCKFMASHT using Theriak/Domino program (de Capitani, Petrakakis, 2010) with an internally consistent thermodynamic database tcdb55c2d (Holland, Powell, 1998, with changes) and different solid solution activity models for feldspars, garnet, biotite, cordierite, spinel, ilmenite, orthopyroxene, and osumilite. Quartz, sillimanite, kyanite, rutile, and titanite were considered as pure phases.

4 RESULTS

According to microprobe analysis, garnet is non-zonal and characterized by increased contents of almandine and pyrope end members ($X_{Fe}0.69 - 0.71$, $X_{Mg}0.27 - 0.29$), low contents of Ca and Mn ($X_{Ca}0.01 - 0.02$, $X_{Mn}0.01 - 0.02$). In garnet rims next to the Crd-Bt aggregate (which replaces garnet) X_{Mg}^{Grt} decreases (to 0.25), and X_{Fe}^{Grt} increases (up to 0.74). This points to the partitioning of Fe and Mg between garnet, cordierite and biotite during retrograde metamorphism (Figure 2).

Sillimanite is characterized by a composition close to stoichiometric; it contains minor FeO (0.4–0.9 wt %).

Alkali feldspar is a mesoperthite with K-rich feldspar host (Ort84–89Ab16–11An0) and almost pure albite lamellae Ab94–95An5–2Ort3–1 (Figure 3). It contains minor barium (BaO 0.3–1.3 wt %).

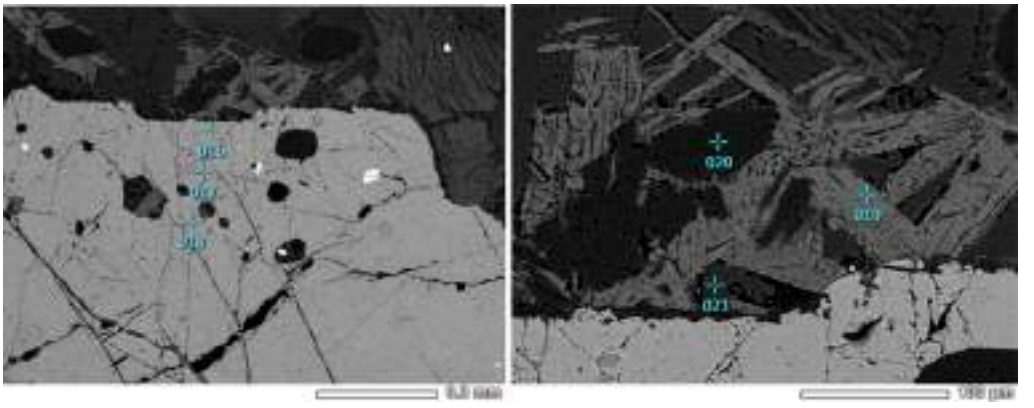

Figure 2. Change the composition of garnet rim next to the Crd-Bt aggregate. Points of analysis: point 19 is biotite, point 20 is sillimanite, point 21 is cordierite.

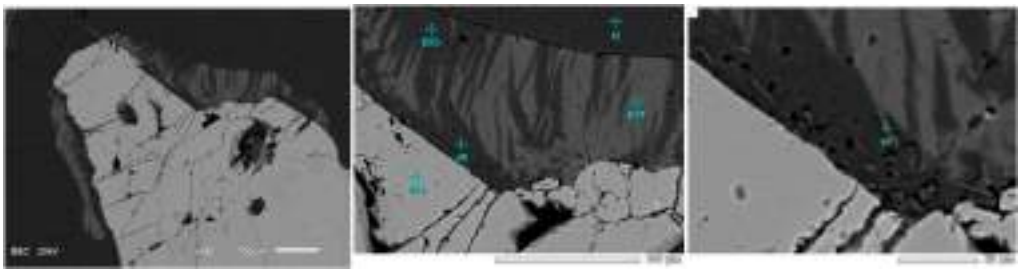

Figure 3. Mesopertite rims around garnet crystals with Sil (II) inclusions. BSE images.

Table 1. Chemical composition for sample 651a.

SiO_2	TiO_2	Al_2O_3	Fe_2O_3	FeO	MnO	MgO	CaO	Na_2O	K_2O	P_2O_5	LOI	Σ
74.88	0.70	12.82	1.14	4.18	0.09	2.20	0.01	1.32	1.36	0.11	0.90	99.71

The mineral of the spinel group corresponds to hercynite, which contains minor zinc (ZnO 4.5–7.7 wt %; 0.09–0.16 a.p.f.u.), chromium (Cr_2O_3 0.3–7.8 wt %; 0.01–0.19 a.p.f.u.) and nickel (NiO up to 0.4–0.6 wt %; Up to 0.01 a.p.f.u.). The content of the hercynite end-member in spinel varies from 0.52 to 0.65, while the magnetite one does not exceed 0.04. The average formula ($n = 6$): $(Fe^{2+}_{0.61}Mg_{0.28}Zn_{0.12})_{1.01}(Al_{1.86}Fe^{3+}_{0.07}Cr_{0.04}Si_{0.01})_{1.98}O_4$.

Ilmenite contains minor magnesium (MgO up to 0.4–1.2 wt % and up to 0.02–0.04 a.p.f.u.) and manganese (MnO up to 0.1–0.6 wt % and up to 0.01 a.p.f.u.). The content of ilmenite end member varies from 0.92 to 0.99. Rutile contains minor FeO (0.3–2.9 wt %).

Cordierite is moderately magnesian with X_{Mg} in the range 0.68 - 0.77. Biotite is characterized by low alumina content (Al_2O_3 17.1–19.1 wt %) and high titanium content (TiO_2 up to 6.0 wt %).

Bulk compositions of the studied sample are reported in Table 1.

During modeling, special attention was paid to the assessment of water activity in the system. To this end, P-T diagrams were constructed at different values of aH2O. As a result, water activity was limited by 0.2 because spinel observed in the rock disappears from the model assemblages at higher water activities (Figure 4, 5). In the diagram calculated for system with $\alpha_{H2O} = 0.12$ (Figure 5), the Grt–Crd–Kfs–Qz–Ilm assemblage consists of spinel at a pressure of 5–6 kbar and a temperature exceeding 870 °C.

5 DISCUSSIONS

Pseudosection modeling and mineralogical analysis show the clockwise P–T path that starts in the rutile stability field (P > 9 kbar) and records the pressure decrease to 6 kbar. The decompression temperature range is 850–950 °C; it could occur against the background of a rise in temperature, or under conditions close to isothermal. This form of the P-T path follows from the assumption that at the early stage of metamorphism the assemblage Grt+Sill+Kfs+Qz+Rt±Ilm was stable in the studied rock. According to the GRAIL geobarome-ter (Bohlen et al., 1983), such equilibrium could take place in the pressure range of 6–8 kbar at 900 °C. As a result of the decompression, rutile was replaced by ilmenite and hercynite began to crystallize

The described scenario is consistent with the data of Tucker and Hand (2016), who also noted the presence of the high-pressure assemblage in the Bunger granulites. But at the same time, it cannot be ruled out that rutile in the studied sample was late and formed due to ilmenite oxidation at low temperatures at the retrograde stage (Bohlen et al., 1983), as indicated by the morphology of ilmenite–rutile intergrowths (Figure 6).

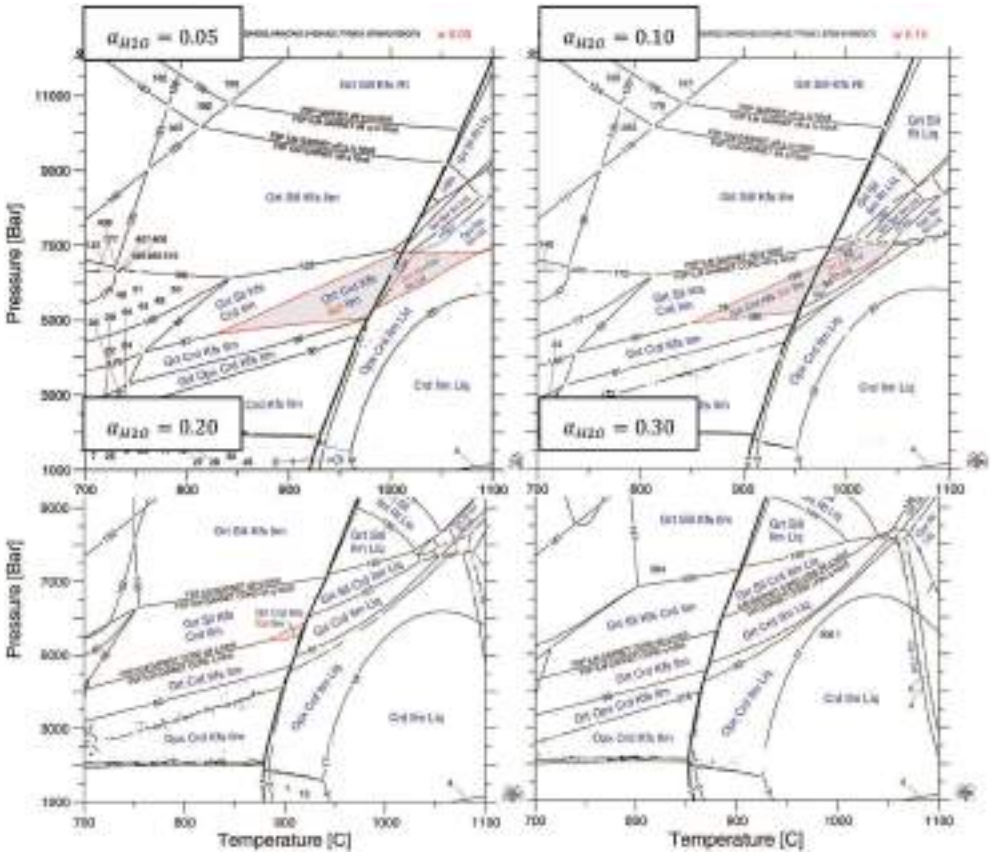

Figure 4. Isochemical P-T phase diagrams for sample 651a calculated for different values of α_{H2O}. Quartz is in excess.

At the second stage, the Grt–Crd–Sp–Qz–Ilm assemblage stabilized and the rock experienced partial melting as a result of isobaric heating at P = 5–6.5 kbar and T > 870 oC. The growth of garnet crystals during heating promoted capture of spinel inclusions. The calculated composition of spinel ($Hc_{68–73}Sp_{30–24}Usp_{2–3}$) agrees closely with the observed one ($Hc_{60–83}Sp_{40–17}$) without taking into account minor elements. Signs of partial melting in the rock (according to Holness et al., 2011) are intergranular quartz films and numerous mesoperthite rims around crystals of cordierite, sillimanite, and garnet (Figure 3, 7).

According to the modeling data, solidus temperature in the studied system is 960 °C at pressure of 6.2 kbar and water activity of 0.12. Partial melting is accompanied by the disappearance of alkali feldspar from the Grt–Crd–Sp–Qz–Ilm assemblage. The calculated composi-tion of the melt is $Qz_{29}Ab_{36}Kfs_{24}Sil_{10}$ whereby quartz, feldspar, and sillimanite are formed due to its crystallization. All these minerals are observed in the studied rock as melt crystallization products (Figure 3, 7). However, in contrast to the calculated composition of feldspar ($Ab_{60}Kfs_{40}An_0$), the reintegrated composition of mesoperthite observed in the sample is characterized by the predominance of the orthoclase mineral ($Ab_{37–49}Kfs_{62–50}An_1$).

It should be noted that the lower temperature limit of stability of hercynite, calculated in the NCKFMASHT system at a given water activity (870 °C), can shift to lower temperatures in the case of spinel enriched with minor elements (Fe^{3+}, Zn, Cr).

At the third stage, isobaric cooling to 750–800 °C occurred. At these temperatures, garnet and cordierite were equilibrated. Evidences of the equilibrium are: (1) the intersection of

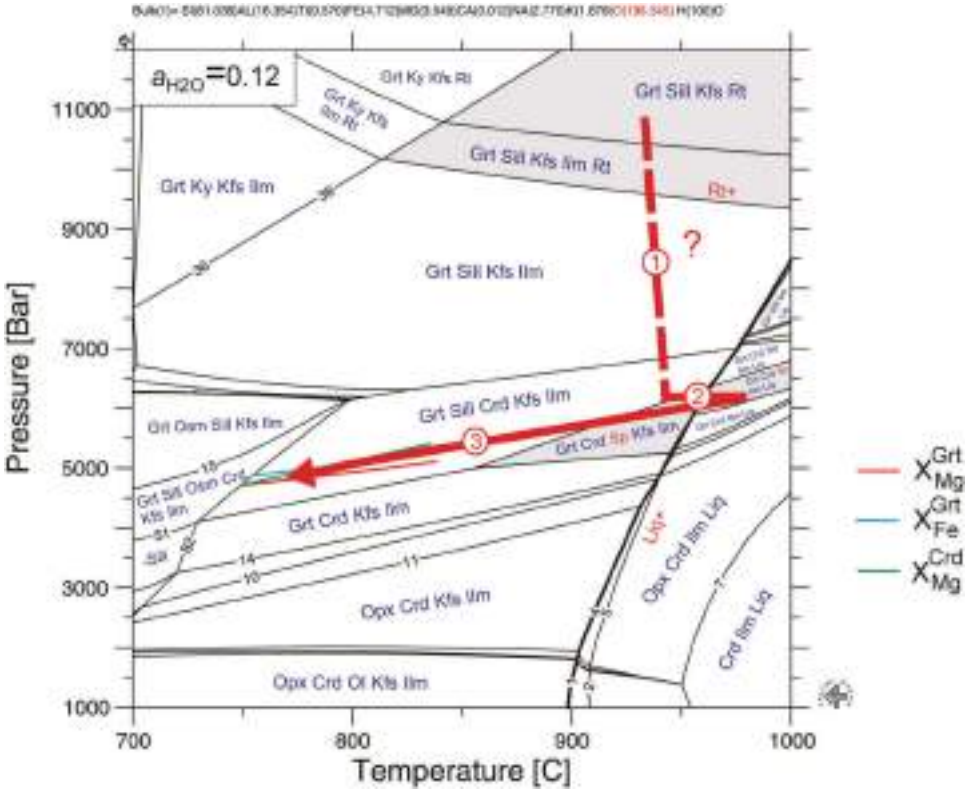

Figure 5. Isochemical P-T phase diagram for sample 651 calculated for α_{H2O} = 0.12. Quartz is in excess. Rutile and spinel stability fields are gray. The solidus line is marked in bold. Red arrow represents the P–T path inferred on the basis of petrographic and mineralogical data.

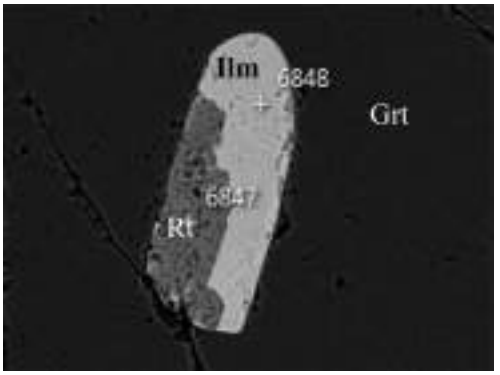

Figure 6. Intergrowth of ilmenite and rutile.

isopleths X^{Grt}_{Fe}, X^{Grt}_{Mg}, X^{Crd}_{Mg} corresponding to observed compositions of garnet and cordierite in the range of 750–800 °C at 5 kbar (Figure 5), (2) temperature estimates obtained with the Grt–Crd geothermometer (Bhattacharya et al., 1988) which vary from 700 to 770 °C at 5 kbar. According to the Ti-in-biotite geothermometer (Henry et al., 2005), high-titanium biotite stabilized under similar conditions (740–770 °C). The latter indicates an in-crease in water activity at the retrograde stage (as modeling shows biotite is stable up to a temperature of 760 °C at α_{H2O} = 0.12 and P = 5 kbar).

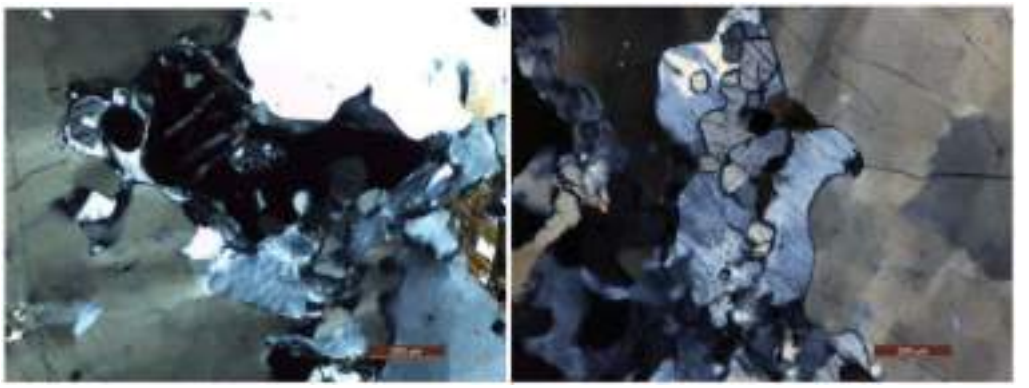

Figure 7. Mesoperthite rims around crystals of cordierite, sillimanite and garnet. Transmitted light, crossed polars.

6 CONCLUSIONS

The following results emerge from the study:

(1) it is shown that granulite metamorphism in the Bunger Hills undergoes at moderate pressure (5–10 kbar), low water activity (aH2O< 0.2), and peak temperature possibly exceeding 900 °C;
(2) the evolution of metamorphism is described by a clockwise P-T path with near-isothermal decompression in the early stage and near-isobaric cooling in the late stage of orogeny that is typical for P-T path associated with collision events

REFERENCES

Bhattacharya A. (1986), Some geobarometers involving cordierite in the FeO-$A1_2O_3$-SiO_2 ($\pm H_2O$) system: refinements, thermodynamic calibration and applicability in granulite facies rocks contribution // Mineralogy and Petrology, V. 94, pp. 387–394.

Bohlen, S. R., Wall, V. J., Boettcher, A. L. (1983), Experimental investigations and geological applications of equilibria in the system FeO-TiO_2-Al_2O_3-SiO_2-H_2O // American Mineralogist, V. 68, pp. 1049–1058.

de Capitani, C., Petrakakis K. (2010), The computation of equilibrium assemblage diagrams with Theriak/Domino software // American Mineralogist, V. 95, pp. 1006–1016.

Gulbin, Y.L., Glazov, A.I. (2013), Morphological evidence for diffusion-controlled growth of garnet from metapelites // Geol. Ore Deposits, V. 55, pp. 686–691.

Gulbin, Y.L. (2013), Modeling of zoning patterns in garnet: Thermodynamic and kinetic aspects // Geol. Ore Deposits, V. 55, pp. 625–636.

Gulbin, Y.L. (2013), Compositional zoning in garnet and kinetics of metamorphic crystallization // Geol. Ore Deposits, V. 55, pp. 613–624.

Gulbin, Y.L. (2015), P–T paths and modeling the evolution of metapelitic mineral assemblages in the MnNCKFMASH system: A case of Northern Ladoga area // Geol. Ore Deposits, V. 57, pp. 699–711.

Gulbin Y.L., Mikhalsky E.V. (2019) Modeling of mineral parageneses and thermobarometry of metavolcanic rocks of the Ruker group in the southern Prince Charles Mountains, East Antarctica // Zapiski RMO (Proceedings of the Russian Mineralogical Society), V. 148, №5, pp. 24–44.

Henry D.J., Guidotti C.V., Thomson J.A. (2005), The Ti-saturation surface for low-to-medium pressure metapelitic biotites: Implications for geothermobarometry and Ti-substitution mechanisms // American Mineralogist, V. 90, pp. 316–328.

Holland T.J.B., Powell R. (1998), An internally consistent thermodynamic data set for phases of petrological interest // J. Metamorphic Geology, V. 16, P. 309–343.

Holness M. B., Cesare B., Sawyer E. W. (2011), Melted rocks under the microscope: microstructures and their intepretation // Elements, V. 7, P. 247 252.

Ravich M.G., Klimov L.V., Soloviev D.S. (1965), Precambrian of East Antarctica // M.: Nedra, 470 p.
Sheraton J.W., Tingey R.J., Oliver R.L., Black L.P. (1995), Geology of the Bunger Hills-Denman Glacier region, East Antarctica // AGSO Bull, No. 244, P. 1–136.
Tucker N.M., Hand M. (2016), New constraints on metamorphism in the Highjump Archipelago, East Antarctica // Antarctic Science, V. 28, P. 487–503.
Tucker N.M., Payne J. L., Clark C., Hand M., Taylor R.J.M., Kylander-Clark A.R.C., Martin L. (2017), Proterozoic reworking of Archean (Yilgarn) basement in the Bunger Hills, East Antarctica // Precambrian Research 298, p. 16–38.
Tucker N.M., Hand M., Kelsey D.E., Taylor R., Clark C., Payne J.L. (2018), A tripartite approach to unearthing the duration of high temperature conditions versus peak metamorphism: An example from the Bunger Hills, East Antarctica // Precambrian Research 314, p. 194–220.

Advances in Raw Material Industries for Sustainable Development Goals – Litvinenko (Ed)
© 2021 Taylor & Francis Group, London, ISBN 978-0-367-75881-3

The principal characterized features of earth's crust within regional strike-slip zones

Aleksei Ageev
Ph.D, Assistant Professor, St. Petersburg Mining University, Saint-Petersburg, Russia

Aleksei Egorov
Doctor of Sciences, head of the Geological Department, St. Petersburg Mining University, Saint-Petersburg, Russia

Nikita Krikun
Ph.D student, St. Petersburg Mining University, Saint-Petersburg, Russia

ABSTRACT: Strike-slip zones are very important geological planet-scale structures. Scientific interest in studying these zones connects with frequent natural hazard (earthquakes, land-slides etc.). Moreover, active tectonics provide a high potential for mineral deposit surveys. This article is a first one in a series of articles and show the main result of modern surface structure of Earth's crust of Baikal-Stanovaya strike-slip zone. Before start, we examined results of geological and geophysical investigation of the earth's crust within most studied strike-slip zone all over the World (San Andreas and Upper-Rhine Graben). It helped us to create an algorithm of comprehensive research of crust investigated region. This algorithm consists from 3 stage. First step was accumulated geological-geophysical information about Earth's crust. At the next step we calculated transformation of geophysical potentional fields and conducted lineaments analysis. The final step was focused on compared individual lineament's schemes with geological maps and created a general tectonic scheme of Baikal-Stanovaya regional strike-slip zone.

1 INTRODUCTION

Regional Strike-slip Zones (RSZ) are geological structures of a planetary scale. The study of their modern structure, deep structure and evolution are fundamental tasks of modern geotectonics. High level of crust's destruction influences on minerogenic survey and metallogeny mapping (Nikolaeva, 2019). World experience in the study of new geological structures indicates that the analysis of the results of comprehensive work on the most studied strike-slip zones of the world plays an important role in the research process. Such comparison is possible only in the course of a model that considers the difference in the geodynamic parameters of the structures under study. In the research process, the authors chose a generalized "zonal-blocking geotectonic model of the earth's crust" (Egorov A.S., Gulin V.D., 2014). The main structural units in this model are blocks with continental, oceanic and transitional types of crusts (areas of stationary geophysical parameters) and interblock zones (gradient zones of geophysical parameters, high seismicity and high heat flow). In that case, interblock zones correspond to suture zones, rifts, tectonic dislocations systems and main faults. The number of faults and the value of tectonic stresses within the interblock zones are several times higher than in the internal areas of relatively stationary blocks.

Nowadays, the most detail-studied by complex geological and geophysical methods is the San Andreas faults system. This tectonic zone is considered as the boundary between the North American craton and the Pacific lithospheric plate. Scientists attribute its foundation to a change in the geodynamic situation on the western edge of the North American continent

from subduction to transform, which occurred in the Paleogene (Armstrong, Ward, 1991; Humphreys, 2003). Currently, the dextral strike-slip component predominates in the San Andreas fault system.

2 DATA & METHODS

The results of comprehensive studies show that the highly seismic strike-slip zone of San Andreas is an extremely complex geological structure. The crust is characterized by a zonal-blocking structure which was mapped during geological and geophysical investigations. The main tectonic units are large crustal blocks of the Pacific and North American plates: Great Valley, Mojave, Transverse Ranges, etc. (Figure 1) Their interaction occurs according to a well-developed system of tectonic dislocations which form 3 spatially joint interblock zones (San Andreas, Walker Lane, East California Shear Zone). The most structural controlling dislocation within San Andreas interblock zone is the San Andreas fault. The large part of tectonic stresses from the plate's interaction are indicating along the main fault. San Andreas fault is a very contrast structure. In potential geophysical fields it corresponds to high-gradient zones. On LANDSAT images and 3D models of relief - straightened areas (10 – 50 km length). Nearby the San Andreas fault develop numerous of secondary faults, which also seismogenic. Geological data show that these secondary faults play a key role in joining San Andreas zone with adjustments interblock zones. Results of detailed investigations of Walker Lane and ECSZ show well-developed fault systems with a network of spatially interconnected dislocations within zones. The main fault was not mapped in both structures.

The most studied trans-regional strike-slip zone in Europe is the Upper Rhine Graben (Germany). This tectonic zone bounds by the Rhine massif from the north and by the Swiss Alps

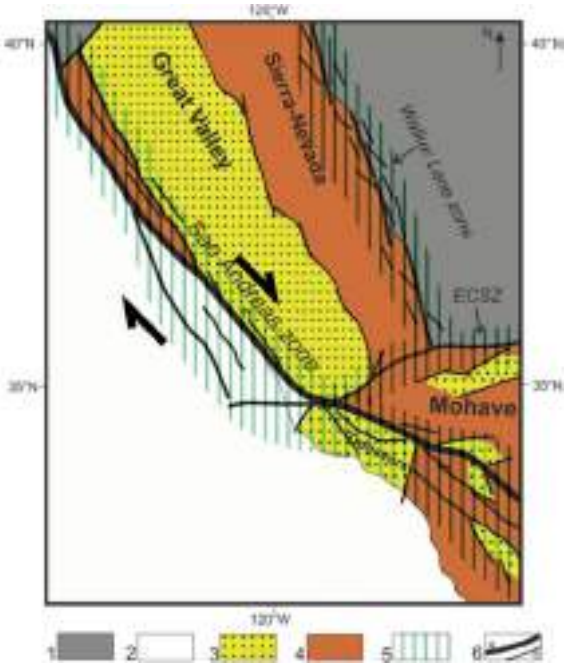

Figure 1. Tectonic scheme of the San Andreas zone.
Legend:1-2 – Lithospheric plates: 1 – North American continental plate; 2 – Pacific Ocean plate; 3-4 – Alpine orogeny stationary blocks with transition type of crust: 3 – Basement covers Tretiary sediments, 4 – Basement covers volcanic sediments; 5 – Interblock zones; 6 – Faults.

from the south (Grimmer, 2017). It is the most seismically active part of the European Cenozoic Rift System. Graben is located in its southern part of it.

The results of geological and geophysical studies show that the crust of this region can be interpreted by a zonal-blocking model. Large blocks of the continental crust are mapped: Moldanubian, Black Forest, Saxon-Thuringian and Swabian (Figure 2). The interblock zone is represented by two elongated "boundary" tectonic faults and a numerous of secondary dislocations (Fracassia, 2005). Researchers in this region identify "boundary" faults as the main structure controlling faults with dominant sinistral kinematics.

These faults mapped by geological surveys and characterize clearly visible structures on remote sensing data. Moreover, these faults correspond to high-gradient zones in potential geophysical fields. "Boundary" faults have a developed system of secondary dislocations. The fault branches extend outside the graben and to its inner region. Both "boundary" and intragraben faults are seismogenic but the intragraben faults mostly correspond normal-fault kinematics.

Scientific results of investigation earth's crust structure of San Andreas and Upper-Rhine Graben help us in studying of a strike-slip zone which develop in the territory of the Russian Federation.

The Neogene-Quaternary Baikal-Stanovaya regional strike-slip zone. It extends for more than 1,500 km east-northeast of Lake Baikal to coastline the Sea of Okhotsk (Ageev, 2016). Large crust geoblocks of the Siberian craton and the Ural-Mongolian ranges belt are most important geological structure of this region.

Research within the San Andreas and the Upper Rhine Graben showes that the first phase of a comprehensive study of the crust should be the spatial modelling of tectonic faults on the surface. In that case, authors formed a geospatial database of geological, geophysical seismological and remote sensing data. The geodatabase was created by ArcGIS 10.3 software, that provided more mobility sharing and updating the database during the research. Information was separated depend on physical properties which data contained. The scale of maps was

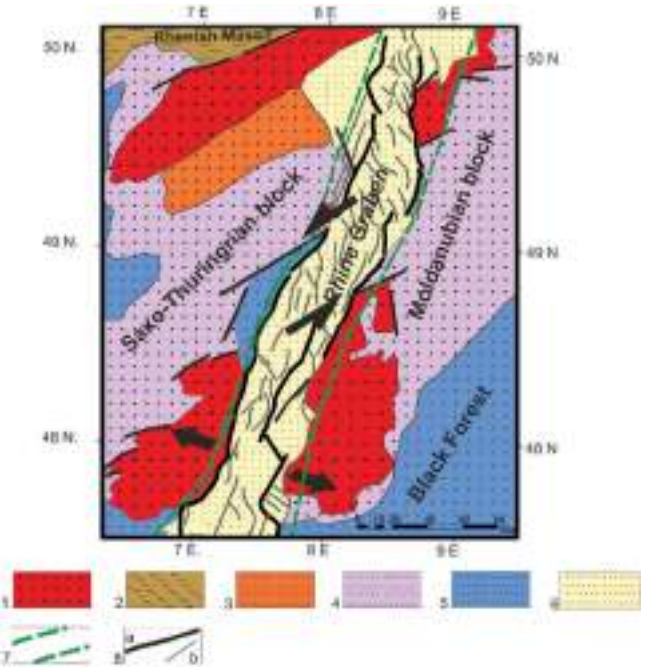

Figure 2. Tectonic scheme of the upper Rhine Graben zone.
Legend: 1 – Variscan crystalline basement; 2 – Devonian sediments; 3 – Permian sediments; 4 – Carboniferous sediments; 5 – Jurassic sediments; 6 – Tertiary sediments; 7 – Interblock zone; 8 -Faults: a – "borders", b – secondary faults.

also important. In that case, we decided to divide all geodata for subdivisions: small-scale; middle-scale and large-scale formats. Small-scale format of data includes: Geological Map of Russia Federation and Adjacent Areas 1:2 500 000; Atlas of Geological Maps of Asia and Adjacent Areas; Tectonic Map of Northern, Central and Eastern Asia; The Atlas of summary maps of the territory of Russia; Map of Active Faults of Russia; In the second group were selected: Geological and Geophysical Maps 1:1 000 000 (lists: O49 – O52; N49 – N52) from All-Russian Geological Institute (VSEGEI);

The main aspect in modeling the lateral distribution of tectonic dislocations were two types of independent lineament analysis: by user (visually) and by computer (PCI Geomatica software). The computer lineament analysis was used only in difficult geological situation and along geotraverses.

The whole complex of georeferenced and systematized geodata was involved in the data process. The most important source for lineaments analysis was satellite images (combined Landsat and visual model of relief). This image covers all investigated region from the lake of Baikal to coastline of the Okhotsk sea. The key features which we tried to identify were straight sections. Mostly it connected with rivers or specific landscape features. At the next step we conducted a lineament analysis of the initial potential geophysical fields (magnetic and gravity fields). The transformants (horizontal and full gradients) were also calculated and have been analyzed. Results of spatial distribution of the earthquake helped in lineament's quality. The catalog of seismic events in the south of the Siberian Platform for the period of instrumental observations from 1960 to 2019 was used in research (U.S. Geological Survey, 2019). The mistake in spatial position of earthquake estimates 1-3 km. In that case the earthquakes data plays secondary role in analysis.

At the first stage of data process we combined georeferenced individual lineaments patterns between each other. Lineaments that were not confirm at least two independent data sources removed from data process. Comparison of georeferenced lineament's schemes conducted in ArcGIS. These procedures led us to reduce a number of lineaments and helped in creation a general scheme of lineaments. The last step was focused on comparison a general lineament pattern with geological, tectonic and active faults schemes. In that case inconsistent lineaments were also deleted.

3 RESULTS

As a result of the studies, a tectonic scheme of the region was compiled. This map shows the zonal-blocking structure of the earth's crust. Several large crustal blocks are identified. A comparison of geophysical fields' linear features, other maps and diagrams made it possible to map and trace spatially interconnected systems of faults and independent faults through the area. Fault systems form an interblock zone, which develops from the southern end of Lake Baikal, then is mapped within the Baikal-Vitimskaya zone, and Khilock-Vitimskiy and Shilkinsky blocks and traces to the east, separating the Aldan and Stanovoy blocks. It should be noted that the main fault does not identified as a single structure. But, a large number of secondary faults are mapped. These faults mostly have echelon and linear form. It can be considered as tectonic "joints" between segments and systems of faults. Most of these faults system form Quaternary and Jurassic depressions. A general shape of interblock zone indicate a bend in a central part of it. In that area we mapped spatial connections with Mongol-Okhotskaya shear zone by group of faults. This situation is similar to San Andreas and adjacent interblock zones. The Mongol-Okhotskaya shear zone older than Baikal-Stanovaya but it also should be investigated in future research.

4 DISCUSSION

The results of the study show that using the model of the zonal-blocking structure of the earth's crust, it is possible to investigate different geodynamic regional strike-slip zones. The main geological units within these structures are blocks and interblock zones. The crust of the

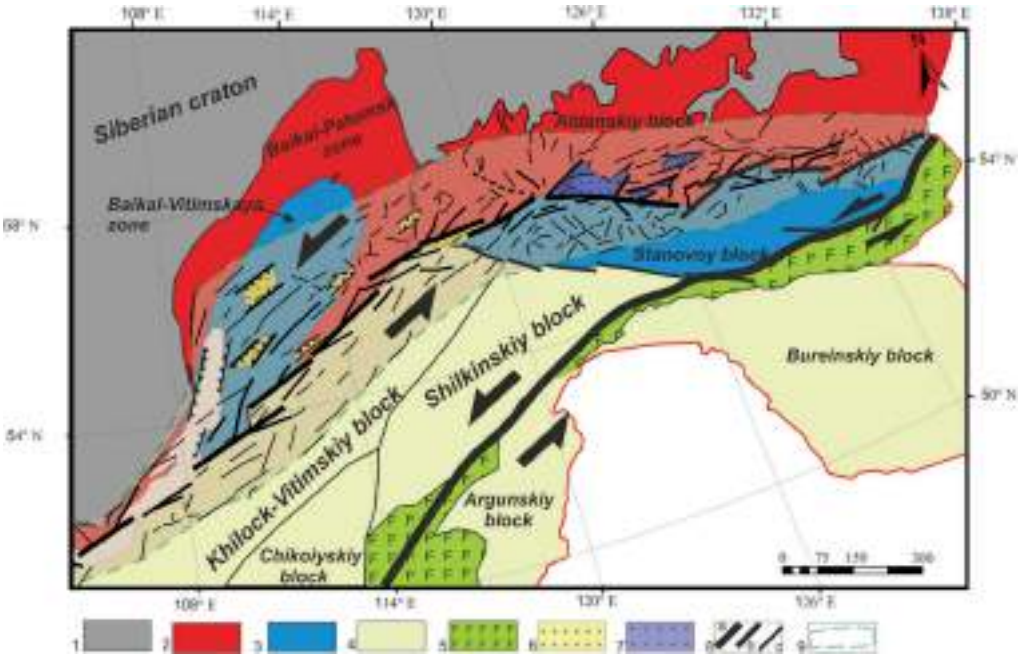

Figure 3. Tectonic scheme of Baikal-Stanovaya strike-slip zone.
Legend: 1 – Continental bocks with Archean basement; 2 - Deformed margins of Archean continental blocks; 3 – Blocks with Caledonian crystalline basement; 4 - Blocks with Cimmerian basement; 5 - Ophiolites; 6 – Neogene-Quaternary basins; 7 – Jurassic basins; 8 – Faults: a –segments of main fault, b –secondary faults with strike-slip kinematics, c – secondary faults with unknown kinematics; 9 – Interblock zone

interblock zones is characterized by the largest number of tectonic dislocations which form spatially interconnected fault systems. It was shown that the shape, quantity, and geographical distribution ensembles of tectonic dislocations within the strike-slip zones are different. These parameters depend on and mainly determined by a value and direction of the vectors of main and local tectonic stresses (Figure 3).

REFERENCES

Ageev, A.S., Ilalova, R.K., Duryagina, A.M. & Talovina, I.V. 2019. A link between spatial distribution of the active tectonic dislocation and groundwater water resources in the Baikal-Stanovaya zone. *Mining Informational and Analytical Bulletin* V.5: 173–180. DOI: 10.25018/0236-1493-2019-05-0-173-180.

Armstrong, R.L & Ward, P. 1991. Evolving geographic patterns of Cenozoic magmatism in the North America Cordillera: The temporal and spatial association of magmatism and metamorphic core complexes. *J. Geophys. Res.*V.96: P.13201–13224. DOI: 10.1029/91JB00412.

Egorov, A.S & Gulin, V.D. 2014. Geological and geophysical deep structure researches of northern Eurasia in the zone-block model of the earth's crust. *6th Saint Petersburg International Conference and Exhibition on Geosciences*: *Investing in the Future* 2014: 133–137. DOI: https://doi.org/10.3997/2214-4609.20140220.

Fracassia, U., Niviere, B. & Winter, T.First. 2005. Appraisal to define prospective seismogenic sources from historical earthquake damages in southern Upper Rhine Graben. *Quaternary Science Reviews* V.24: 403–425.

Grimmer, J.C., Ritter, J.R., Eisbacher, G.H. & Fielitz, W. 2017. The Late Variscan control on the location and asymmetry of the Upper Rhine Graben. *International journal of Earth Sciences* № 106: 827-853. DOI: 10.1007/s00531-016-1336-x.

Humphreys, E, Hessler, E., Dueker, K., Farmer, G., Erslev, E. & Atwater, T. 2003. How Laramide-Age Hydration of North American Lithosphere by the Farallon Slab Controlled Subsequent Activity in the Western United States. In: The lithosphere of Western North America and its geophysical characterization. *Klemperer S.L., Ernst W.G. (Eds.), Bellwether Publishing. Ltd. For the Geological Society of America. The George A. Thompson Volume International Book Series* Volume 7: 524–544. DOI: 10.2747/0020-6814.45.7.575.

Nikolaeva, E., Talovina, I, Duriagina, A., Vorontcova, N., Krikun, N. 2019. The Main Factors Influencing of Minor Intrusions on the Formation of Nickeliferous Weathering Crust on the Example of the Sakhara and the Elov Deposits (Urals). *19th International Multidisciplinary Scientific GeoConference SGEM 2019* Vol.18, Issue 1.1: 625–630. Bulgaria: SGEM 2019 Conference Proceedings. ISBN 978-619-7408-76–8.

U.S. Geological Survey. 2018. *2017, Earthquake Facts and Statistics*: accessed March 22 at URLhttps://earthquake.usgs.gov/earthquakes/browse/stats.php (last accessed 20.01.2020).

Advances in Raw Material Industries for Sustainable Development Goals – Litvinenko (Ed)

Dyke-like and veined bodies' complex of the Elov deposit (the Northern Urals)

E. Nikolaeva
Assist. Prof., Mining university, Saint-Petersburg, Russia

I.V. Talovina
Prof., Head of the Hystorical and dynamic geology department, Mining university, Saint-Petersburg, Russia

G. Heide
Prof., Institutsdirektor, Technische Universität Bergakademie Freiberg, Freiberg, Germany

ABSTRACT: The object of study is the Elov deposit, which is located in the Sverdlovsk region (the Northern Urals, Russia). Based on a comprehensive analysis of geological, mineralogical and petrographic data of the dyke-like and veined bodies of the Elov deposit, the patterns of influence of the veined rocks' composition and quality, as well as the distribution of ore mineralization in them has been researched. Further study of this topic will help to expand the region's prospects for the nickel mineralization's exploration.

Keywords: Elov deposit, Urals, nickeliferous weathering crust, minor intrusions of gabbros and granitoids, dykes, veined bodies

1 INTRODUCTION

The formation of nickel-bearing weathering crusts is the leading geological-industrial type in the world in terms of reserves and mining of nickel. In Russia the main deposits of nickel-bearing weathering crusts are located in well-developed mining regions of the Urals and have been forming the raw material base of the cobalt-nickel industry developed in the Urals for many years.

The formation of nickel-bearing hypergenic weathering crusts is spatially confined to ultramafite formations, the bright examples of which are dunite-harzburgite complexes of the ophiolite formation type and dunite-clinopyroxenite massifs of the zonal formation type.

Nickel-bearing weathering crusts and nickel deposits associated with this type' crusts are mainly developed on ophiolite type' harzburgites and dunites, which in the Urals are represented by a considerable number of large, medium and small massifs confined to deep-seated faults and forming a series of meridional ultramafic belts. The formation of nickel-bearing weathering crusts occurs less often on the dunite-clinopyroxenite massifs of the zonal formation type, confined mainly to the Platiniferous Belt of the Urals.

The geological position and structure of many ultrabasic massifs of the Urals are interpreted ambiguously in the scientific literature despite the long period of study. In this regard, more detailed study of both the mineralogical and petrographic composition of the Urals' massifs' rocks is required.

2 GEOLOGY

The Elov deposit is located on the eastern frontier area of the Kola (Serov) massif in that part of it where hyperbasites are on the border of large protrusion of gneiss-shaped diorites, which were classified by I.S. Lisov (1968) among Pre-cambrian (Figure 1).

The deposit has a very complex geological structure, it is composed of hyperbasites serpentinized to varying degrees or completely transformed into serpentinites and penetrated by dykes and dyke-like bodies of various compositions all over. The hyperbasites presented dunites, peridotites and pyroxenites. Peridotites are the predominant rocks. Dunites are spread less and often interspersed with peridotites. Pyroxenites are found in the eastern part of the deposit mainly, where they fringe the Kola (Serov) massif in the form of wide (100-300 m) ribbon in contact with the Pre-cambrian gneiss-like diorites and granitoids.

Also pyroxenites were found in the southwestern part of the deposit among apoperidotite serpentinites in the form of bodies with thickness of up to 8-10 m.

In the northwestern part of the deposit the hyperbasites are on the border of diorites fresher in age, also numerous apophyses and dykes fall back into hyperbasites. These bodies have submeridional strike and steep mostly eastern pitch, their thickness of up to several tens of meters is.

In addition to the aforementioned dikes and apophyses there is a large number of weathered vein-like bodies having different compositions, a wide variety of shapes, differing thicknesses and various dips and strikes in the weathering crust of hyperbasites.

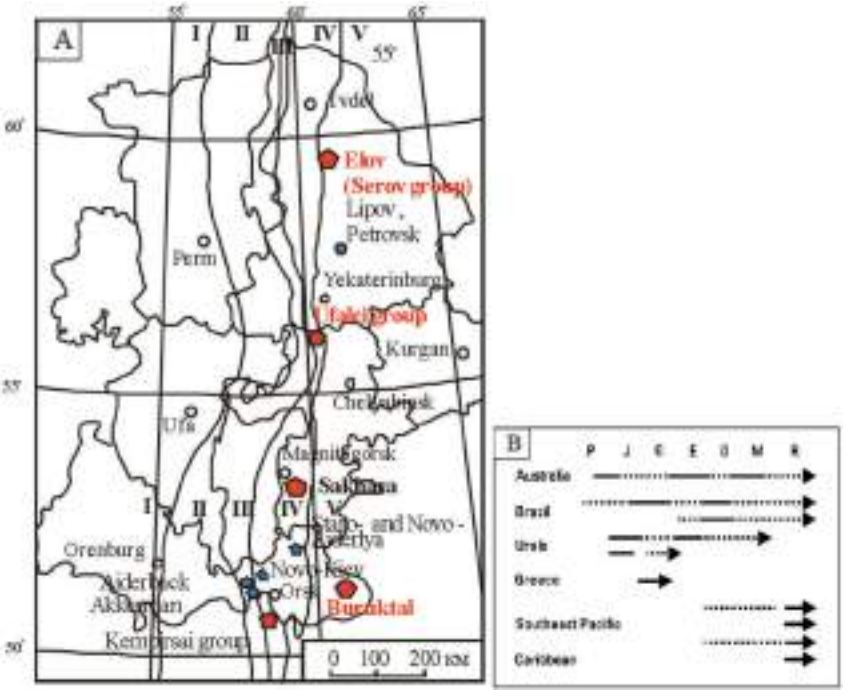

Figure 1. (A) Main tectonical units of the central and northern Urals with the nickelhydrosilicate ore deposits (after Mikhailov, 2002) and (B) Periods of nickel laterite formation in various provinces (after Marsh et al., 2013).

Tectonic zones: I, the East-European platform; II, the Fore-Ural megazone; III, the Central-Ural megazone; IV, the Tagil-Magnitogorsk megazone; V, the East-Ural megazone. Main supergene nickel deposits: the Buruktal deposit, the Ufalei group (the Cheremshanka, the Sinara, the Rogozha deposits), the Serov group (the Elov deposit). P, Paleozoic, J, Jurassic, Є, Cretaceous, E, Eocene, O, Oligocene, M, Miocene, R, Recent.

According to exploratory drilling's and mining works' data loose weathering products of vein-rocks in weathered hyperbasites are found in the upper part of the geological record much more often than vein-shaped bodies in fresh hyperbasites at depth.

Considering the data of measurements of dip and strike of vein-shaped bodies in prospect holes and cut acrosses, we can conclude that the vein-shaped bodies of southwestern strike in the central part of the Elov deposit prevail. The vein-shaped bodies of both northwestern and southeastern strike are equally spread. The vein-shaped bodies of northeastern strike are widespread in this area to a much lesser extent. The largest of them resemble "feathers" in shape with steeply going down "trunks". In the southern part of the deposit, the vein-shaped bodies are spread much less, the strike is mainly northwestern and southwestern, the pitch is steep.

In the east of the Elov deposit the shallow dipping apophyses of diorites are widespread and they form the lower parts of the geological record.

Nickel-bearing ore mineralization of the Elov deposit (Figure 2) is confined to the weathering crust of ultramafic rocks of peridotite's formation which all nickel deposits of the Urals and the North Kazakhstan are related with.

The Elov deposit (Figure 3) contains a large number of minor intrusions in contrast with all other Urals' deposits and for the formation of the weathering crust with equivalent nickel content as in other deposits with similar composition it could be required twice the amount of nickel in the source serpentinites or double expansion of decayed and weathered serpentinites, from which fully leached nickel was redeposited in orebodies.

According to calculations of the ratio of minor intrusions height to the seam height of serpentinites in the central part of the Elov deposit minor intrusions estimated 40% of total

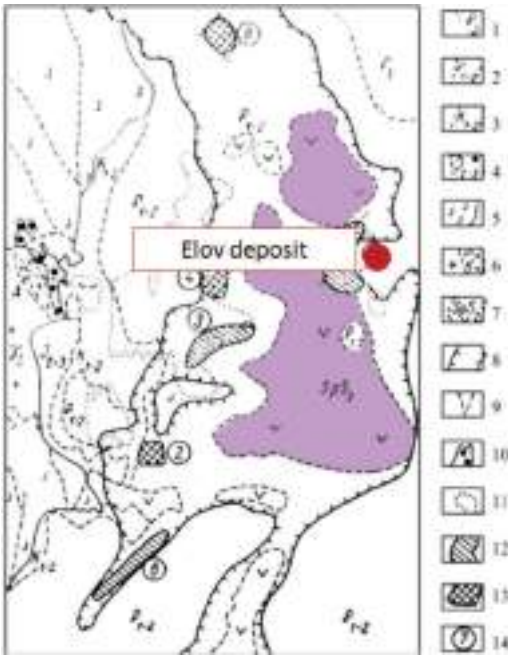

Figure 2. Schematic geological and technological map of deposits of the Serov group (after Vershinin et al., 1988).
1–4, Meso-Cenozoic deposits of the weathering crust; 5–6, Paleozoic formations; 7, day stones of serpentinites; 8, contours of serpentinites in accordance with magnetic survey and drilling; 9, zones of tectonic dislocations; 10, chalcopyrite-magnetite skarns; 11, nodular-conglomerate sedimentary iron ores in the deposits of the Myssov suite; 12–14, deposits of supergene nickel ores of various technological types: 12, ores for alkaline hydrometallurgical process, 13, ores for blast smelting process; 14, numbers of deposits. The Serov group of deposits: 7, Elov; 6, Katasmin; 8, Ustey; 2–4, others.

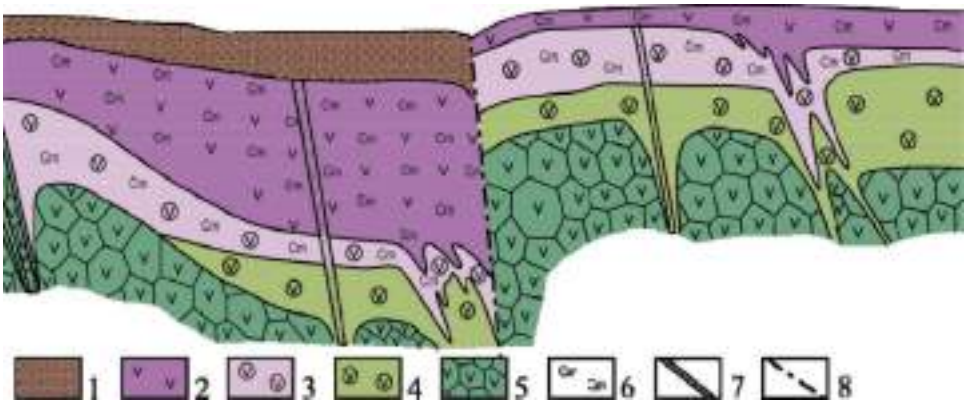

Figure 3. Geological record of the weathering crust of the Elov deposit (after Berkhin et al., 1970).
1, nodular-conglomerate sedimentary iron ores (K_1); 2, nontronited serpentinites; 3, leached serpentinites; 4, disintegrated serpentinites; 5, unaltered serpentinites; 6, chamosites; 7, chlorite vein-rock; 8, fractures.

rocks thickness, sometimes in some small areas volume of vein-shaped bodies exceeds volume of the serpentinites.

3 COMPOSITION AND STRUCTURE

The composition of the vein-shaped bodies is different. Among them pyroxenites, gabbros, gabbro-porphyrites, odinites, spessartites, diorites and granitoids are noted. One part of the vein-shaped bodies is associated with hyperbasites, and the other part of them refers to granitoids derivatives. Some vein-shaped bodies may have a local contact-reaction-metasomatic genesis, i.e. they are the result of exposure to hyperbasites of post-magmatic liquids associated with granitoids.

The vein-shaped bodies of local contact-reaction-metasomatic genesis have a mutable composition, which varies from gabbroids to granitoids, and often a zonal structure. Zonation in most cases is asymmetric. The near-contact parts of the vein-shaped bodies are usually composed of amphibole rocks with relics of pyroxene and have different thicknesses (from a few centimeters to 1-2 meters). The following zones are represented by gabbroids, diorites, and, less commonly, granitoids sequentially to the center. Contacts between marked types can be either gradual or abrupt. Gabbroids in composition and structure resemble issites, hornblende microgabbros or metamorphic norites such as gabbro-amphibolites. They often have a banded structure, and the direction of banding coincides with the direction of contacts of the vein-shaped bodies with the surrounding hyperbasites. Gabbroids are sometimes represented by rocks of the amphibolite type, in which rocks of the diorites' and granitoids' composition are found in the form of vein-like aggregates and splices with tortuous outlines. In the vein rocks, all of the above varieties are not always present, and more often one or two varieties are absent. Amphibole rocks in the form of angular-shaped "detached masses" of up to 5-10 cm in size are observed in the diorite composition rocks. Narrow reaction rims of chlorite, tremolite and talc with a thickness of up to fractions of a meter, rarely up to 1 meter, are found at the contacts of the metasomatic vein bodies with the hyperbasites. Moreover, chlorite is formed mainly due to vein rocks, and tremolite and talc appear due to hyperbasites and serpentinites. The thickness of the contact-reaction rims depends on the thickness of the vein-shaped bodies. A thin biotite rim is occasionally present before the chlorite rim at the contacts of granitoids or quartz diorites with hyperbasites. Hyperbasites in the near-contact zones are transformed into antigorite serpentinites. The thickness of antigorite serpentinites is usually within a few meters.

When compiling a geological map of the weathering crust of the Elov deposit, some of the many varieties of rocks described above were combined into several types:

1. the group of hyperbasites includes dunites, peridotites and serpentinites;
2. the group of gabbroids includes vein pyroxenites, gabbros, gabbro-porphyrites, amphibole near-contact rocks such as issits, also odinites and other amphibolites;
3. the group of dioritoids includes diorites, quartz diorites, spessartites, granodiorites, plagiogranites, granites, plagiaplites and albitites.

4 TECTONICS

Paleozoic rocks of the deposit reflect traces of intense tectonic activity. Exploration work revealed a large number of joints and fractured zones of both submeridional and sublateral (East-West, EW) directions. Many of the largest tectonic faults, especially those with an EW trending, are controlled on the present surface of the relief by small rivers and narrows, and the largest submeridional faults in the eastern part of the deposit have steep stair-stepping benching towards the Sos'vin depression. The geological map shows mainly tectonic dislocations, renewed by adjustment movements immediately preceding the encrustation stage and later ones occurring in the Meso-Cenozoic period (cf. Ageev et al. 2019).

In Paleozoic age rocks a highly eroded weathering crust is well developed. The maximum crust thickness according to exploratory drilling wells data reaches 85 meters, and the thickness of nickel-bearing crust with industrial nickel contents in individual sections is up to 50 m. It is represented mainly by the lower zones, i.e. the zones of leaching and integration. The weathering crust has been most fully preserved under Meso-Cenozoic deposits, especially along tectonic dislocations and joints, where strongly decomposed clay products and ochres developed after ultrabasic and basic rocks decomposition are also noted along with leached rocks.

Almost all products of ultrabasic rocks' weathering crust are nickel-bearing in the deposit, including the vein rocks under favorable conditions.

Ores associated with weathering products of ultrabasic rocks account for 76% of their total volume in the deposit. Of these, 18% are ochres and heavily ocherized leached nontronitized serpentinites. 24% of the total ore mass is associated with the weathering products of the vein rocks.

Initially, the weathering crust on the deposit had a wider development scale and greater thickness. Its upper clay and ocher products are mostly eroded at present. The erosion crust was eroded several times throughout the subsequent history of the development of the region, as a result of which the crust was almost completely eroded in some areas.

The free-open textured products of the weathering crust were transferred to the lower parts of the ancient relief of the deposit and were deposited at the bottom of lakes and swamps. They were a source of accumulation and formation of iron bean-conglomerate ores.

The Elov deposit is characterized by a shallow bedding of rocks in comparison with a number of other deposits of the Serov orefield.

In the western part of the deposit, the weathering crust directly lies under the Quaternary age deposits at a depth of the first tens of meters. Further east, as hyperbasites sink, the depth of nickel-bearing crust increases, reaching 80 meters. Meso-Cenozoic deposits appear in the geological record, at the base of which are bean-conglomerate ores. Up the geological record, bean-conglomerate ores are replaced by glauconite-quartz sands, mudstones (or argilites), silica gaizes and diatom earth.

5 PROCESSING

Currently, three different processes (Figure 4) are used to extract the nickel and cobalt elements from the mined rocks. The Caron process and high-pressure-acid leaching (HPAL) are mainly used for the oxide ore subtypes. For the nickel clay deposits, the HPAL method is also used with priority, whereas for the serpentine subtypes, a pure melting method is preferred.

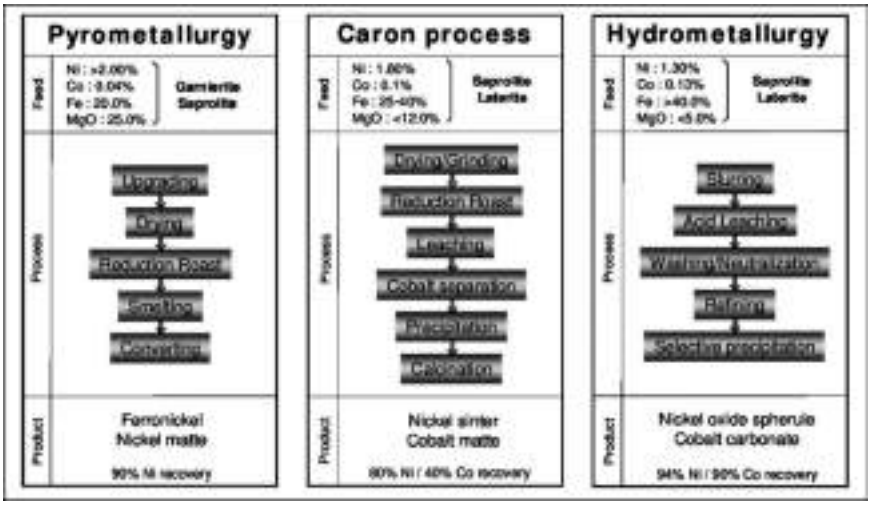

Figure 4. Main processes for the extraction of nickel out of lateritic rocks.

Ongoing research is developing new extraction methods, such as the Dni-Hydrometallurgy process developed by DirectNickel, which can also process the entire laterite profile without prior separation (cf. Kobylyanski et al. 2019). But because of the complexity needed to handle and process the nickel-cobalt laterites, much research has focused on ore delineation and mineralogical identification for distinguishing rocks. Thus it is important to characterize the mineralogy of the Elov deposit in more detail (cf. Lvov et al. 2017).

6 MATERIALS AND METHODS

6.1 *Samples*

For the investigation there were nine samples, which were sampled during an excursion by leading of Prof. Dr. Irina Talovina (Saint Petersburg Mining University) and Prof. Dr. Gerhard Heide (TU Bergakademie Freiberg) in the active open pit Elov nearby the town Serov in September 2014. The samples are crude ore as well as country rock that occur within the open pit area. In the following, the samples are listed in Table 1.

6.2 *Analytical methods*

The mineralogical composition of the samples was determined by using x-ray diffraction phase analysis. All samples were prepared as powder preparations. The rocks were crushed

Table 1. The investigated samples with Nickel content, %.

Sample	Name	Ni
SV 02	Porphyritic serpentinite	0.117
SV 04	Chromite ore	0.056
SV 06	Talc-chlorite-schist	0.542
SV 07	Limonite ore	1.160
SV 08	Gangue rock	0.199
SV 09	Contact-zone of SV08	0.163
SV 10-1	Silicate nickel ore	0.101
SV 10-2	Silicate nickel ore	0.979
SV 11	Oxide nickel ore	1.030

with a hammer down to a grain size < 400 μm. The bulk samples were subsequently divided using quarter cross. Further crushing was done using the ball mill XRD-Mill McCrone with ZrO2-grinding bodies. Technical ethanol (96%) was used for cooling and to guarantee careful grinding. After drying, the samples were homogenized by means of an Ardenne vibrator and finally sieved with a 200 μm sieve into an aluminum cuvette using the side-loading procedure. The measurements were executed with URD 6 (Mineralogical laboratory TU Bergakademie Freiberg) with Co-radiation.

To investigate the swelling capable minerals which show mainly wide reflexes in the 14 Å area, texture preparations were produced in the traditional way. The selected samples were first measured in an air-dried state, afterwards they were saturated in ethylene glycol vapor and then measured again. The ethylene glycol accumulates in the interlayers of the minerals and causes a widening of the structure, thereby increases the layer distance. After the second measurement, all texture preparations were annealed at 400 °C and measured again. The last measurement was executed after an annealing process at 550 °C.

Thermal analyses were carried out in the mineralogical laboratory of the TU Bergakademie Freiberg by Dipl.-Chem. Margitta Hengst. All measurements were realized by means of the STA 409 PC, and a heating rate of 10 kelvin per minute, up to a maximum temperature of 1200 °C. As carrier gas, purified air was used for all analyses. The reference material for the DTA analyses was corundum (cf. Földvari 2011).

The observations on the scanning electron microscope (SEM) were mainly examined on polished thin sections of the solid rocks. Individual measurements were also carried out on strewn slides. For the investigations it was possible to use the CarryScope JCM-5700 from the museum "Terra Mineralia Freiberg". This SEM is equipped with a Bruker EDX (133eV). The focus of this analytical method was the determination of the spinel group minerals. Further questions arose with regard to the distribution of the various valuable elements inside the rock units, primarily nickel. As far as possible, this method allowed the investigation of the local coupling of nickel to the various minerals.

6.3 *Results*

The chemical analyses show a significant accumulation of nickel in various rocks of the open pit. Most of the silicate dominated areas of the deposit contain higher nickel concentrations, however, they are not high enough to reach economic relevance. The rocks display nickel contents between 0.101% and 0.542%. An exception is the major amount of silicate nickel ore (SV 10-2), which at 0.979% shows significantly increased nickel contents of economic importance. It is note-worthy that only the unaltered areas of the silicate nickel ore have significantly elevated contents, while the secondary silicified zone has only a very low nickel content of 0.101%. Since the biggest difference lies in the mineral composition, in this case the increased content of serpentine and especially smectite in the non-silicified areas, the nickel must be linked to exactly these minerals. It can be assumed that these are typical nickel-containing nontronites (cf. Brindley 1984b, Brindley et al. 1973).

The highest nickel contents were detected in the oxidic type nickel ore of SV 11 (1.03%) and in the limonite ore of SV 07 (1.16%). Thus, these areas are most enriched when considering the absolute contents. As far as the limonite ore is concerned, it can be assumed that the nickel is primarily coupled to nickel-rich goethite and very occasionally to nickel sulphides. The rock contains neither smectite nor talc, and the serpentine branch veins (apophysis) in which EDX analyses did not show any major nickel content, are the result of later secondary formation. According to the elevated position of the dehydroxilation peak, the thermal analyses of goethite indicate a significant foreign metal substitution, further substantiating the thesis of nickel-rich goethite (cf. Talovina 2012, Talovina et al. 2008, 2010, 2011, 2012). Although nickel sulphides have been detected in limonite ore, their absolute contents are negligible compared to the substitutional placement in the goethite structure. This is corroborated by the missing peaks in the powder diffraction pattern as well as by the low sulphur content of the sample. It merely amounts to 0.10% sulphur content compared to the 1.16% nickel content. In the oxidic type nickel ore (SV 11), the nickel carrier cannot be reliably determined.

However, enrichment in the silicate components seems to be plausible, especially in chlorite and smectite as well as in goethite, which also has increased d values. Also in this particular rock the serpentines showed no relevant nickel content throughout the EDX measurements.

7 CONCLUSION

The Serov group of deposits is one of the sedimentary-infiltration formations. The Orsk-Khalilovsk, Aydyrlinsk and other deposits, except the Elov deposit, belong to this kind of formations in the Urals. In this type a significant role belongs to the nickel-containing ore-forming ferruginous chlorite, i.e. shamosite (Fe5Al)(AlSi3O10)(OH)8. The deposits of this type had experienced a rather complex history of formation, including the stage of epigenesis (destruction, transportation and deposition with the formation of ferrous sedimentary rocks) in addition to the lateritogenesis stage (cf. Yudovich et al. 2011).

The vertical zonal profile in the nickel weathering crust of the Elov deposit is observed (from the bottom up): serpentinized ultramaficites (substrate) − serpentinite zone − nontronite zone − oxide-iron zone. Separately, it is worth noting the shamosite zone, which belongs to the converted part of the weathering crust of the Elov deposit, has a limited distribution and replaces serpentinite, nontronite and oxide-iron zones in part or completely.

The research displays a very diverse mineralogy in the rocks of the Elov deposit. It was shown that different types of rocks from variously weathered areas of the deposit have relevant nickel contents. Due to the different mineralogy of the nickel-bearing minerals between laterite and saprolite, both a selective mining and a selective processing of the individual types of ore should be considered.

ACKNOWLEDGEMENTS

The work is carried out with financial support of Ministry of Education and Science of Russian Federation according to grant program "Research and development in priority areas of development of Russia's scientific and technical complex for 2014 – 2020", the project RFMEFI61620X0127.

REFERENCES

Ageev A. S., Ilaliva R. K., Duryagina A. M., Talovina I. V. A link between spatial distribution of the active tectonic dislocation and groundwater water resources in the Baikal-Stanovaya shear zone. *Gornyy informatsionno-analiticheskiy byulleten'*. 2019;5:173–180. [In Russ]. DOI: 10.25018/0236-1493-2019-05-0-173-180.

Bugelskiy, J. J., I. V. Vitovskaya, A.P. Nikitina. 1990. *Ekzogennye rudoobrazujushhie sistemy kor vyvetrivanija (Exogenic Ore-forming Systems of Weathering Crusts*). Moscow, Nauka, 365 p. (in Russian).

Földvari M. 2011. *Handbook of thermogravimetric system of minerals and its use in geological practice*. In Occasional Papers of the Geological Institute of Hungary, Vol. 2, 180 p.

Gottman, I. A., E. V. Pushkarev. 2009. Geologicheskie dannye o magmaticheskoi prirode gornblenditov v gabbroul'tramafitovyh kompleksah Uralo-Alyaskinskogo tipa (Geological data on the magma nature of hornblendites in gabbroultramafic complexes of the Ural-Alaskan type). *Litosfera*, *2*, 78–86 (in Russian).

Kobylyanski, A., Zhukova, V., Petrov, G., Boduen, A.Y. 2019. Challenges in processing copper ores containing sulfosalts. DOI: 10.1201/9781003017226-18. In book: *Scientific and Practical Studies of Raw Material Issues*, pp.120–128.

Lazarenkov, V. G., I. V. Talovina, I. N. Beloglazov, V. I. Volodin. 2006. *Platinovye metally v gipergennyh nikelevyh mestorozhdenijah i perspektivy ih promyshlennogo izvlechenija (Platinum metals in supergene nickel deposits and prospects for their commercial extraction*). St Petersburg, Nedra, 188 p. (in Russian).

Lvov V., Sishchuk J., Chitalov L. Intensification of Bond ball mill work index test through various methods//*17th International multidisciplinary scientific geoconference and expo SGEM* - 2017, Vol. 17, Issue 11, pp. 857–864. DOI: 10.5593/sgem2017/11/S04.109.

Marsh, E., E. Anderson, F. Gray. 2013. Nickel-Cobalt Laterites – A Deposit Model Chapter H of Mineral Deposit Models for Resource Assessment. – In: *Scientific Investigations Report 2010–5070-H*. Reston, USGS, 38 p.

Mikhailov, B. M. 1999. Nickel ores in the Urals. *Lithology and Mineral Resources*, *35*, 4, 351–364.

Mikhailov, B .M. 2002. Perspective of mineral base of nickel industry in Urals. *Regionalnaya Geologiya i Metallogeniya*, *15*, 97–109.

Marin, Y .B., V. G. Lazarenkov. 1992. *Magmatic formations and their ore-bearing*. St. Petersburg, Mining University (SPbGGI), 166 p.

Nikolaeva, E.; Talovina, I.; Duriagina, A.; Vorontcova, N.; Krikun, N. 2019. The main factors influencing of minor intrusions on the formation of nickeliferous weathering crust on the example of the Sakhara and the Elov deposits (Urals). *19th International Multidisciplinary Scientific GeoConference SGEM 2019*; SGEM; Sofia Vol. 19, Issue 1.1,: 625–630. Sofia: Surveying Geology & Mining Ecology Management (SGEM). (2019) DOI:10.5593/sgem2019/1.1/S01.077.

Nikolaeva, E.S., Talovina, I.V., Nikiforova, V.S., Heide, G. 2019. Chemical composition and genesis of serpentinite group minerals in nickeliferous weathering crust of the Elov deposit (Urals). DOI: 10.1201/9781003017226-1. In book: *Scientific and Practical Studies of Raw Material Issues*, pp.3–10.

Talovina, I. V., G. Heide. 2016. Serpentines of Chrysotile-pecoraite series as genesis indicators of nickel deposits in the Urals weathering crusts. *Journal of Mining Institute*, *221*, 629–637. DOI 10.18454/ PMI.2016.5.629.

Talovina, I. V., V. G. Lazarenkov, S. O. Ryzhkova, V. L. Ugolkov, N. I. Vorontsova. 2008. Garnierite in Nickel Deposits of the Urals. *St. Petersburg State Mining Institute (Technical University), Lithology and Mineral Resources*, *43*, 6, 588–595.

Talovina, I. V. 2012. *Geohimija uralskih oksidno-silikatnyh nikelevyh mestorozhdenij (Geochemistry of the Uralian oxide-silicate nickel deposits*). St. Petersburg, Natsionalnyi mineralno-syrevoi universitet "Gornyi". 270 p. (in Russian).

Talovina, I. V., N.I. Vorontsova, S. O. Ryzhkova O. P. Mezentseva, A. G. Pilugin. 2012. Harakter raspredelenija redkozemel'nyh jelementov v rudah Elovskogo i Buruktalskogo gipergennyh nikelevyh mestorozhdenij (Pattern of rare earth element distribution in ores of the Elov and Buruktal supergene nickel deposits). *Zapiski Gornogo Instituta*, *196*, 31–35 (in Russian).

Talovina, I. V., V. G.Lazarenkov, N. I. Vorontsova, O. P. Mezentseva, S. O. Ryjkova, A. G. Pilugin. 2010. *Geochemistry of impurity elements in Buruktal supergene nickel deposit, South Urals*. Freiberg – St. Petersburger interdisziplinares Kolloquium junger Wissenschaftler. Technische Universitat Bergakademie Freiberg. 40–43.

Talovina, I.V., V. G. Lazarenkov, U. Kempe, M. Tichomirowa, N. I. Vorontsova, A. G. Pilugin. 2011. *Value in Millerite and Genesys of Chamosite Nickel Ores in the Elov Supergene Deposit (Serov Group), North Urals*. Scientific Reports on Resource Issues. Vol.1: Latest Developments in Mineral Industry – Geology, Mining, Metallurgy and Management. TU Bergakademie Freiberg. 30–34.

Talovina, I. V. 2012. *Geochemistry of supergene nickel deposits of the Urals*. PhD Thesis, G.-M. Sciences: 25.00.09., St. Petersburg, 270 p.

Volchenko, Y. A., K. S. Ivanov, V. A. Koroteev, T. Auger. 2007. Strukturno-veshhestvennaja evoljuciya kompleksov Platinonosnogo pojasa Urala pri formirovanii hromit-platinovyh mestorozhdenii uralskogo tipa (Structural-compositional evolution of the Ural Platinum Belt complexes during the formation of platinum-chromite deposits of the Ural type). Part 1. – *Litosfera*, *4*, 73–101 (in Russian).

Yudovich, Y. E., M. P. Ketris. 2011. *Geochemical indicators of lithogenesis (lithological geochemistry*). Syktyvkar, Geoprint, 742 p.

Advances in Raw Material Industries for Sustainable Development Goals – Litvinenko (Ed)
© 2021 Taylor & Francis Group, London, ISBN 978-0-367-75881-3

Longwall panel width optimization

D. Belova
Postgraduate student, St. Petersburg mining University, St. Petersburg, Russia

A. Sidorenko
PhD, Associate professor, St. Petersburg mining University, St. Petersburg, Russia

A. Meshkov
«SUEK-Kuzbass»

ABSTRACT: The article discusses the issues encountered by mining companies in Russia when extracting coal through the use of fully mechanized longwalls. The article presents the results of an analysis of coal mining operations in the world's largest coal producers (USA, Australia, and Russia). As a result of the analysis, it has been determined that longwall panel width depends on a range of geological and engineering factors, such as average annual production, panel length, working height, depth of cover, etc. Using the cases of several Australian mines, the authors examine the influence of longwall panel dimensions on water inflows in the longwall face and mine faces taking into account the influence of overburden pressure and fracture density. The issue of massive water inflows at the thick-seam coal mine named after V. D. Yalevsky in the Kuznetsk Basin is considered. The results of mathematical modelling and economic evaluation for different longwall panel dimensions presented in the article make it possible to determine the range of optimal longwall panel dimensions with due consideration of working heights.

1 INTRODUCTION

When facing volatility and tough competition in the global coal market, one of the key issues for coal mining companies is to reduce their production costs. The main cost-reducing method in underground coal mining is to deploy a fully mechanized longwall system, which delivers excellent results in terms of productivity and economic performance if there are no mining constraints. However, as the main coal-mining regions in Russia are characterized by complicated geological settings, it negatively influences equipment performance indicators. This is why searching for optimal engineering solutions for the effective use of advanced equipment is an important practical task for Russian mines. The longwall method is the most popular method of underground coal mining in Russia. Such parameters of longwalls as panel width and length have a significant impact on productivity and safety. It should be noted that Russia has not yet accumulated any experience in using longwall faces with a length of more than 400 m (only one mine has been operating with a panel width of 400 m since 2017), which makes analyzing the experience accumulated by the top coal-producing countries of particular interest.

2 LITERATURE REVIEW

One of the global coal mining leaders is the United States of America in terms of not only production indicators but also the state of technology used in mining operations. When analyzing data on American longwall mining operations over the last 35 years, it can be noted

that over this period the share of panels with widths ranging from 122 to 183 m decreased from 81% in 1984 to 5% in 2018, with a large share taken by panels having a width over 305 m (Figure 1). It should be stressed that there is a common upward trend in panel width seen in all the top coal-mining countries and the number of longwalls being operated in the U.S. almost halved over the same period due to the use of state-of-the-art equipment in favourable geological settings and an increased concentration of production.

If we look at how longwall panel width influenced average annual production in U.S. coal mines over a period from 2013 to 2018 (Figure 2), it becomes obvious that longwalls with panel widths exceeding 400 m are characterized by the highest production rates in each of the years analyzed (Fiscor, 2014-2019).

It should be kept in mind that the choice of longwall panel dimensions depends on geological settings and engineering parameters, such as working height and depth of cover.

Based on the analysis of data on U.S. mines operating in 2018, it can be argued that, as a rule, thick coal seams are mined using panel widths of up to 350 m, whereas medium-thick seams are mined using bigger panel widths.

The influence of the depth of cover on the choice of panel width is the following: the greater the depth, the less likely the use of panel widths exceeding 300–350 m.

Each of the above factors influencing the choice of panel width is, in its turn, influenced by overburden pressure and face ventilation conditions.

At the same time, panel dimensions are undoubtedly interrelated, which makes it necessary to find the optimal panel length when determining the optimal panel width. This requirement is based on the fact that geological data on the block of the seam being mined is unevenly distributed. In 2018, panels with widths ranging from 350 to 400 m had the biggest length

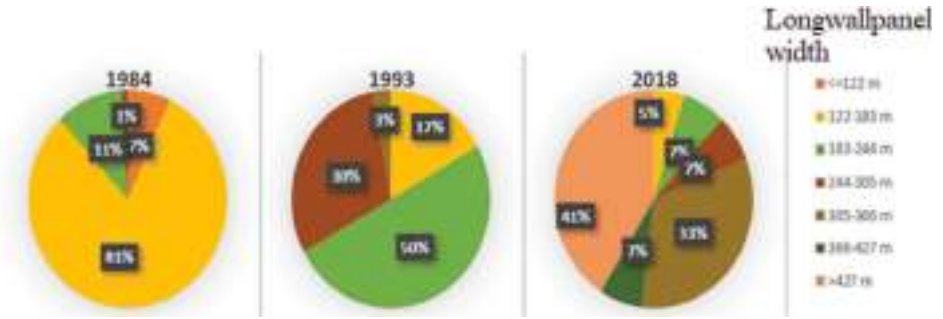

Figure 1. Shares of U.S. mines active in 1984, 1993, and 2018 based on longwall panel width.

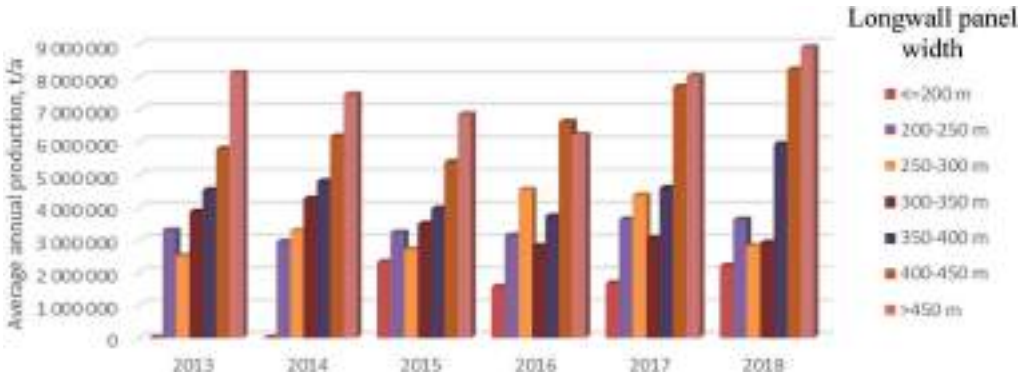

Figure 2. The dependence of average annual production on longwall panel width at U.S. mines for years 2013 to 2018.

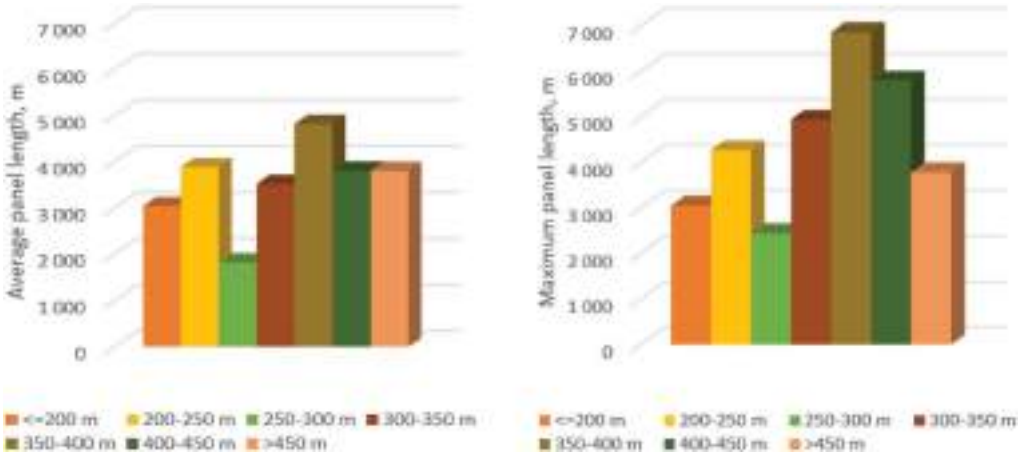

Figure 3. The dependence of average and maximum panel lengths on panel width in the U.S. in 2018.

(about 7 km) along with the biggest average length (Figure 3). Based on these figures, it can be assumed that an increase in panel length sets the stage for an increase in panel width.

Under ideal geological settings, i.e. when the coal seam is flat-lying and free of such geologic structures as faults and joints, the methane content is low, and water inflows are regular as mining operations are conducted far enough from river valleys or lake basins or other sources of massive water inflows, an increase in panel dimensions undoubtedly leads to an increase in equipment utilization efficiency and a growth in the concentration of production at minimum cost. However, when geological settings are not ideal, the feasibility of increasing panel length should be studied from an economic perspective. The main questions arising in this process are: what restrictions are there on increasing panel dimensions and how much do these restrictions affect the productivity indicators of one or another mining sequence?

The positive results of increasing panel dimensions (a decrease in the number of assembly and disassembly operations in the mine, a decrease in the unit cost of panel preparation, an increase in face productivity, more regular methane emissions, and a decrease in coal loss due to chain pillars) in real-life geological settings should be considered along with negative consequences (an increase in absolute methane emissions from the seam being mined into the working area, an increase in methane emissions from adjacent seams into the mined-out areas, an increase in the length of assembly and disassembly operations in the working area, an increase in initial capital costs due to the cost of equipment, an increase in the variability of geological settings within one panel, as well as an increase in loads on load-bearing elements and, as a result, a bigger influence of overburden pressure).

An example of a mine characterized by negative results of an increase in panel dimensions is the mine named after V. D. Yalevsky (the Kuznetsk Basin). The section of coal seam No. 52 being mined is affected by the Srednyaya Salanda River valley causing massive water inflows into the longwall face and the mine faces. As a rule, when there are massive water inflows, it is recommended that reserves should be mined in a bottom-up sequence to prevent water from flooding the faces (Chemezov, 2019). However, an increase in panel dimensions has resulted in the fact that the geological and geometrical characteristics of the coal seam within one panel are so different on the up-dip and down-dip sides that the extraction sequence has to be changed. When mining in a top-down sequence, there is a sharp drop in face productivity.

It is considered that the main reason causing massive water inflows is an increase in panel dimensions. For example, in a report on one of the Australian mines dated October 29, 2008 (Gale, 2008), the author analyzes the effect of changes in panel width on water inflows into working areas. Using computer modelling tools, the author shows that with an increase in panel width, there is a bigger zone of destressed strata, which causes stress redistribution and, as a consequence, a growing zone of high rock pressure resulting in extra fracturing. An

increase in fractre density entails an increase in water inflows at the face ends. However, such a parameter as the depth of cover should also be taken into account. At shallow depths, the influence of these processes is especially great, since the river valley, as a rule, is impacted by mining operations even if there are impermeable layers. However, with an increase in the depth of cover, the impact of mining operations on the layers located closer to the surface diminishes, which suggests that there is such a depth of cover at which an increase in panel dimensions does not have a significant impact on water inflows into the longwall face and the mine faces.

According to the results of studies conducted at another Australian mine in 2015 (Skorulis& Minchin, 2015), the impact of longwall mining operations can be graphically represented in the following way (Figure 4):

The dimensions of each zone are calculated individually for each kind of geological settings and each set of panel dimensions. The results of calculations make it possible to predict, to some degree, the intensity of water inflows into longwall faces, which, in turn, enables engineers to take precautions against water inflows and tackle the issue of a drop in face productivity.

3 MATERIALS AND METHODS

In order to find the optimal panel width, mathematical modelling and economic evaluation of the dependence between panel width and performance indicators were carried out. In the model, the total unit costs for the main items as well as the net present value (NPV) were taken into account. A range of panel widths from 200 to 450 m with a step of 50 m was analyzed. The model was built using the parameters of geological settings at the mine named after V. D. Yalevsky (SUEK-Kuzbass).

Mathematical modelling and economic evaluation were carried out taking into account the following cost items: unit production costs, unit development costs, total unit costs. As the next step, the price for coal as of the moment of modelling was taken to calculate the income based on different production volumes, which was later discounted.

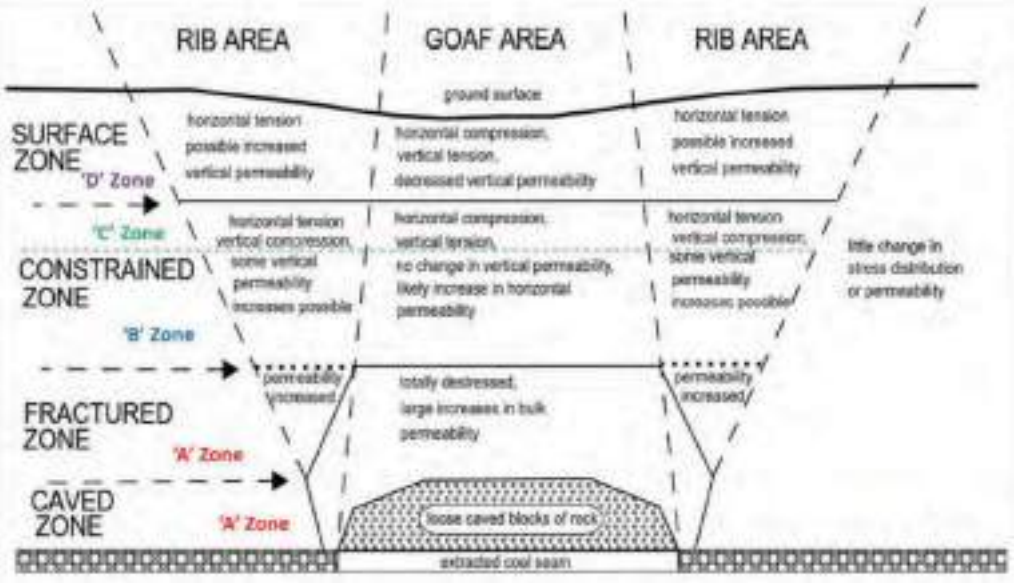

Figure 4. Zones of disturbance and hydrogeological effects following longwall mining (Skorulis& Minchin, 2015).

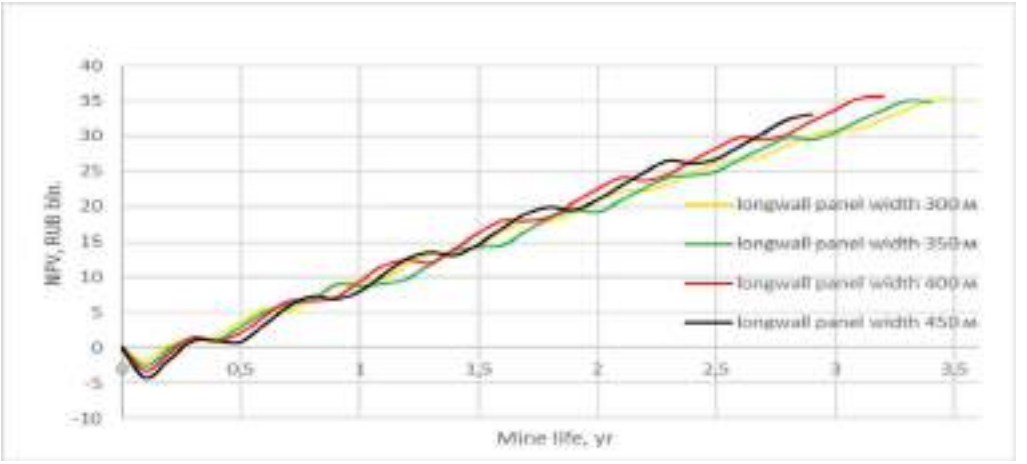

Figure 5. Changes in NPV over time depending on longwall panel width.

4 RESULTS

As a result of mathematical modelling and economic evaluation, unit development costs and unit production costs were calculated for each panel width option, based on which the net present value for the most cost-effective options was found (Figure 5).

5 DISCUSSION

Assuming that the calculation error associated with the inaccuracy of the initial data and other factors is 10%, the optimal panel width ranges from 300 to 450 m. This is a range within which the total unit costs are at a minimum.

After calculating the net present value for this range of longwall panel widths and analysing its change over time, it becomes clear that a panel width of 400 m is the optimal one, since it results in the highest net present value over the shortest period possible (Figure 5). However, a panel width of 450 m could also be an optimal solution but for the fact that there are dimension limits, which, when exceeded, result in an increase in coal loss.

6 CONCLUSION

The analysis of longwall mining practices in the top coal-producing countries has revealed that there is a global upward trend in longwall panel dimensions, with panel widths reaching 400 to 500 m and panel lengths reaching 6 to 8 km, which is a result of utilizing reliable high-performance equipment. However, there is a range of factors limiting the use of such panels. Among them are significant methane emissions, and limited panel length. The main factors limiting panel length are the limited size of the area being mined, the presence of faults and joints, as well as complex geometry and geological settings accompanied by massive water inflows. It has also been revealed that longwall panel dimensions are interrelated: an increase in panel length sets the stage for an increase in panel width. In addition, longwall panel width is greatly affected by working height, since an increase in panel width results in an increase of coal volume within the panel and, consequently, a decrease in unit development costs. The results of mathematical modelling and economic evaluation show that using longwall panels with widths bigger than 400 m in thick coal seams is impractical, which is also confirmed by the fact that no such panels are used in the top coal-producing countries.

Further research will be conducted with the view to solving the issue currently relevant to Russian mines, which is finding optimal longwall panel dimensions in mines characterized by complex seam geometry and geological settings and influenced by massive water inflows.

REFERENCES

Skorulis A., Minchin W., 2015. Report «Estimated Height of Connected Fracturing above Dendrobium longwalls», https://www.south32.net

Chemezov E.N. Industrial safety principles in coal mining. Journal of Mining Institute. 2019. Vol. 240, p. 649–653. DOI: 10.31897/PMI.2019.6.649

Fiscor, S. February 2014. The Landscape for U.S. Longwalls changes. Coal Age, The Magazine for Coal Mining and Processing Professionals: 26–32.

Fiscor, S. February 2015. US Longwall Operators Ramp Up Production. Coal Age, The Magazine for Coal Mining and Processing Professionals: 30–38.

Fiscor, S. February 2016. U.S. Longwall Operators Scale Back Production. Coal Age, The Magazine for Coal Mining and Processing Professionals: 18–22.

Fiscor, S. January-February 2017. U.S. Longwall Operations: How slow can we go? Coal Age, The Magazine for Coal Mining and Processing Professionals: 26–32.

Fiscor, S. January-February 2018. Longwall Production Rebounds in 2017. Coal Age, The Magazine for Coal Mining and Processing Professionals: 24–28.

Fiscor, S. January-February 2019. Longwall Production Remains Steady. Coal Age, The Magazine for Coal Mining and Processing Professionals: 24–28.

Gale, W., 2008. Report «Assessment of Longwall Panel Widths and Potential Hydraulic Connection to Bowmans Creek - Ashton Mine», http://www.ashtoncoal.com.au

Ralston, J.C., Hargrave C.O., Dunn M.T., August 2017. Longwall automation: trends, challenges, and opportunities. International Journal of Mining Science and Technology: 733–739.

Ordin, A.A., Metelkov, A.A., Kolenchuk, S.A., 2014. Instructional guidelines on optimization of fully mechanized production face length and output in flat coal seam mining. Fundamental and engineering questions of mining sciences: 266–272.

Trackemas J.D., 2013. Factors considered for increasing longwall panel width. Graduate Theses, Dissertations, and Problem Reports. 175.

Mills K.W., O'Grady P., 1998. Impact of longwall width on overburden behavior. Coal Operators' Conference, University of Wollongong& the Australian Institute of Mining and Metallurgy: 147–155.

McMillan, D., December 2014. Selecting a longwall panel. RPMGlobal PERSPECTIVES: 4.

Kazanin O.I., Sidorenko A.A. & Meshkov A.A. Organizational and technological principles of realization of the modern high productive longwall equipment capacity. Ugol' – Russian Coal Journal, 2019, no. 12., pp. 4–13.

Singh T.N., B. Singh. 1985. Model simulation study of coal mining under riverbeds in India. International Journal of Mine Water 4, no. 3: 1–10.

Jeffery, R.I., J.W. Summers, and M.D. North. 1991. The numerical analysis of subsurface deformation in relation to minewater ingress at Wistow Colliery. In 4th International Mine Water Congress, Ljubljana, Slovenia, Yugoslavia, September.

Golubev D. D., April 2018. Development of the technological schemes of the extraction of coal seams for modern mines. Topical Issues of Rational Use of Natural Resources: Proceedings of the International Forum-Contest of Young Researchers, ed. Litvinenko, St. Petersburg, Russia: 55–60.

Nguyen, K.L., Gabov, V.V., Zadkov, D.A., Le, T.B., 2018. Justification of process of loading coal onto face conveyors by auger heads of shearer-loader machines. IOP Conference Series: Materials Science and Engineering, № 327: 1–6.

Advances in Raw Material Industries for Sustainable Development Goals – Litvinenko (Ed)
© 2021 Taylor & Francis Group, London, ISBN 978-0-367-75881-3

Design of seismic-resistant linings for rock burst conditions

Vitalii V. Glinskii
Postgraduate student, Saint-Petersburg Mining University, Saint-Petersburg, Russian Federation

V.L. Trushko
D.E.Sc., full professor, Saint-Petersburg Mining University, Saint-Petersburg, Russian Federation

ABSTRACT: In the deep horizons development of deposits, mining and geological and technical conditions are significantly complicated. In mine workings dynamic phenomena are appeared, therefore they lead to performance decline of mining enterprises and injuries of miners. Actual task is the development of designs and justification of the rational parameters of seismic-resistant reinforcing linings, ensuring the stability of the mine workings throughout the entire period of their exploitation and the safety of mining. An analysis of the experience of using reinforcing rockbolt linings in Russian and foreign mining enterprises and a comparative assessment of seismic resistance and the effectiveness of using various types of rockbolts. The basic requirements for reinforcing rockbolt linings are formulated to ensure the stability of mine workings in the conditions with dynamic phenomena. As a result of research, it was found that the most effective application of frictional rockbolts, since they come into operation immediately after installation, retain high bearing capacity under dynamic stresses (75-110 kN).

1 INTRODUCTION

In the development of deep horizons of deposits, geological and mining and technical conditions are greatly complicated. Dynamic phenomena such as rock bump reduce the efficiency and productivity of the mining enterprise and lead to injuries to miners. Proceeding from this, the development of rational parameters of seismic-resistant reinforcing linings, which ensure the stability of the mine workings, the reliable maintenance throughout the entire period of their exploitation, the safety of mining operations and the constancy of the mining enterprise's work, becomes an actual task in the development of deep deposits.

Mainly combined seismic-resistant rockbolt linings in mine workings with the manifestation of dynamic phenomena from rock bump and mass explosions in preparatory mine workings and used coupling (Chunlin Li, C. 2010). The relatively recent studies have shown that friction-type rockbolt linings have the highest strength and deformation indicators.

Exploitation reliability in mine workings, which liable to dynamic loads and in areas, which affected by mass explosions is low. The wooden lining in this case has low efficiency, because the beams are destroyed, the legs are pressed inside the output contour. Dumps and the zone of destroyed rocks in the roof, depending on the type of rock, reach 2-3 m. The arch malleable lining doesn`t provide the necessary stability of mine workings, because such phenomena as deflection of the upper part of the lining, breaks of clamps, and destruction of the tie lead to a loss of stability of the lining structure with increasing deformations.

The main reason for the low efficiency of the considered lining constructions under dynamic phenomena is the discrepancy between the work mechanism of the deformation processes arising in rocks under the action of seismic waves.

2 REQUIREMENTS FOR ROCKBOLT LININGS

The designed rockbolt lining must satisfy the following requirements (Trushko V.L., Protosenya A.G., Matveev P.F., Sovmen H.M. 2000) to ensure the stability of mine workings in the conditions of dynamic forms of rock pressure manifestations:

- providing functional purpose in economic and technological ways;
- starting working in a short time after installation (up to 3-6 hours);
- assumption of a change in the shape and size of the cross section of the mine when it`s position in space deviates from the initial one,
- assumption of a change in the direction and magnitude of the maximum static and dynamic stresses in the rock mass, without a significant change in the construction of the elements and the technology of erection lining;
- maximum use of the own load-bearing capacity of the rock mass, including due to it`s hardening to the level necessary to perceive the total influence of static and dynamic loads for the required period;
- providing the possibility of reinforcing the originally selected lining in zones of influence of increased seismic effects, tectonic disturbances, couplings of mine workings stoping without significantly changing the constructional elements of the lining;
- ensuring the stability of the mine workings in conditions with genesis of oscillatory processes in the border zone of rock mass;
- preservation of the load-bearing capacity and stability of the lining interaction with the rock mass under periodic exposure to dynamic phenomena.

The peculiarities of the work of rockbolt linings are determined by the variability of the distribution of stress fields in the tectonically active rock mass, the random character of the dynamic influences on the lining, and the frequent change of geological conditions during mining works.

Based on this, the type and parameters of lining are chosen for typical mining, geological and technological conditions of the designed mine working, providing for the possibility of changing both the shape of its cross section and the parameters of the lining during the period of mining works.

Rockbolt linings must satisfy the following technological and design requirements for implementation these conditions:

- ensuring the stability of production and the safety of work in it throughout the entire service life;
- quick entry into work, preservation of the calculated load-bearing capacity and resistance to dynamic influences throughout the entire service life of the lining;
- assumption of changing the shape of the cross section of the mine working without changing the construction of the lining;
- possession of an effective reinforcing effect on the rock mass;
- increasing the load-bearing capacity of the border zone of the rock mass in order to prevent loss of stability of the mine working in areas of possible dynamic manifestations of rock pressure;
- possession of the necessary amortizing properties (compliance) during the development of oscillatory processes in the rock mass under the influence of dynamic phenomena;
- the possession of increased load-bearing capacity, necessary in conditions of highly weakened rocks around the output contour of mine working;
- the lining construction must be technologically advanced in the manufacture and construction, transportable, accessible for monitoring the load-bearing capacity and maintenance during exploitation.

3 ROCKBOLT LINING GROUPS

In the mining industry of the Russian Federation are mainly classical types of linings such as shotcrete and rockbolt lining from supporting structures - compliant metal lining and monolithic concrete lining are used.

As seismic-resistant linings it`s recommended to use reinforcing constructions of rockbolt linings and combined linings, which preserve the calculated load-bearing capacity and stability under the influence of seismic effects and throughout the entire period of exploitation (Wen, J., Yang, C., Su, H., & Ning, D. 2015). The rockbolts should come into work quickly after installation and have contact with the rock mass along the entire length of the rockbolt (Gospodarikov, A. P., & Zatsepin, M. A. 2019).

Consider the traditional types of rockbolt constructions used in the mining industry of the Russian Federation which have been successfully tested in domestic mines.

As a seismic-resistant rockbolt constructions were fastened, which are retaining the load-bearing capacity under the influence of seismic effects (Li, C. C., Stjern, G., & Myrvang, A. 2014). This condition is most satisfied with the rockbolt, which had the presence of continuous contact with a massive. Based on this in this work two groups are considered: first group is rockbolts which are entering into work immediately or shortly after installation; second group is rockbolts which are entering into work after several hours of installation (Li, C. C. 2017).

The first group includes following rockbolts:

(1) Combined cemented roof rockbolt (CCRR). This slot-and-wedge rockbolt (Figure 1) is a structure that has a wedge-slot metal rockbolt with a modified wedge as reinforcement, which is fixed in the array by both the wedge itself and the cement-sand mortar that fills the well along the entire length before the rockbolt is inserted into it. Designs of this rockbolt are selected to specific conditions, changing the length of the rockbolts, the diameter of the rockbolts, the density of their placement, the diameter of the wire mesh, the thickness of the shotcrete and the backlog of the lining from the face of mine working (Small, J. C. 2016).

(2) Frictional rockbolt type Swellex (FR). This frictional rockbolt (Figure 2) consists of a special hollow pipe with a C-shaped cross section with plugs at the ends, which is fixed in the well by the pressure of a special fluid pumped into the pipe (Li, D., Masoumi, H., Saydam, S., & Hagan, P. C. 2018).

(3) Resin-grouted roof rockbolt (RGRR). Steel and polymer rockbolt (Figure 3) are lock and solid, consisting of a reinforcing bar, ampoules with polymer concrete components, a nut and a base plate (Protosenya A.G., Kolosova O.V., Ogorodnikov Y.N. 2003).

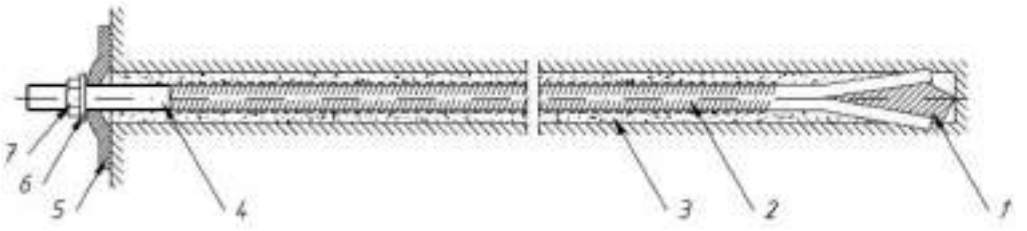

Figure 1. Combined cemented roof rockbolt (1 - metal wedge, 2 - rod of circular or periodic profile, 3 - cement-sand mortar, 4 - section of the rod with thread, 5 - base plate, 6 – spacing washer, 7 - tension nut).

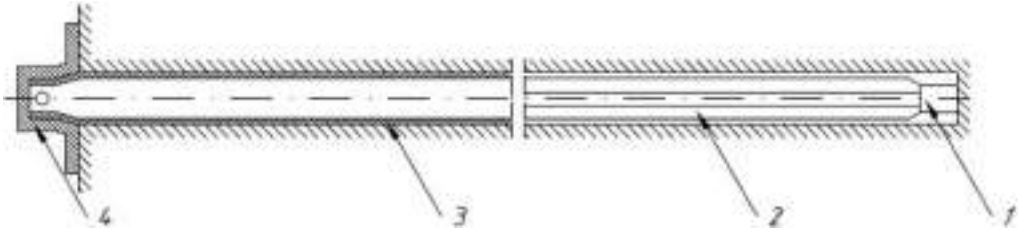

Figure 2. Frictional rockbolt type Swellex (1 - a sealed rockbolt shank, 2 - a special section hollow pipe before liquid injection, 3 - a special section hollow pipe after liquid injection, 4 - a special type base plate).

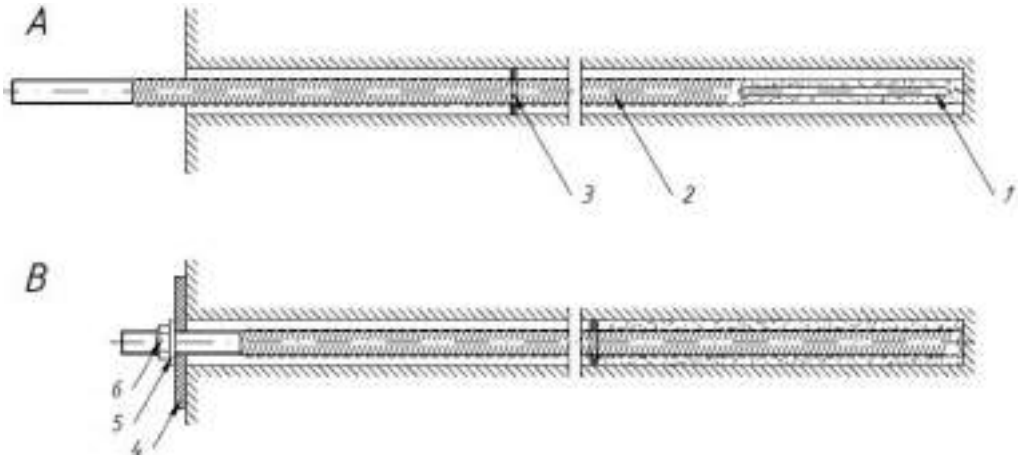

Figure 3. Resin-grouted roof rockbolt during installation (a) and after it (b) (1 - a steel rod of a periodic profile, 2 - quick-hardening composition based on synthetic resins, 3 - a rubber ring, 4 - a base plate, 5 - spacing washer, 6 - a tension nut).

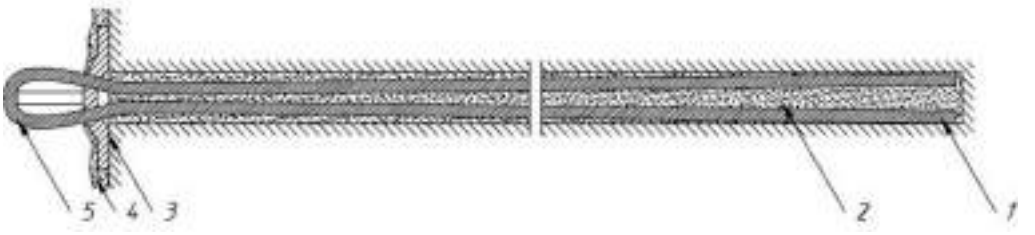

Figure 4. Cable rockbolt (1 - wire rod, 2 - cement-sand mortar, 3 - special wedge-shaped supporting element, 4 – shotcrete, 5 – hinge of wire rod).

The second group includes following rockbolt:

(1) Cable rockbolt (CR). This rockbolt (Figure 4) consists a loop end, an oval-type base plate with a notch and a special locking wedge (Trushko O.V. 2016).

4 TASKS OF WORK

The first task is determination of the load-bearing capacity of seismic resistant rockbolts in rock mass, exposed to dynamic effects.

The second task is testing construction technologies of seismic resistant rockbolts and the estimation of their labor intensity.

5 METHODOLOGY

The tests were carried out in the conditions of the Severouralsk bauxite mines in the limestone rocks with a compressive strength of 62-75 MPa at a depth of 200-400 m. Each type of rockbolt had a length of 2.5 m. and a diameter of 36 mm.

The tests were as follows:

(1) One rockbolt of each type was installed in a specific mining area;

(2) Measurements were made of the installation time of each of the rockbolts to determine the complexity of the work and the average time for each type of rockbolt was displayed;
(3) Throughout the day, data on the bearing capacity of each of the rockbolts were recorded. The first measurements were made at the installation stage if it was possible to make the installation technology of the rockbolt. Then the measurements were made after 1 hour, 2 hours and 24 hours.

6 ANALYSIS OF RESULTS

Average results of mining tests in Table 1 are presented.

Table 1. Average results of mining tests.

Rockbolt type	Number of tested structures	Average load-bearing capacity of the rockbolt (kN) from the moment of installation (hour)				Unit labor for installation of one rockbolt (person per hour)
		0	1	2	24	
Combined cemented roof rockbolt (CCRR)	3	69	-	-	110	0,16
Cable rockbolt (CR)	4	0	-	-	60-85	0,18
Resin-grouted roof rockbolt (RGRR)	3	0-60	80	140	180	0,18
Frictional rockbolt (FR)	2	100-110	100-110	100-110	100-110	0,10

When analyzing the results, the following conclusions were generated:

(1) The load-bearing capacity of the CCRR ensures normal exploitation and it may apply as a permanent lining;
(2) RGRR tests have shown high performance. Due to the application of polymer concrete with high-strength fast-acting composition, it was possible to achieve rapid entry into work. RGRR has a high resistance to seismic effects and can be used such as temporary and permanent linings;
(3) Experimental data showed that FR is the most effective of the common constructions. FR come into exploitation immediately after installation and have high load-bearing capacity (100-110 kN). FR has contact with the rock along the entire length and it is technological in installation (the average installation time of the rockbolt was not more than 1 min, excluding drilling of the hole);
(4) The technology of CR construction and their load-bearing capacity are less than CCRR, which ensures their normal exploitation and it may apply as a permanent support. However, the slow curing of concrete strength does not allow the use of CR such as a temporary lining.

7 CONCLUSION

Due to the high seismic resistance of FR, high and constant load-bearing capacity, workability, this rockbolt construction can be recommended as rockbolt in difficult mining and geological conditions with exposed to dynamic forms of rock pressure.

It can be used both as temporary and as permanent lining.

REFERENCES

Chunlin Li, C. 2010. A new energy-absorbing bolt for rock support in high stress rock masses. International Journal of Rock Mechanics and Mining Sciences, 47(3), pp.396–404. https://doi.org/10.1016/j.ijrmms.2010.01.005

Gospodarikov, A. P., & Zatsepin, M. A. 2019. Mathematical modeling of boundary problems in geomechanics. Gornyi Zhurnal, 2019(12), 16–20. doi:10.17580/gzh.2019.12.03

Li, C. C., Stjern, G., & Myrvang, A. 2014. A review on the performance of conventional and energy-absorbing rockbolts. Journal of Rock Mechanics and Geotechnical Engineering. Chinese Academy of Sciences. https://doi.org/10.1016/j.jrmge.2013.12.008

Li, C. C. 2017. Principles of rockbolting design. Journal of Rock Mechanics and Geotechnical Engineering, 9(3), 396–414. doi:10.1016/j.jrmge.2017.04.002

Li, D., Masoumi, H., Saydam, S., & Hagan, P. C. 2018. Mechanical Characterisation of Modified Cable Bolts Under Axial Loading: An Extensive Parametric Study. Rock Mechanics and Rock Engineering, 51 (9), pp. 2895–2910. https://doi.org/10.1007/s00603-018-1475-4

Protosenya A.G., Kolosova O.V., Ogorodnikov Y.N. 2003. Seismic-resistant designs of lining of mine workings in the development of shock-hazardous deposits. Journal of Mining Institute, 154, pp. 153–156.

Small, J. C. 2016. Geomechanics in soil, rock, and environmental engineering. Geomechanics in soil, rock, and environmental engineering, pp. 1–535

Trushko V.L., Protosenya A.G., Matveev P.F., Sovmen H.M. 2000. Geomechanics of massifs and dynamics of deep mine workings. Saint-Petersburg Mining Institute, p. 396.

Trushko O.V. 2016. Types and designs of antiseismic lining a used in the development of ore deposits. "Izvestiya Tula State University" (Izvestiya TulGU), pp. 120–130.

Wen, J., Yang, C., Su, H., & Ning, D. 2015. Theoretical analysis and application of composite arch for bolt-shotcrete steel frame supported tunnel in weak and fractured rock mass. Tumu Gongcheng Xuebao/China Civil Engineering Journal, 48(5), 115–122.

Advances in Raw Material Industries for Sustainable Development Goals – Litvinenko (Ed)
© 2021 Taylor & Francis Group, London, ISBN 978-0-367-75881-3

Results of plasma-impulse technology application at uranium Inkay deposit, Kazakhstan

A.V. Chekulaev
Geophysic Engineer of Scientific-production center «GeoMIR», Saint-Petersburg, Russia

A.S. Egorov
Doctor of Geological and Mineralogical Scienses, Head of the Department of Geophysical and Geochemical Methods of Prospecting and Exploration of Mineral Deposits, Saint-Petersburg Mining University, Saint-Petersburg, Russia

A.A. Molchanov
Doctor of Engineering Sciences, Proffessor at the Department of Geophysical and Geochemical Methods of Prospecting and Exploration of Mineral Deposits, Saint-Petersburg Mining University, Saint-Petersburg, Russia

ABSTRACT: This article discusses the methodology for increasing the uranium extraction, in the process of development of hydrogen type uranium deposits of the Republic of Kazakhstan. The analysis of the effectiveness of the standard repair work and methods was applied. The plasma-impulse technology (PIT) using is proposed to increase the permeability of the ore-layer decolmatate the well filters and as a result, intensify the leaching process. The article reviews the physical impact of PIT on the reservoir. Due to the resonant effects in the reservoir as a result of the elastic impact, the process of uranium transition to the mobile form is intensified. A schematic model of the elastic resonance action on a uranium-containing ore-layer using PIT is presented. Positive results were obtained on the application of the proposed technology on some uranium ore deposits of the Republic of Kazakhstan at all stages of their development – while the opening of a deposit, blocks acidification and leaching. Based on the results of testing the technology, a combination of PIT with standard methods of repair and restoration work was developed. The application of the author's methodology intensifies the process of uranium transition to the mobile form due to resonance at dominant frequencies and stabilizes the metal yield. High flow rates of pumping wells with an increased or stable metal yield will increase uranium production, its extraction rate and, accordingly, shorten the life of the deposit.

1 INTRODUCTION

The method of the drillhole in situ leaching (ISL) in uranium deposits was developed and widely used in the Republic of Kazakhstan. It is characterized by high environmental safety, low costs and simplification of technological operations (Turaev. N. & Zherin. I. 2005). ISL development system is considered to be the specified mode of technological wells. The principal operations of the ISL technological system are the well injecting, pumping and monitoring (Figure 1).

Sulfuric acid solution with a concentration of 5–30 grams per liter, less often up to 50 grams per liter, is used as a leaching reagent (acid solution). The acid solution is supplied through injection wells and penetrated into ore horizons, where selective transfer of natural uranium ions to a productive solution takes place. The productive solution with dissolved uranium rises to the surface through pumping wells. Monitoring wells are used for observation and process control.

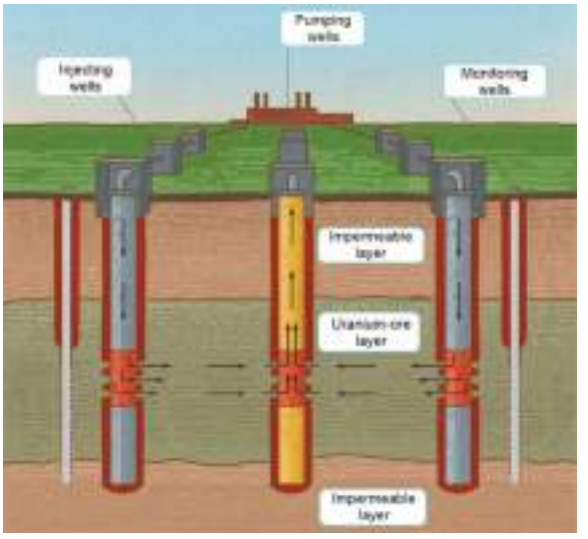

Figure 1. Technological scheme of drillhole in situ leaching of hydratogenous uranium deposits.

2 PROBLEM DEFINITION

It should be noted that the leaching rate in beds depends on many geological and technological parameters. There are two principal parameters - the coefficient of permeability of ore horizons and the uranium concentrations. Due to high permeability of the sedimentary reservoirs at a low metal values of hydratogenous uranium deposits, the drillhole in situ leaching method is the only possible method for their efficient and profitable development.

The decreasing of productive intervals permeability is one of the principal problems of ISL method application to the due to the clogging (colmatation) of well-filters (Evteeva L., 2002) and near-well zones of technological wells (Gorbatenko O. et al, 2018). A similar problem is observed in the process of development of uranium deposits in Kazakhstan in depths more than 500 meters. It is necessary to achieve high production rates of pumping wells, to ensure a stable metal yield, to increase the interrepair cycles (IRC) in technological wells, and to reduce the number and time of repair and restoration works (RRW). Therefore, the solution of this problem is of significant technological and economic interest.

Currently, there are standart technologies increasing well productivity. There are three principial types of RRW applied to recover the permeability:

- physical methods of RRW - flushing, pumping by airlift, hydrodynamic and pneumatic treatments;
- chemical methods of RRW based on the using of highly concentrated sulfuric acid or ammonium fluoride;
- physicochemical (complex) methods of RRW.

Each of the RRW methods has its advantages and disadvantages, however, the average interrepair cycle of wells achieves 20 - 25 days, sometimes achieves 1.5 - 2.0 months. Besides, application of standart RRW methods requires the shutdown of wells and the additional expenses.

Our investigations have shown that the main well colmatant is drilling clay. The clay content in the solid phase varies from 42 to 98.2% and on average is of 76%. The rest part of the colmatant is represented by the sand of various fractions, mainly from 0.1 to 0.5 mm, destroyed in the process of ion exchange in the injecting wells and insignificant amounts of gypsum.

3 METHODOLOGY

To increase the uranium extraction, the authors developed and patented plasma-impulse technology (PIT) for creating a series of high - power electrohydraulic impulses in the hydrosphere of the well (Molchanov A. et al, 2014). The manufactured equipment "Pritok-1M" (Figure 2) can be used for decalmation of the well-filter, wellbore zone, and interwell space to restore the permeability of the reservoir and increase the mobility of the acid solution (RU Pat. No. 2685381 to LLC SPC «GeoMIR»). This technology has been successfully tested in the Inkai uranium field.

This process of plasma - impulse action occurs due to the expansion of the plasma channel and its subsequent "collapse", which has alternating stresses on the filter, near the wellbore zone and on the reservoir as a whole (Molchanov A. & Chekulaev A., 2019). As a result of repeating repression-depression cycles, elastic hydraulic waves propagate along with the bed-layer skeleton and in its porous medium, improve the capacitive and filtration properties of this bed-layer. At the same time, the filter intervals and the near-well zone are cleared from the clay and mud slush colmatant particles, as well as the precipitation of salts.

Pressure impulses open the natural channels in the reservoir and contribute to the formation of new ones that have increased hydraulic conductivity (Figure 3). Due to the resonant effects in the reservoir as a result of the elastic impact, the process of transition of uranium to the mobile form is intensified (Molchanov A. & Chekulaev A.,, 2019). The penetration depth of

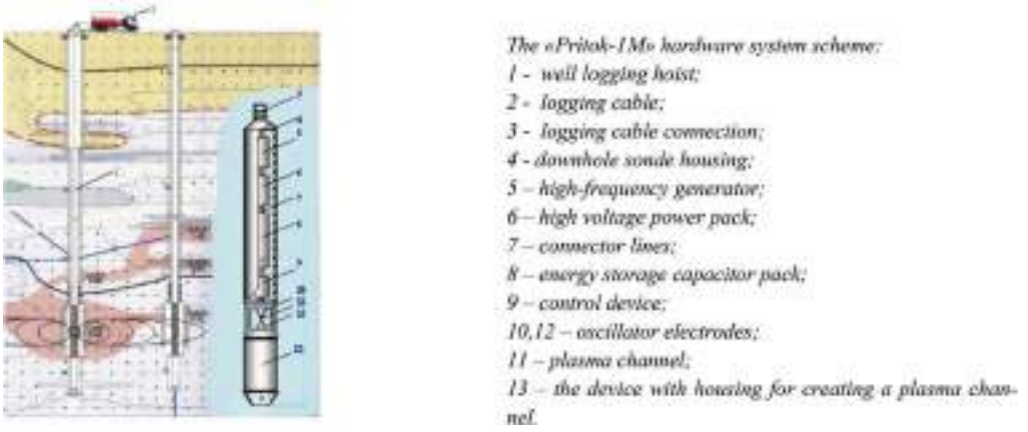

Figure 2. Construction of the «Pritok-1M» hardware system.

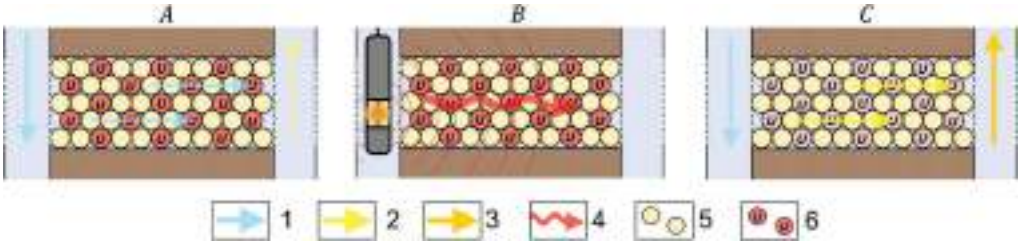

Figure 3. Schematic model of the plasma-impulse impact on the ore-layer. A- the usual model of uranium leaching. B- the ore-layer treatment by PIT. C - intensified leaching process. 1 – direction of injected acid solution; 2- direction of acid solution with a low concentration of uranium; 3- direction of acid solution with a high concentration of uranium; 4- elastic wave exposure of PIT; 5- rock grains; 6-uranium-containing rock grains.

elastic energy due to directional radiation achieves 50-75 meters or more, which significantly exceeds the exposure range of the traditionaly applied RRW methods and, in combination with acid treatment, contributes to deeper leaching of metal from wells of long-operating cells with low uranium extraction (Molchanov A. & Demekhov., 2014).

4 RESULTS

Application of PIT in the period of the blocks acidification provides reducing the time of uranium transition to the mobile form and to intensify the leaching process due to the deep penetration of the acid solution into the interwell space. It also provides the uranium extraction and high production rates of pumping wells for a long time with an IRC of 80 - 120 days. (Table 1).

Table 1. Operating mode of wells after the PIT application (LLP "JV"Inkai" 2016-2017 y.).

№	Number of well	Date of RRW	production rate after PIT, m^3/hour	0.7 production rate after PIT, m^3/hour	IRC, days	Q/Q_{max} %	U, mg/l
1.	30-6-3	10.05.16	8.30 – 1.84	5,81	50	22	15
2.	30-6-4	11.05.16	8,89	6,22	65	63	17,4
3.	32-0d-1	26.11.16	8,01	5,60	45	48	34,3
4.	32-2-2	24.11.16	11,04	7,728	120	55	31-23
5.	32-4-4	14.12.16	7,88	5,51	120	42	44,4-31
6.	32-6-3	22.11.16	9,53	6,671	50	57	42,6
7.	80-6-1	08.08.16	9,23	6,46	30	62	84,3
8.	80-6-4	05.05.16	9,82	6,87	75	78	47,4
9.	80-8-3	26.11.16	7,35	5,14	180	77	55
10.	16-18d-3	06.12.16	The bottom of the well filter after the PIT was filled with sand				
11.	16-20d-5	11.12.16	11,33	7,93	240	71	45,6
12.	16-26d-2	16.12.16	5,01	3,50	120	23	90 - 64
13.	81-6-3	19.12.16	12,63	8,84	240	80	274
14.	81-4-1	Without PIT treatment (control)	10.25	7,17	230	96	162

To study the effectiveness of the PIT treatment in wells in the period of their acidification, the commissioned well No.81-6-3 was treated with a complex of PIT and pneumatic pumping. The control well No.81-4-1 (without any treatment) was located in the same cell. The increase in metal extraction in No.81-6-3 well occurred in 12 days earlier than in the control well No.81-4-1. The metal extraction in the samples stabilized at the value of 264 mg per liter and lasted more than 150 days. In the control well: output - 174 mg per liter. Over the period from January 20 to June 9 in the No.81-6-3 well treated by PIT, the metal extraction was 43.2% higher than in the untreated control well 81-4-1 (Figure 4).

Moreower, this technology has been successfully tested at the Akdala uranium field, Central and East Mynkuduk uranium fields of the Republic of Kazakhstan. So, RRW applying PIT in the mynkuduk and inkuduk-horizons were carried out in 36 pumping and 54 injection wells. During development after drilling, acidification and leaching of technological blocks No. 30, No. 32, No. 16, No. 80, No. 81, No. 83 and No. 66, the IRC increased from 15-20 days to 80-150 days, with the flow rates of pumping wells within 10-11 m^3/h, an increase, and stabilization of the metal yield are observed.

Figure 4. Comparison of metal extraction in wells No. 81-6-3 and No. 81-4-1.

5 CONCLUSION

1. The author's plasma-impulse technology (PIT) accelerates the transition of uranium in sedimentary layers to the mobile form due to the parametric resonance of layers at dominant frequencies.
2. Applying the PIT in combination with standard methods of repair and restoration works (RRW) provides deep cleaning of the filter and the near-wellbore zone, as well as intensify the operating modes of technological wells at all stages in the process of uranium deposits development.
3. Experience in the application of PIT at the Inkai uranium field demonstrated opportunities of the efficiency increasing of uranium development. It was justified by our investigations of 36 pumping and 54 injection wells of the inkuduk and mynkuduk horizons in the Inkai uranium field at various stages of it's development. At the same time, the interrepair cycle of pumping wells increases in several times, which allows reducing the number of RRW and, accordingly, reduce the production expenses.

REFERENCES

Gorbatenko, O. 2018. The results and prospects of applying plasma impulse technology for increasing of efficiency of technological wells operating mode of uranium from deposits which are developed by the method of drillhole in situ leaching (Inkay deposit, republic of Kazakhstan). A.Molchanov & A.Chekulaev. *25 World Mining Congress*. 2018. Kazakhsatn, Astana.

Evteeva, L. 2002. Types of well collation during underground uranium leaching and methods of struggle. *II International Scientific and Practical Conference "Actual problems of uranium industry"*, JSC "NAC Kazatomprom", Almaty, 2002.

Molchanov, A. & Demekhov, Y. 2014. Increasing the efficiency of uranium mining from deposits of hydrogenous type, developed by the method of underground well leaching of the Republic of Kazakhstan (on the example of the Vostochny Mynkuduk deposit). *VII International Scientific and Practical Conference. "Actual problems of uranium industry"*, Almaty, 92–98. September 25-27, 2014.

Molchanov, A. 2018. Plasma-impulse technology applying for intensification of hydratogenous uranium deposits. Y.Demekhov & A. Chekulaev *«Ecology and social development»*. № 4. 34–42. 2018.

Molchanov, A. 2014. Plasma-impulse technology application for increasing the efficiency of uranium extraction from hydrogenous type deposits, developed by the drillhole in situ leaching". D.Dmitriev & V.Sidora. *Scientific and technical bulletin "Karotaznik"*, No. 3, 29–40. 2014.

Molchanov. A. & Chekulaev. A. 2019. Efficiency of parametric resonance application to the process of mining ore deposits developed by the method of underground well leaching. *Scientific and technical bulletin "Karotaznik"* No. 295, 3–14. 2019.

Patent of the Russian Federation, No. 2685381 "Method of uranium and related elements extraction on the technology of drillhole in situ leaching with plasma-impulse effect on the hydrosphere of the well" (priority 15.05.2018), patentee: LLC SPC "GEOMIR" (RU).

Turaev. N. & Zherin. I. 2005. Chemistry and Technology of Uranium: *A Textbook for Universities/- Moscow. Federal state unitary enterprise central scientific research institute of economics of information of "ROSATOM"*, 2005. p. 83–89.

Advances in Raw Material Industries for Sustainable Development Goals – Litvinenko (Ed)
© 2021 Taylor & Francis Group, London, ISBN 978-0-367-75881-3

Geomechanical issues in the development of the Udachnaya diamondiferous pipe

K.A. Anisimov
Postgraduate student, Saint-Petersburg mining university, Saint-Petersburg, Russian Federation

D.G. Sokol
Postgraduate student, Saint-Petersburg mining university, Saint-Petersburg, Russian Federation

V.P. Zubov
Professor, Saint-Petersburg mining university, Saint-Petersburg, Russian Federation

ABSTRACT: The data of researches and observations of the geological settings on the Udachnaya kimberlite pipe since the commissioning of the underground mine was considered in this article. The main geomechanical parameters that complicate mining were studied; recommendations on the future researches were given.

1 INTRODUCTION

Nowadays, Udachny Mining and Processing Division (MPD) develops two primary diamond deposits: Udachnaya and Zarnitsa, as well as Dellyuvialnaya and Ruchey Piropovy placer deposits of the Udachnaya kimberlite pipe (Brief report by independent experts on the reserves and resources of diamond deposits of the ALROSA group of companies, 2018).

The Udachnaya kimberlite pipe has a crucial meaning to the development of the Udachny MPD. This deposit is located in the Daldino Alakit diamondiferous area, close to the city of the same name. The pipe can be traced as a single ore body from the surface to a depth of 250 m. Downstream it splits into two independent ore bodies – East (EOB) and West (WOB), separated by a block of host secondary rocks of the upper-Cambrian period (Figure 1) (Drozdov, 2015).

For a long time, the pipe had been mined as an open-pit. Udachny open-pit was put into production in 1971, and it has been functioning for over 40 years. Open-pit mining was completed in 2016; the depth of the open-pit was 640 meters at the time of the completion.

The Udachny underground mine was put into production in 2014. The development of the ore reserves, which lie below the bottom of the open-pit with absolute elevation of -320 m, is provided by three vertical shafts located south of the pit: cage shaft, air shaft and skip shaft. Moreover, main opening adits are driven into the sides of the open-pit at -170 m and -290 m levels, and they are connected with West and East airway crosscuts at -380 m level through the runaway No.1 (Nikitin, 2017).

2 RESEARCH

The development of the underground reserves of the Udachnaya pipe was started at the level of 260/-320 m WOB and EOB. There were ore reserves left in the pit sides on these levels. Mining method, which was applied to develop these reserves: sublevel caving with the side ore drawing, showed excellent results providing a sufficiently high volume of ore mass production with low rates of loss and dilution. More than half of the ore mined on the pit sides was dumped at the

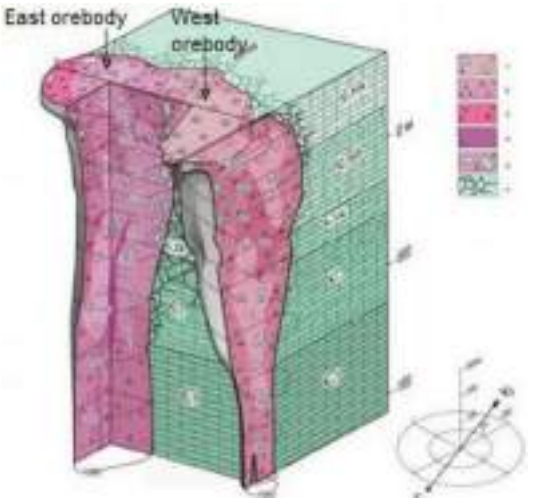

Figure 1. Geological structure of the kimberlite pipe (G.S. Von der Flaas representation).
1 – autolithic kimberlite breccia (phase III); 2 – kimberlite breccia (II); 3 – kimberlite breccia of the massive structure (phase I); 4 – porphyritic kimberlite (phase IV); 5 – kimberlite breccia with large xenoliths of host rocks; 6 – crushing area of host rocks.

bottom of the pit; some of the reserves were transported to the Processing Plant No. 12 (PP No. 12) in the city of Udachny. The bottom of the pit at -320 m and -365 m levels was also destroyed to create a movable and friable safety cushion. This ore safety cushion is a three-dimensional moving rock mass with a designed height of up to 65 meters, which provides a seal between the underground mining and the open-pit space. The safety cushion is going to be slowly lowered following a decrease in the level of mining operations in accordance with the designed mining method of the kimberlite pipe (Drozdov, 2015; Piven`, 2011).

A high-performance method of combined shrinkage stoping and caving with one-stage stoping and areal ore drawing is implemented (Figure 2) to develop primary reserves, located below the bottom of the pit up to the level of 600 m. This mining method is unique for diamondiferous deposits of the Far North, since earlier such methods had not been used in such difficult climatic conditions. There has also been a significant change in technology for creating a safety cushion between the open pit and the underground mine. Traditionally, the bottom of the pit is either left forming a pillar of kimberlite rocks of the sufficient thickness, or artificial filling mass is made (Aikhal, Mir, Internatsionalny mines), when designing the development of a diamondiferous deposit. The movable and friable ore safety cushion was designed at the Udachny mine. Low-performance cut-and-fill mining methods are commonly implemented in the fields of the Far North. These methods allow reducing the negative climate impact on the underground mining, reducing the influence of hydrological parameters and increasing the safety of personnel in mining zones (Kovalenko, Tishkov, 2017). The method of combined shrinkage stoping and caving with a friable safety cushion is used in the countries of the African continent (Finsh and Kimberly mines). This method has a higher productivity rate: it was possible to achieve and maintain the mine's productivity at the same level as in open-pits with the introduction of these mining methods in the mines of South Africa at a cost-per-ton of ore much less than that of the cut-and-fill mining methods (Chadwick, 2012).

Diesel load-haul-dumpers and self-propelled drillers are used at the drawing-off levels. It is planned to use electrical equipment on the main haulage levels, in particular, a belt conveyer is used on the main haulage level at the elevation of -480 m, ore gets onto it from an underground crushing facility. The projected production rate for 2018 was 2.7 million tons. The mine was supposed to reach full production capacity by 2019, ensuring the production of

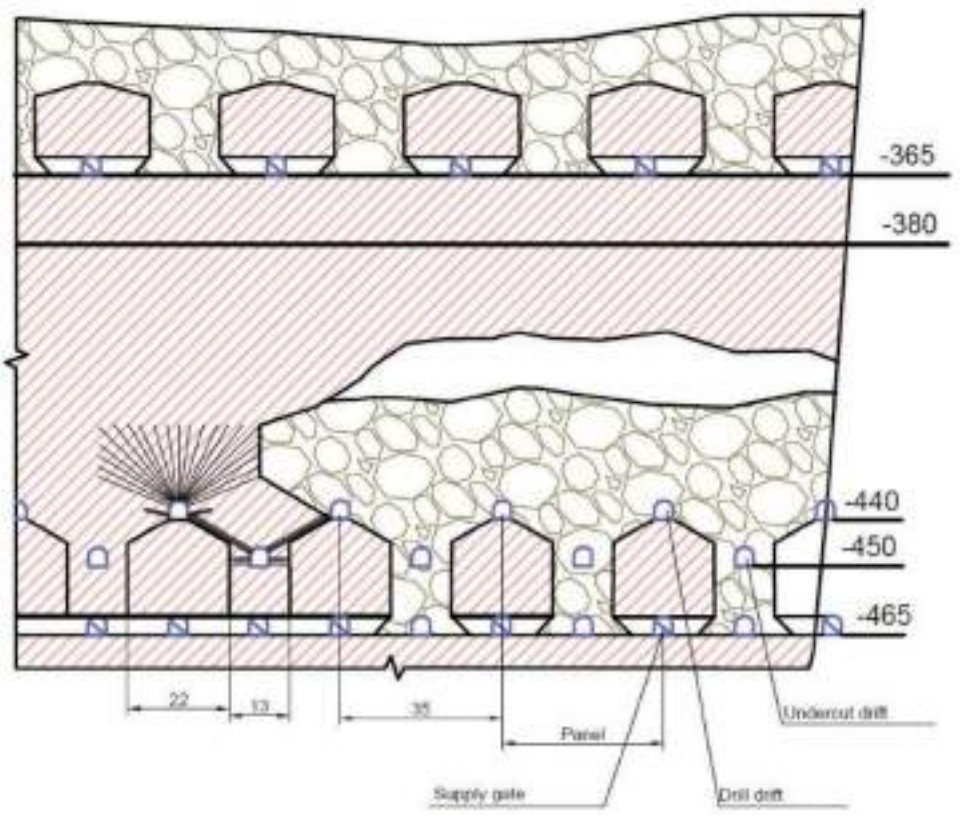

Figure 2. Part of the combined shrinkage stoping and caving method; the lay out of the workings on the -450 m level (undercutting level).

4.0 million tons of ore annually, however, as for the III quarter of 2019, 1836 thousand tons of ore were mined, ensuring that the plan was not fulfilled almost twice (The quarterly report of ALROSA PJSC for the 3rd quarter of 2019, 2019).

The development of the Udachnaya kimberlite pipe is extremely difficult, climatic and geological conditions have a significant impact on the development process. The main factors that have a critical value for the operation of the underground mine are the following:

- Kimberlite pipe is located in the extreme climatic conditions of the Far North, almost at the level of the Arctic Circle. The pipe is located in the permafrost area with a large frost depth of rocks. Sharply continental climate is described by large daily temperature swings, which negatively affect the stability of rock masses (Balek, Sashurin, 2016);
- Water cut is distributed highly uneven in the developed rock masses, the geological structure of the pipe and surrounding rocks is formed without natural aquicludes, which leads to the free promotion of aggressive and high-salinity brines with a total salinity of up to 400 g/l (Balek, Sashurin, 2016);
- The rock mass, which surrounds the pipe, is extremely disturbed, host rocks and kimberlite rocks have a network of deep (up to 50 meters) fractures and various disturbances located randomly. Cases of groundwater breakthroughs in mines due to penetration of fractures during drilling wells, etc., were recorded (Balek, Efremov, 2016; Kovalenko, Tishkov, 2016);
- Ore and rock masses have low stability; the dependence of the kimberlite's stability on the time of its contact with the mine's air has been established: it drops significantly over the year, increasing the cost of fastening and maintaining mine workings (Bokiy, Zoteev,

Pul, 2019). The most disturbed mass is the mass of waste rocks in the space between the WOB and EOB; it contains many disturbances and manifestations of fracturing;

- Many zones of increased fracturing, hazardous places of low coherence, caused by various hydro-geomechanical, geomechanical and other factors were particularly highlighted. Special timbering plans are often designed for such zones and there is special monitoring of the state of the underground mines (according to PJSC ALROSA);
- The mine is hazardous in terms of gas emission; there have been cases of oil and gas occurrences during mining on the levels of -260 m/-380 m that negatively affect the development of the field (Brief report by independent experts on the reserves and resources of diamond deposits of the ALROSA group of companies, 2018).

The development of the Udachnaya kimberlite pipe is a big challenge for Russian science, forming a certain number of extremely unique and often advanced solutions. The Yakutniproalmaz Institute was initially involved in the development of all design decisions; part of the work was carried out in Saint-Petersburg at the Institute GIPRONIKEL LLC, the Institute of Mining of Ural Branch of RAS carried out the research work and technical solutions. Therefore, technological parameters of the development process of the Udachnaya kimberlite pipe have been studied for a long time taking into consideration the wishes of the direct customer – PJSC ALROSA.

However, the following negative factors that affect mining process were noted in the first few years of the mine's operations:

1. A methane-air mixture exploded during the driving of the runaway due to the strong gas contamination of the mine and insufficient ventilation. Gas manifestations were repeatedly recorded in the mine atmosphere during further mining operations, there were also oil products ignitions after the production cycle of the blast hole drilling (according to the regional department of the Russian Ministry of Emergency Situations).
   These negative factors are caused by the content of petroleum bitumen in the host rocks. Its content on different mining depth varies from 0.6 to 2.35%, and lower in the section (level -480 m/-1080 m) decreases to 0.01%. According to group analysis, bitumen contains about 50-60% oils, 40-45% resins, and in the lower part of the section the oil content decreases to 15-20%. Oil in the area of the Udachnaya pipe contains less resins (30-35%) compared to bitumen, and its asphaltene content does not exceed 4%. The gas content of the field is due to the presence of gases dissolved in oil and brines, however, the rocks themselves have almost no sorption capacity. The gas content of the field was assessed to a depth of 800 m; the main gases are hydrocarbon mixtures with predominant methane content. Petroleum bitumen in kimberlites complicates the ore processing, and their presence in rocks have a great impact on the conduction of blasting operation in the underground conditions;
2. Multiple rock falls were observed both from the roof and from the sides of the workings, this is especially typical for the ore body – kimberlite ores are very easy to flake and crumble, starting their destruction in an extremely short time. Moreover, kimberlites of the East ore body are different from the ones of the West ore body in their characteristics (Balek, Efremov, 2016; Drozdov, 2009).
   These phenomena are mostly observed either in the ore body or in zones of increased fracturing and at contacts with the ore body. Kimberlites of the EOB and WOB change the values of all physical and mechanical properties by 1.1-1.6 times with the increase in depth. The average bulk density varies through the blocks in the upper levels of the field (elevation of +300 m/-280 m) from 2.34-2.37 to 2.48-2.6 t/m^3, and on "deep" levels (elevation of -280 m/-1080 m) – from 2.52-2.62 to 2.62-2.69 t/m^3. In terms of unconfined compressive strength, kimberlites of the EOB and WOB are considered soft (σ = 10-35 MPa) and very soft (σ = 4-10 MPa) rocks. Hardness coefficient of the host rocks on the Protodyakonov's scale of hardness ranges from 1 to 8, and the coefficient of kimberlites varies from 5 to 7. The lowest values of the hardness coefficient are recorded in crushing zones, less often in zones of hydrothermal changes, and its maximum values coincide with intensely silicified rocks;

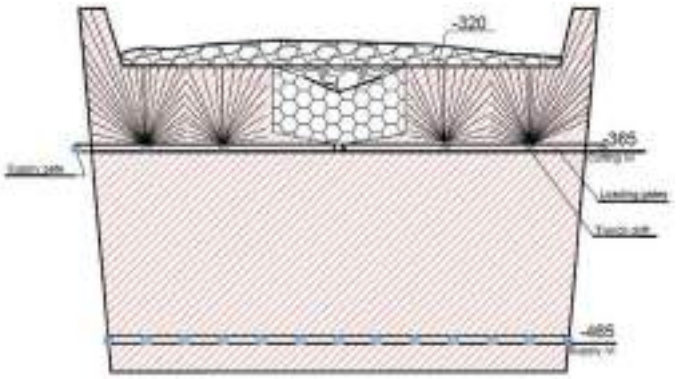

Figure 3. Part of the mining method with the creation of the safety cushion.

3. Increased wear of machinery and equipment associated with the aggressive type of brines, which penetrate underground mines, was observed during the operation of the mine. There have been cases of breakthroughs of brines into the interior of the mine due to the bursting through fractures or disintegration of the underground cavities filled with them (Kovalenko, Tishkov, 2017; Bokiy, Zoteev, Pul, 2019; Sokolov, Smirnov, Antipin, Nikitin, Tishkov, 2018).
   Groundwater is represented by calcium chloride brines with an average salinity of 300-400 g/l. The total gas saturation of brines can reach up to 1.2 m^3/m^3. The chemical composition of the aquifer is abnormal: sodium chloride brines have a high content of sodium, sulfates, and bromine. Hydrogen ion concentration (pH) value is 7.75. Filtration properties of kimberlites are variable: water conductivity varies from 1-2 to 70 m^2/day (average conductivity is 40 m^2/day), however, it always exceeds equivalent parameters of the host rocks. The negative impact of the water inflow in the underground mine will increase with further development of the kimberlite pipe;
4. Numerous safety violations have been recorded since the beginning of the operation of the mine to the present moment, resulting in personnel injuries, including deaths at the mine (according to the regional department of the Russian Ministry of Emergency Situations)
   The management of the Udachny MPD was faced with the lack of personnel trained to work in the underground conditions of the mine during the period of transition to the underground operation of the enterprise. At the same time, method of combined shrinkage stoping and caving with one-stage stoping and areal ore drawing requires the highest quality of the conducted mining operations and high professionalism of personnel. Moreover, there are no similar mines which use combined shrinkage stoping and caving method among underground mines in the territory of Russian Federation;
5. It is planned to extract mineral resources in the WOB and EOB simultaneously in a descending order by the flow-sheet of the mine. The friable safety cushion is supposed to be gently lowered with the lowering of the mining, conducting work on two levels of the working -480 m and -580 m (Figure 3). At the same time, the destroyed bottom of the open-pit formed into the ore friable safety cushion should go down, increasing the depth of the pit, as well as forming and exposing the mass of the host rocks located between the East and West ore bodies.

3 RESULTS

Mass of the host rocks located between the East and West ore bodies consists of extremely disturbed rocks, especially in the contact zone. The mass at the elevation of -580 m is

comparable in volume with the volume of both ore bodies. It becomes impossible to control the state of the inner-pipe mass as the mining operations deepen. Active processes of flattening of the sides, which gradually come down onto the ore cushion, are already taking place in the pit, further ensuring the inability to safely come to the bottom of the pit and restricting visual observation of the smoothly exposing mass.

The parameters of the safety cushion were calculated by the specialists of the Institute of Mining of Ural Branch of RAS, taking into consideration the collapse of the known volume of the sides with the known geometry and location (Sokolov, Smirnov, Antipin, Nikitin, Tishkov, 2018). However, in the case of uncontrolled destruction of the inner-pipe mass, it is impossible to give an accurate estimation of the volume of collapsed rocks on the safety cushion, including giving a reliable prediction of the height and the place of the collapse. At the same time, if the thickness of the safety cushion is insufficient, there is a real threat of transfer of the impact energy through the safety cushion to the underground mines. This transfer can cause dangerous deformations of the underground mines, up to creating emergency situation at the field.

The results of the analysis of the actual state and development prospects of mining operations in the EOB and WOB indicate that ensuring a cost-effective and safe extraction of reserves of the Udachnaya Pipe is problematic without developing measures to eliminate dangerous geomechanical situations caused by an increase the depth of mining operations. Initial data for predicting such situations can be obtained using the modeling method on models of equivalent materials of large-scale geomechanical processes in block rock masses developed at St. Petersburg Mining University (Zuev B.Yu., Zubov V.P., Smychnik A.D., 2019; Zuev B. Yu., Zubov V. P., Fedorov A. S., 2019). This method allows you to study the stress-strain state of the rock mass located between the EOB and WOB for various stages of development of mining operations, and on this basis to take preventive measures aimed at increasing the efficiency of mining ore bodies.

4 CONCLUSION

The current state of the Udachny mine can be called steady and stable. The production capacity required by the engineering design is achievable with the existing mining technology. It is suggested based on the analysis of the geological conditions of the pipe to adjust the parameters of the mining methods as mining operations are deepened to maintain the production volume. There is a steady tendency to the degradation of the mining conditions:

- An increase in the volume of underground brines penetrating into the workings directly affects mining operations, the safety of the underground workings, and the condition of the machinery and equipment;
- The process of destruction of the access crosscut of the bottom of the blocks composed of kimberlite, which will experience high loads, is going to begin after the start of the extraction process using combined shrinkage stoping and caving method. Open access to mine air is going to accelerate the destruction of walls of the workings;
- Geomechanical issues will occur associated with the weakening of the sides of the open-pit and with the violation of the initial state of the rock mass during the mining of the West and East ore bodies. The mass located between the ore bodies is extremely disturbed. There is a possibility of partial relaxation, and fracturing, and sudden uncontrolled collapses of rocks on the safety cushion with a decrease in level of the mining operations and exposure of this rock mass. In case of uncontrolled collapse of the rock mass, there is a possibility of exceeding the maximum allowable stability of the cushion up to serious dynamic impacts on the underlying workings.

These factors, which impact the mining of the kimberlite pipe, require further scientific research. At the same time, the inner-pipe mass requires special attention, including field studies and research operations to identify and prevent dangerous uncontrolled collapses.

REFERENCES

Balek A. E., Efremov E. Yu. Justification of the geomechanical conditions of the underground mining of the diamond pipe "Udachnaya pipe". Innovative geotechnologies in the development of ore deposits, 2016, pp. 173–176.

Balek A. E., Sashurin A. D. The problem of assessing the natural stress-strain state of a rock mass during subsurface development. Mining Information and Analytical Bulletin, special issue, 2016, pp. 9–23.

Bokiy I. B, Zoteev O. V, Pul V. V. Analysis of the process of subsidence of the rock pillow during mining of the western ore body of the Udachnaya pipe using a collapse system, Mining Journal, No. 2, 2019, pp. 43–46;

Brief report by independent experts on the reserves and resources of diamond deposits of the ALROSA group of companies, Micon International Co Limited, 2018, http://www.alrosa.ru/wp-content/uploads/2013/11/Alrosa-Summary-Report-Final-RUS.pdf

Chadwick J., Automated Finsch, International Mining, 2012, pp. 10–13.

Drozdov A.V. Geotechnological problems of developing the deep horizons of the Udachnaya pipe. Subsoil use problems: issues of integrated development of deep-seated mineral deposits, 2009, pp. 110–121.

Drozdov A.V. Mining and geological features of the deep horizons of the Udachnaya pipe. Mining Information and Analytical Bulletin, No. 1, 2011, pp. 153–165.

Drozdov A.V. Mining, geological and technological problems in the construction of the Udachny underground mine. Mining Information and Analytical Bulletin, No. 2, 2015, pp. 125–131;

Kovalenko A. A., Tishkov M. V. Assessment of the underground method of mining the Udachnaya pipe field using a self-collapsing system. Mining Information and Analytical Bulletin, No. 4, 2017, pp. 117–128.

Kovalenko. A.A., Tishkov M.V. Evaluation of development of the Udachnaya pipe field. Mining Information and Analytical Bulletin, No. 12, 2016, pp. 173–174

Nikitin I.V. Optimization of opening parameters during underground mining of open-pit reserves of a kimberlite deposit. Topical Issues of Rational Use of Natural Resources, No. 1, 2017, pp. 21–28;

Piven` G.F. Technologies for the development of sub-quarry reserves of the Udachnaya pipe. Notes of the Mining Institute, No. 1, 2011, pp. 359–361.

Sokolov I.V., Smirnov A.A., Antipin Yu.G., Nikitin I.V., Tishkov M.V. Justification of the thickness of the safety cushion when working out the quarry reserves of the Udachnaya pipe with caving systems. Technology mining operations, FTRPRI, No. 2, 2018, pp. 52–62.

The quarterly report of ALROSA PJSC for the 3rd quarter of 2019, ALROSA PJSC, 2019, http://www.alrosa.ru/wp-content/uploads/2019/11/3-квартал-2019-года.pdf.

Trushko V.L., Protosenya A.G., Prospects of geomechanics development in the context of new technological paradigm. Journal of Mining Institute, Vol. 236, 2019, pp. 162–166.

Yakubovskiy M.M., Sankovsky A.A., Drilling and blasting design based on invariable mining parameters. Journal of Industrial Pollution Control, Vol. 33, 2017, pp. 931–936.

Zuev B.Yu., Zubov V. P., Fedorov A. S. Application prospects for models of equivalent materials in studies of geomechanical processes in underground mining of solid. Eurasian mining, No. 1, 2019, pp. 8–12.

Zuev B.Yu., Zubov V.P., Smychnik A.D. Determination of static and dynamic stresses in physical models of layered and block massifs. Mountain Journal, No. 7, 2019, pp. 61–66.